



PONTIFICIA UNIVERSIDAD CATOLICA DE CHILE
Facultad de Ciencias Biológicas
Programa de Doctorado en Ciencias Biológicas
Mención Ciencias Fisiológicas

**INSULIN-LIKE GROWTH FACTOR 2 PROMOTES OVARIAN CANCER GROWTH
AND RESISTANCE TO TRADITIONAL CHEMOTHERAPY**

Tesis entregada a la Pontificia Universidad Católica de Chile en cumplimiento parcial de los requisitos para optar al Grado de Doctor en Ciencias con mención en Ciencias Fisiológicas

Por

JURRIAAN BROUWER-VISSER

Director de Tesis: Gloria S. Huang, MD

Co-director: Ricardo D. Moreno Mauro, PhD

2014

GENERAL INDEX

LIST OF FIGURES	III
LIST OF TABLES	IV
LIST OF ACRONYMS	V
ABSTRACT	VI
RESUMEN	VII
GENERAL INTRODUCTION	1
IGF2 overview	1
Gene structure of IGF2	2
The different IGF2 proteins	5
Regulation of IGF2 function	6
Involvement of IGF2 in drug resistance	11
The IGF signaling pathway as a possible therapeutic target	12
Ovarian cancer overview	15
Origins of ovarian cancer	17
Subtypes of ovarian cancer	18
Treatment of ovarian cancer	19
Drug resistance in ovarian cancer	21
Hypothesis	25
Aims	25
MATERIALS AND METHODS	27
Ethics statement	27
Cell lines and reagents	27
IGF2 gene expression analysis in clinical samples of ovarian cancer	27
Quantitative PCR	28
Sequencing of β -tubulin	28
Proliferation kinetics and cytotoxicity assays	28
ELISA for receptor phosphorylation and IGF2	29
Stimulation of cells with conditioned media	29
Western blot analysis of protein expression	29
Therapeutic studies in xenograft-bearing mice	29
IGF2 and IR knockdown	30
IGF2 overexpression	30
Migration Assay	30
Clinical Specimens	31
Immunohistochemistry	31
Cell cycle and apoptosis analysis	31
Drug efflux analysis	32

Statistical analysis	32
Chapter I: Insulin-like Growth Factor 2 Expression Modulates Taxol Resistance and Is a Candidate Biomarker for Reduced Disease-Free Survival in Ovarian Cancer	33
Abstract	34
Statement of Translational Relevance	34
Introduction	35
Results	37
Activation of AKT by Taxol	37
IGF2 regulation by Taxol	40
Evaluation of paired sensitive and resistant HEY ovarian cancer cells	41
IGF2 knockdown in Taxol-resistant cells	46
IGF2 expression in epithelial ovarian tumors	48
Discussion	55
Acknowledgements	58
Supplemental Figures	59
Chapter II: Insulin-Like Growth Factor 2 Silencing Restores Taxol Sensitivity in Drug Resistant Ovarian Cancer	64
Abstract	65
Introduction	65
Results	66
Discussion	91
Acknowledgements	94
Supplemental Figures	95
Chapter III: Overexpression of Insulin-like Growth Factor 2 in an ovarian cancer cell line leads to increased xenograft growth and neutrophil infiltration	102
Objectives	103
Aims	103
Results	104
Phenotype of IGF2 overexpression in HEY cells	104
IGF2 conditioned media stimulates HEY cells	108
HEY-IGF2 xenografts have an increased growth rate	110
HEY-IGF2 conditioned media stimulates and attracts HL60 cells	115
GENERAL DISCUSSION	119
CONCLUSIONS	126
REFERENCES	127

LIST OF FIGURES

Introduction

Figure 1: The IGF2 gene with its variants, promoters and isoforms	3
Figure 2. Stage of diagnosis and five-year survival rate by stage of diagnosis of ovarian cancer between 2003 and 2009 in USA	16

Chapter I

Figure 1. Effect of Taxol treatment on AKT phosphorylation	39
Figure 2. Taxol-induced IGF2 mRNA expression	42
Figure 3. Potentiation of Taxol treatment by the IGF1R inhibitor NVP-AEW541	45
Figure 4. Effect of IGF2 depletion by siRNA transfection in HEY and HEY-T30 cells	47
Figure 5. Representative images of IGF2 immunohistochemical staining	49
Figure 6. Correlation between IGF2 expression and clinicopathologic factors in ovarian tumors	53
Figure S1. Inhibition of IGF1R by NVP-AEW541	60
Figure S2. Constitutive IGF1R activation in HEY-T30 cells	61
Figure S3. Evaluation of cisplatin cytotoxicity in HEY and HEY-T30 cells	62
Figure S4. IGF2 depletion by siRNA transfection in HEY-T30 cells	63
Figure S5. Quality control assays for IGF2 immunohistochemistry	64

Chapter II

Figure 1	70
Figure 2	73
Figure 3	77
Figure 4	81
Figure 5	86
Figure 6	90
Figure S1. A2780-T15 β -tubulin mutation	97
Figure S2. Knockdown by siRNA and shRNA	98
Figure S3. Correlation between IGF2 and ABCB1 mRNA	100
Figure S4. Cell doubling time	101
Figure S5. Xenograft growth curve of animals from D5W group until first treatment.	102

Chapter III

Figure 1	107
Figure 2	110
Figure 3	113
Figure 4	118

LIST OF TABLES

Table 1. Characteristics of the study population	50
Table 2. IGF2 expression in LMP tumors and epithelial ovarian carcinoma (EOC)	54
Table S1. Sequences of primers and oligonucleotides	96

LIST OF ACRONYMS

ABCB1: Adenosine triphosphate-binding cassette sub-family B member 1
ANOVA: ANalysis Of VAriance
ATP: Adenosine TriPhosphate
CDDP: cis-diamminedichloroplatinum(II)
D5W: 5% Dextrose Water
DMSO: DiMethyl Sulfoxide
ELISA: Enzyme Linked ImmunoSorbent Assay
EOC: Epithelial Ovarian Carcinoma
ERK: Extracellular signal Regulated Kinase
EV: Empty Vector
FACS: Fluorescence Activated Cell Sorting
FBS: Fetal Bovine Serum
FIGO: Federation Internationale de Gynecologie et d'Obstetrique
GAPDH: GlycerAldehyde 3-Phosphate DeHydrogenase
GFP: Green Fluorescent Protein
IC₅₀: Inhibitory Concentration 50%
IGF1/2: Insulin-like Growth Factor
IGF1R: Insulin-like Growth Factor 1 Receptor
IGFBP: Insulin-like Growth Factor Binding Protein
IR: Insulin Receptor
LMP: Low Malignant Potential
LOI: Loss Of Imprinting
MSA: Microtubule Stabilizing Agent
MTD: Maximum Tolerated Dose
NA: Not Applicable
ND: Not Detectable
OSE: Ovarian Surface Epithelium
PI3K: Phosphatidylinositol-4,5-bisphosphate 3-kinase
PPIB: PeptidylProlyl Isomerase B
RT-qPCR: Reverse Transcriptase quantative Polymerase Chain Reaction
RTK: Receptor Tyrosine Kinase
SD: Standard Deviation
SE/SEM: Standard Error of the Mean
SEER: Surveillance, Epidemiology, and End Results
SRB: Sulforhodamine B
TCGA: The Cancer Genome Atlas
TMA: Tissue Micro Array
UTR: UnTranslated Region

ABSTRACT

Ovarian cancer remains the deadliest gynecological cancer worldwide with relatively little advancements in its treatment. Limited knowledge of its molecular origins and the absence of clear symptoms lead to late diagnosis resulting in advanced disease and a poor five-year survival prognosis. Even though initial surgery and chemotherapy treatment reduce pathology, the disease recurs often and frequently develops resistance to standard chemotherapies. The Insulin-like Growth Factor (IGF) signaling axis is involved in several cancers and increased *IGF2* expression is suggested to be associated with poor survival in women with ovarian cancer. Here, we sought to determine the role of IGF2 in ovarian cancer growth and chemoresistance. We observed that Taxol, a standard chemotherapy agent commonly administered to patients with ovarian cancer, induced increased *IGF2* expression in two ovarian cancer cell lines. Similarly, cell lines resistant to multiple microtubule-stabilizing agents also showed increased levels of *IGF2* expression. Inhibition of the IGF-signaling pathway with a small-molecule inhibitor or knockdown of *IGF2* mRNA sensitized the cells to Taxol, both in cell culture and in xenografts. Immunohistochemistry of ovarian tumor samples showed a significant correlation between high *IGF2* expression, advanced stage, tumor grade and decreased disease-free survival. Analysis of mRNA data of *The Genome Cancer Atlas* of serous ovarian cancer also revealed a significant correlation between increased *IGF2* mRNA and reduced progression-free and overall survival.

When *IGF2* was constitutively overexpressed in an ovarian cancer cell line, increased xenograft growth was observed as compared to the control-transfected parental cell line. Along with increased growth rate, increased numbers of infiltrating neutrophils were present in the *IGF2*-overexpressing xenografts. Furthermore, we observed that a human neutrophil-precursor cell line migrated significantly more to the conditioned media of the *IGF2*-overexpressing HEY cell line *in vitro*.

These findings suggest an important role for IGF2 in tumor growth and responsiveness to standard chemotherapy for ovarian cancer, as well as a potential new target for the precision treatment of certain ovarian tumors.

RESUMEN

Cáncer de ovario sigue siendo la enfermedad ginecológica más mortal en el mundo con relativamente pocos avances en su tratamiento. El conocimiento limitado de sus orígenes moleculares y la ausencia de síntomas claros llevan a un diagnóstico tardío que resulta en una enfermedad avanzada y un mal pronóstico en los primeros cinco años. Aunque la cirugía inicial y el tratamiento con quimioterapia reducen la patología, a menudo la enfermedad recurre y frecuentemente se desarrolla resistencia a la quimioterapia. La vía de señalización del factor de crecimiento semejante a la insulina (IGF) esta involucrada con varios tipos de cáncer y la expresión aumentada de *IGF2* podría estar asociada con baja supervivencia en mujeres con cáncer de ovario. En este estudio, buscamos determinar el rol de IGF2 en el crecimiento y quimioresistencia de cáncer de ovario. Observamos que Taxol, una quimioterapia estándar típicamente administrada a pacientes con cáncer de ovario, induce el aumento en la expresión de *IGF2* en dos líneas celulares de cáncer de ovario. Similarmente, líneas celulares resistentes a múltiples agentes estabilizantes de microtubulos también mostraron un aumento en los niveles de expresión de *IGF2*. La inhibición de la vía de señalización de IGF con un inhibidor de molécula pequeña o con el knockdown del mRNA de *IGF2* sensibilizaron las células a Taxol, tanto en cultivo celular como en xenografts. Inmunohistoquímica de muestras de cáncer de ovario mostraron una correlación significativa entre una alta expresión de *IGF2*, estado avanzado, grado del tumor y disminuida supervivencia libre de enfermedad. Análisis de los datos de mRNA de *The Genome Cancer Atlas* de cáncer de ovario seroso también reveló una correlación significativa entre altos niveles de mRNA de *IGF2* y la reducida supervivencia libre de progresión y general. Cuando IGF2 fue sobreexpresado constitutivamente en una línea celular de cáncer de ovario, se observó un aumento en el crecimiento de xenograft comparado con la línea celular parental control transfectada. Junto con esta aumento en crecimiento, había un aumento en la presencia de neutrófilos infiltrantes en los xenografts de *IGF2*-sobreexpresado. Además, observamos que una línea celular humana de precursor neutrofilico migraba significativamente mas hacia el medio condicionado de la línea HEY con sobreexpresión de *IGF2 in vitro*. Estos resultados sugieren un rol importante de *IGF2* en el crecimiento tumoral y en la respuesta a quimioterapia estándar en cáncer de ovario, así como un potencial nuevo blanco para el tratamiento preciso de ciertos tumores de ovario.

GENERAL INTRODUCTION

Ovarian cancer treatment has advanced relatively little over the last decades and outside surgery and standard chemotherapy treatment, there are few precision treatment options available. To further the development of treatment for this disease we need to better understand the molecular origins of this cancer, establish better diagnostic assays and interpret the tumor's response to chemotherapy treatment. Even though many signaling cascades are involved in tumorigenesis, one that has specifically piqued our interest is the Insulin-like Growth Factor signaling pathway and one of its ligands, IGF2. In the following sections, we will summarize the current data published on IGF2 signaling and ovarian cancer in order to fully understand the difficulty of its treatment.

IGF2 overview

IGF2 is a small peptide, part of the Insulin-Like Growth Factor signaling family. Other members include the signaling peptide IGF1, at least six different binding proteins and the receptors IGF1R and IGF2R. As the name indicates, there is much homology in form and function between insulin and the Insulin-Like Growth Factor family. The insulin gene itself is located just upstream of *IGF2* on chromosome 11 and IGF2 can also signal through the insulin receptor in both mice and humans (Livingstone, 2013).

The IGF-axis has a variety of roles for metabolism and proliferation. IGF2 is of great importance during development both in mice and humans. Mice with homozygous null-mutated or paternal heterozygous null-mutated *Igf2* give rise to a dwarfed but viable embryo, showing its importance in the regulation of growth during development (Baker *et al*, 1993; Liu

et al, 1993). In humans during adult life, hepatocytes are the major producer of IGF2, but its physiological role seems to be of less importance (Holthuisen, 2003). IGF2, unlike IGF,1 is not greatly dependent on Growth Hormone and therefore changes little during puberty.

However, IGF2 is involved in a variety of diseases such as Beckwith-Wiedemann syndrome, Wilms' tumor and Ewing's sarcoma (Harris & Westwood, 2012). The childhood Beckwith-Wiedemann syndrome is an overgrowth syndrome that is accompanied by *IGF2* overexpression and often leads a type of renal tumor called Wilms' tumor (Rancourt *et al*, 2013). A related rare tumor type, Ewing's sarcoma, is also characterized by increased *IGF2* expression (Manara *et al*, 2007).

In recent years, IGF2 has been shown to be involved in a variety of adult malignancies, usually leading to a worse prognosis in case of its overexpression (Singer *et al*, 2004; Lu *et al*, 2006). These examples show the importance of regulating IGF2 function. Research has shown many different levels at which this signal is regulated, from its expression to its binding and bioavailability (Chao & D'Amore, 2008; Harris & Westwood, 2012).

Gene structure of *IGF2*

The *IGF2* gene is located on chromosome 11 in a highly imprinted region. Normally, the *IGF2* maternal allele is methylated, and expression occurs only from the paternal allele. This imprinting is done reciprocally between *IGF2* and its downstream neighbor *H19*, which is usually expressed only from the maternal allele (Ratajczak, 2012). The insulin gene is located upstream of the *IGF2* gene and read-through transcripts of *INSIGF2* have been described. This transcript, mainly found in beta cells of the pancreas, encodes for a fusion consisting of the

first 138 amino acids of the *IGF2* gene along with 62 amino acids of the insulin gene (Kanatsuna *et al*, 2013).

Currently, there are four different variants of *IGF2* described in the RefSeq database, originating from four different promoters (P0-P4). The fifth promoter P1 is further upstream, near the insulin gene and does not have a RefSeq entry as of yet (Figure 1).

The gene has nine exons, of which only exons 7, 8, and part of exon 9 encode for the preproprotein. An isoform 2 has also been described, using an alternatively spliced exon 4 (exon 4b) as part of the coding sequence (Mineo *et al*, 2000; Li *et al*, 2011).

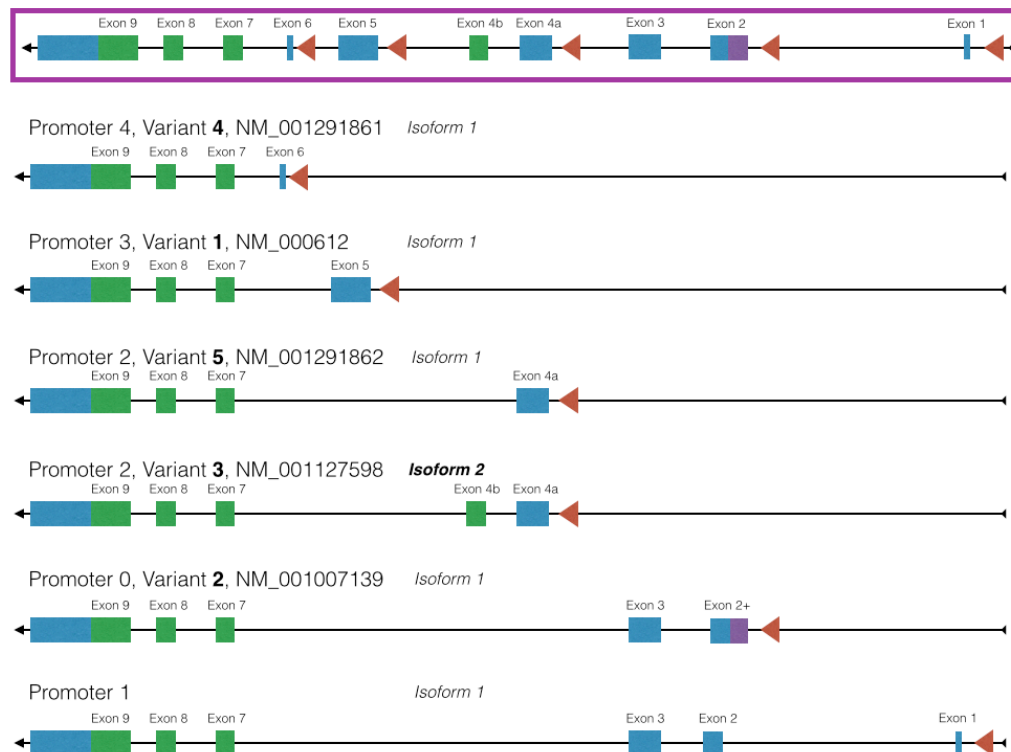


Figure 1: The *IGF2* gene with its variants, promoters and isoforms

In blue are the non-coding exons, green the coding exons, red arrows promoters.

Different promoters are used in different stages of development. Promoters P2-P4 are used during fetal development, as is P0; although this promoter is initially expressed only in fetal skeletal muscle, later in development it is detected in most tissue types. P1 is also called the liver-specific promoter as it is expressed only in the liver during adult life (Lui & Baron, 2013). In malignancies where IGF2 is upregulated, often the re-activation of the “fetal” promoters is detected. In immortal cell lines P3 is usually the most active promoter (Holthuizen, 2003). Promoter 1 is the most distant from the coding sequence and transcribes exons 1, 2, 3, 7, 8, 9. Promoter 2 comes before exon 4 and gives rise to both protein isoforms 1 and 2 by means of alternative splicing of exon 4, leading to a transcript of exons 4a/b 7, 8, 9 where unlike exon 4a, exon 4b is described to be part of the coding sequence (Mineo *et al*, 2000). Promoter 3 in front of exon 5 leads to the transcript consisting of exons 5, 7, 8, 9. Finally, promoter 4 located in front of exon 6 leads to a transcript of exons, 6, 7, 8, 9. Promoter 0 is in front of exon 2, giving rise to a transcript of exons 2, 3, 7, 8 and 9. Exon 2 transcribed from P0 is slightly larger than exon 2 transcribed by P1 since the transcript initiation site is upstream of the splice donor site of P1, giving rise to a unique P0 5' UTR (Monk, 2006). Other elements in the *IGF2* gene include an miRNA (*miR-483*) in the intron between exon 8 and 9, which appears to be important in the regulation of *IGF2* translation. Five tag-Single Nucleotides in the non-coding part of the *IGF2* gene that decrease the chance of ovarian cancer have been described. Specifically the SNP rs4320932 showed a 13% decrease in ovarian cancer chance per copy present (Pearce *et al*, 2011).

The different IGF2 proteins

The main isoform of IGF2 (isoform 1), translated from exons 7, 8 and part of 9, gives rise to a 180-residue pre-pro-protein. A 24-residue signal peptide is cleaved off to give the 156 residue pro-protein. This pro-protein consists of the 67 residues of mature IGF2 plus the 89 residues of the e-domain and has up to four O-glycosylation sites. The weights of proteins range from 10 to 19 kDa, depending on cleavage. At least three non-mature IGF2 forms have been described to have biological activity: besides the 1-156 residue pro-IGF2, also the two so-called big IGF2s (1-87 and 1-104) (Greenall *et al*, 2013). The different intermediate forms of IGF2 are present in detectable quantities in the serum of both healthy people and patients affected by malignancies (Huang *et al*, 2014).

In gastrointestinal stromal tumors, 91% of a cohort of tumors showed the presence of *IGF2* mRNA, while benign tissue was negative. By immunohistochemistry, 65% of IGF2 was of the “big” kind (Rikhof *et al*, 2012). Big-IGF2 has also been suggested to be one of the main culprits of non-islet cell tumor-induced hypoglycemia, a condition where the tumor produces so much IGF2, the patient suffers of hypoglycemia (Hizuka *et al*, 1998). All four forms (mature IGF2 and three pro-proteins, 1-87, 1-104 and 1-156) have similar effects on proliferation and bind to IGF1R and IR-A/B. Worth noting is that the IGF2 binding to IR-A increases survival and motility, whereas insulin binding to IR-A only has metabolic effects (Belfiore *et al*, 2009). Even though the non-mature forms bind to at least the binding proteins IGFBP2, 3 and 5, they are unable to form the ternary structure with the Acid Labile Subunit. Conversely, pro-IGF2 binds more strongly to IGF2R than mature IGF2, increasing its

internalization and degradation, suggesting mature IGF2 might have evolved to avoid inactivation by the IGF2R (Greenall *et al*, 2013).

Regulation of IGF2 function

As IGF2's functions are essential for the correct development of an organism, its usage is exquisitely regulated (Bruchim *et al*, 2014). Loss Of Imprinting, meaning both alleles are expressed, occurs but does not necessarily indicate disease (Cui *et al*, 2003). LOI occurs normally by a decrease in binding of the enhancer-blocking element CCCTC-binding factor (CTCF) to the *IGF2-H19* imprint control region. This allows for increased DNA-methylation, silencing the maternal imprinting, which results in bi-allelic expression. A population of healthy Chinese babies showed a 20% of LOI in cord blood (Dai *et al*, 2007), a similar percentage to that observed in cohort of neonates in the USA (Rancourt *et al*, 2013). In adults, transcription from the P1 promoter in the liver is also bi-allelic under normal circumstances (Monk, 2006). LOI occurs in the prostate of older men and mice by the reduction of CTCF expression. Bi-allelic expression has extensively been observed in cancers, but often is not enough to explain the large increases of IGF2 seen in tumors. Similarly, during development *IGF2* expression is much higher than during adult life, but in both stages expression is mainly mono-allelic, indicating different ways of regulation (Ekstrom *et al*, 1995). Oxidative stress has been linked to LOI of the *IGF2* gene through the NF-kB pathway. CTCF expression is reduced by the binding of NF-kB p65/p50 heterodimer to its promoter, leading to *IGF2* LOI (Yang *et al*, 2014).

The cancer genome atlas study of colorectal cancer samples, found a focal amplification of the *IGF2* gene in 7% of the studied tumors, the most common amplification observed in that study. This amplification is expected to lead to an increase in *IGF2* expression as well as the previously mentioned *miR-483* (Cancer Genome Atlas Network & Getz, 2012). This miRNA (*miR-483-5p* specifically) is located in one of *IGF2*'s introns and has been shown to regulate *IGF2* expression (Liu *et al*, 2013). This positive feedback loop is described to function through DHX9, an RNA helicase. Upon overexpression of this miRNA in an Ewing's cell line, the stability of the *IGF2* mRNA was not increased, but the number of transcripts was. DHX9 binds directly to the promoter 3 of the *IGF2* gene, thereby altering the structure and allowing for faster transcription. The importance of *miR-483* as a dominant driver oncogene of *IGF2* has been confirmed in a new primary organoid system of colorectal cancer (Li *et al*, 2014b). Other more distant miRNAs have also been shown to regulate *IGF2* expression. Directly comparing tumorigenic and non-tumorigenic breast cancer tissue by miRNA profiling, found *miR-100* to inhibit the expression of *IGF2*. When this miRNA was stably overexpressed, *IGF2* was downregulated and xenograft growth was inhibited. This effect was rescued by the overexpression of *IGF2*. Reporter gene assays showed that *IGF2* was a direct target of *miR-100* while mTOR and IGF1R were unaffected by its overexpression. In a small set of patient breast cancer samples there was a significant negative correlation between expression of *miR-100* and *IGF2* (Gebeshuber & Martinez, 2013).

MiR-615-5p, located in an intron of the homeobox family member *HOXC5*, is a miRNA described to regulate *IGF2* expression in pancreatic ductal adenocarcinoma. Similar to *miR-100*, its expression decreases *IGF2* on the mRNA, protein and secretion level. Mutating

the 3' UTR region of *IGF2* inhibits the binding of this microRNA, and subsequent overexpression of *miR-615-5p* ceases to negatively affect *IGF2* expression, indicating *IGF2* is the direct target. Xenografts overexpressing *miR-615-5p* had smaller tumors with less staining for *IGF2* (Gao *et al*, 2014).

ZFP57 is an embryonic stem cell-specific transcription factor that is also important in anchorage-independent growth in a fibrosarcoma cell lines. *ZFP57* binds to imprinting control region of imprinted genes, one of which is *IGF2*. Overexpression of *ZFP57* allowed 3T3 cells to grow under anchorage-independent conditions, which could be reverted by the addition of an IGF2-neutralizing antibody, showing the direct relation between these two genes. In tumor samples of the pancreas, esophagus and breast, *ZFP57* was overexpressed, while showing a positive correlation between *ZFP57* and *IGF2* expression in esophagus and breast cancer samples (Tada *et al*, 2014).

In mice and humans, it was observed that the activating transcription factor *E2f3* binds to the P2 of *Igf2* (P3 in humans) and is downregulated with age. *E2f3* is the only *E2f* family member that has been shown to be overexpressed in cancers. Overexpression of *E2f3* led to increased *Igf2* expression, suggesting direct regulation. A strong correlation was shown between *Igf2* and *E2f3* expression in both human bladder and prostate cancer samples. Interestingly, even though *IGF2* and *E2F3* are overexpressed in Wilms' tumors, no correlation was found between the two, suggesting one of the many other regulators is responsible for *IGF2* expression in this malignancy (Lui & Baron, 2013).

In esophageal squamous cell carcinoma, the inhibitor of DNA binding 1 (ID1), a dominant negative helix-loop-helix protein, activates the PI3K/AKT pathway through IGF2 and IGF1R.

Analysis of patient samples showed a correlation between the increased expression of *ID1* and *IGF2*. Overexpression of *ID1* increased *IGF2* secretion from cell lines, leading to increased tumor growth in mice, which could be reversed by knocking down *IGF2* or by treatment with IMC-A12, an anti-IGF1R blocking antibody. Interestingly, IGF2 in the serum of the mouse increased as well, allowing for an interesting set of experiments with instigator tumors of *ID1* overexpressing cells and responder tumor of untransfected cells. The IGF2 secreted by the instigator tumor allowed the responder tumor to grow more rapidly, even when the responding cells were injected intravenously (Li *et al*, 2014a).

IGF2 signaling can be modulated on several levels once the protein has been processed. The quantity of receptors on the membrane will alter the intensity of intracellular signaling and IGF2's final effect on the cell's fate (Holthuisen, 2003). This goes for both the IGF1 receptor and the IGF2 receptor, but in opposite ways. IGF1R is a receptor tyrosine kinase and signals downstream to the PI3K/AKT and mTOR pathways. An increased number of IGF1R on the membrane will allow for increased signaling by IGF2. Conversely, IGF2R is not an RTK and internalizes and recycles IGF2 upon its binding, thereby attenuating IGF2's signaling action. Notably, *IGF2R* is a paternally imprinted gene that under normal conditions is transcribed only from the maternal allele (Ludwig *et al*, 1996). An increased number of IGF2Rs will therefore decrease the amount of IGF2 signaling. Of interest is that the IGF2 pro-protein in its various stages of processing has a much lower affinity for the IGF2R (Greenall *et al*, 2013). By expressing mainly "big" IGF2, tumors can avoid the binding of IGF2 to IGF2R (Hizuka *et al*, 1998), thereby increasing autocrine and paracrine signaling.

At least 6 binding proteins can bind IGF2 to stabilize the protein and allow for its transport, with IGFBP-2, -3 and -5 being the most common ones (Holthuisen, 2003). This binary complex can cross the capillary endothelia and can be separated by the action of metalloproteases. Certain tumor cells have an increased expression of these enzymes likely to increase the amount of free IGF2 available. Only the mature form of IGF2 has the possibility to form a ternary complex both with one of the binding proteins and the acid labile substrate. This complex does not have the ability to exit the vascular system and greatly increases the stability of IGF2. Similar to avoiding the IGF2R, tumors avoid this ternary complex formation by secreting mainly “big” IGF2. (Greenall *et al*, 2013).

Another potential important interaction is between p53 and IGF2. Loss of p53 leads to activation of IGF/AKT/mTOR signaling, while *IGFBPs* are also target genes of p53. Elegant experiments with mice with differing allelic expressions of *Igf2* and *Trp53* showed *Trp53*-null homozygote mice were lethal if *Igf2* was not paternally expressed, showing that *Igf2* is necessary for the survival of *Trp53* knock out mice. In tumor formation studies, mice with heterozygous *Trp53* form spontaneous tumors that can be accelerated by bi-allelic expression of *Igf2*. Conversely, conditional knock out of *Igf2* delays the formation of tumors in these heterozygous *Trp53* mice. This suggests *Igf2* favors tumor formation by the inhibition of *Trp53* activity (Haley *et al*, 2012).

Involvement of IGF2 in drug resistance

Our group has shown that *IGF2* is upregulated after Taxol treatment of ovarian cancer cell lines. Cell lines made resistant to Taxol and other microtubule-stabilizing drugs showed constitutive *IGF2* increase. Inhibition of IGF2 signaling in the Taxol-resistant cell line HEY-T30 by the small molecule inhibitor NVP-AEW541 or by siIGF2 reverted sensitivity and decreased proliferation (Huang *et al*, 2010). In xenografts, this cell line showed resistance to Taxol as well, which could be reverted by knocking down *IGF2*, but not by IMC-A12 treatment. Another Taxol resistant ovarian cancer cell line, A2780-T15, was also sensitized by *IGF2* knockdown (Brouwer-Visser *et al*, 2014). The importance of IGF2 in clinical response was further demonstrated by a large cohort of patients samples showing a significant decrease in progression-free survival in patients with high IGF2-positive staining (Huang *et al*, 2010), while we used the data obtained by the Cancer Genome Atlas of ovarian cancer (Cancer Genome Atlas Research Network, 2011), to show that an increase in *IGF2* mRNA leads to worse progression free survival and worse overall survival.

In a set of head and squamous cell carcinoma cell lines made resistant to CDDP, IGF2 was shown to be an important factor in the conference of resistance. Knocking down *IGF2* in the resistant cell lines sensitized the cells, while overexpression of *IGF2* in sensitive cell lines made them more resistant to CDDP (Ogawa *et al*, 2010).

Interestingly enough, high circulating IGF2 in epithelial ovarian cancer seems to lead to better progression-free survival and overall survival, where in the cellular microenvironment the exact opposite was observed (Huang *et al*, 2014). This could be explained by the fact that most

IGF2 in an adult human is produced by the liver and not by the tumor. Low circulating IGF1, IGF2 and IGFBP3 were indicators of poor outcome, whereas lower IGFBP2 was related with better outcome.

In neuroblastoma cells, knockdown of achaete-scute complex homolog 1 (*ASCL1*, a basic helix-loop-helix activating transcription factor) led to increased expression of *IGF2*, mainly from promoter 4. Both isoforms of promoter 2 (with either exon 4a or 4b) were detected, as well as a hetero-duplex of the two splice variants. Neuroblastomas are commonly treated with retinoids that induce differentiation of the tumors cells. *ASCL1* was observed to be downregulated after treatment, which in turn led to the overexpression of *IGF2* (Li *et al*, 2011).

The IGF signaling pathway as a possible therapeutic target

Much effort has gone towards developing the IGF1 receptor as a therapeutic target. Imclone with cixutumumab, Amgen with ganitumab and Pfizer with figitumumab developed humanized antibodies against IGF1R, but clinical trials have been disappointing so far (Yee, 2012). The only IGF1R antibody that is still in development is dalotuzumab from Merck. These unfavorable results could be due to the fact that patients were not selected on their status of the IGF signaling pathway and that resistance to IGF1R inhibition is quickly acquired through compensatory signaling through the IR-A/B (Shin *et al*, 2013). Ganitumab's effectiveness has been shown to correlate with *IGF2* expression and *PTEN* mutational status. Only in cell lines with active *PTEN* and increased *IGF2* expression did the antibody show activity. Only cell lines that do not depend heavily on insulin receptor signaling are affected by

ganitumab (Beltran *et al*, 2014). One way to possibly avoid the compensation occurring between the IGF1R and insulin receptors, is inhibiting the highly similar ATP-cassette of these tyrosine kinases. Small molecule inhibitors such as NVP-AEW541 and OSI-906 (Linsitinib) have the ability to block IGF1R, hybrid and IR signaling, but have shown little effectiveness in phase II trials, which has led to halted development. Importantly, even though IGF2 can bind to both IR-A and IR-B, the inhibition of IR-B will lead to hyperglycemia and might explain the negative results obtained with small inhibitors such as NVP-AEW541 (Gao *et al*, 2011). Few antibodies that target IGF2 directly have been developed for clinical use. MEDI-573 from AstraZeneca is an antibody that targets both IGF1 and IGF2 and is expected to go to phase III trials during 2014. The advantage of this antibody is that it inhibits IGF1/2 signaling through the IGF1R, IR-A, IR-B and hybrid receptors, without affecting insulin signaling through the insulin receptor (Gao *et al*, 2011), thereby avoiding acquiring of resistance seen with antibodies against only IGF1R. DX-2647 is a humanized antibody against IGF2 and binds both mature and “big” IGF2 (Dransfield *et al*, 2010). Both MEDI-573 and DX-2647 only bind to free IGF2 and not in complex with binding proteins, which might limit their use in cancer treatment but may be advantageous for patient with non-islet cell tumor-induced hypoglycemia (Fukuda *et al*, 2006). Another novel way of targeting the regulation of *IGF2* expression is through the infection with vectors that cause cells to lyse under the control of *IGF2*-related promoters. A double promoter-expressing vector is in pre-clinical development and depends on the usage of P3 and P4 of *IGF2* by tumors cells. Only tumor cells use these promoters in adult humans and subsequently only these cells will express the diphtheria toxin and subsequently be lysed. Early data show that the double promoter vector to be more

effective than the treatment with both P3 and P4 vectors separately (Amit *et al*, 2013). A similar approach is taken with Ad315-E1A, where replication of an adenovirus is regulated by the *H19* promoter. Only cells that have LOI of *IGF2* will allow this adenovirus to replicate which finally leads to cell lysis. This similar method of action is used by H101 (Oncorine), where the adenovirus is only replicated in p53-deficient cells. This virus is approved for use in China and is administered by direct injection into the tumor (Nie *et al*, 2012).

These data suggest an important role for IGF2 in a variety of processes important for cancer. Taken together with the fact that its signaling is most important during development, it makes for an attractive target in cancer treatment.

Ovarian cancer overview

Cancer is the leading cause of death for men and women between the ages of 40 and 79. Even though ovarian cancer is not a type of cancer that is diagnosed frequently (1.3% of all cancers), it is the fifth most common cause of cancer-related deaths in women in the USA (Of all deaths due to cancer, 2.4% are due to ovarian cancer) (Siegel *et al*, 2014). In Chile, ovarian cancer is both the ninth most frequent type of cancer diagnosed and cause of cancer-related death in women, leading to 406 deaths in 2011 (DEIS-MINSAL). The majority of patients are diagnosed between the ages of 40 and 79 (with a median of 63 years). Being the most lethal of gynecologic malignancies, the five-year survival rate is only 44.6%. Five-year survival has remained relatively stable over the years and has only increased from 33.6% in 1975 (Howlader *et al*, 2014), due to improved surgical techniques and standard treatment with a platinum and Taxol. In Chile, deaths due to ovarian cancer have remained relatively stable between 1997 and 2011 (from 3.0% to 3.6%) (DEIS-MINSAL).

These statistics illustrate the difficulty of diagnosing and treating ovarian cancer. A major cause for the low survival rate is the advanced stage at which ovarian cancer is diagnosed. If ovarian cancer is diagnosed in an early stage, localized to the ovary, there is a cure rate of 92% (Coleman *et al*, 2013). However, the majority of patients (61%) are diagnosed at a more advanced stage, with metastasized cancer in the abdominal cavity; on the parietal and visceral peritoneum, including the omentum. Ascites can also occur when diaphragmatic lymphatics are blocked, preventing normal drainage. At advanced stages the five-year survival rate is only 27% (Figure 2).

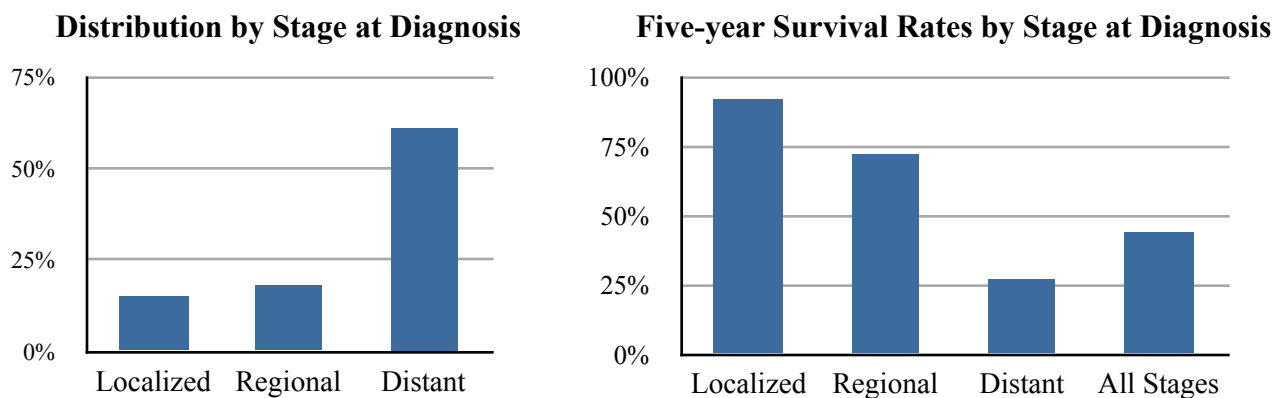


Figure 2. Stage of diagnosis and five-year survival rate by stage of diagnosis of ovarian cancer between 2003 and 2009 in USA

Adapted from (Siegel *et al*, 2014)

Previously, ovarian cancer was thought to be asymptomatic until reaching an advanced stage, but analyses of patients' symptoms have shown that a combination of pelvic or abdominal pain, bloating, increased abdominal size, difficulty with eating and feeling full quickly more than twelve times per month for less than a year warrants further evaluation for ovarian cancer (Andersen *et al*, 2008). While much research is done to determine serum markers that can detect early stage ovarian cancer, CA-125 is the most important marker being used clinically (Mor *et al*, 2005). CA-125 corresponds to a transmembrane mucin is important for adhesion, motility and invasion and is present in 80% of all ovarian cancers. It is shed from the membrane and detectable in the blood. Unfortunately, CA-125 is increased in only 50% of patients with early stage ovarian cancer and its utility is primarily to detect recurrence of ovarian cancer (Bast & Spriggs, 2011). Another recently FDA-approved serum marker to monitor recurrence and progression is HE4 (WFDC2); this gene was seen amplified in ovarian carcinomas and increased levels in the blood correlated both to tumor stage and histological

markers with similar specificity and sensitivity to CA-125 (Hellström *et al*, 2003; Molina *et al*, 2011).

Risk factors include nulliparity, early and late menopause and family history of ovarian cancer (Visintin *et al*, 2008). Conversely, oral contraceptive pills decrease the incidence of ovarian cancer, giving rise to the incessant ovulation theory (Kim *et al*, 2012). This theory states that the chance of ovarian cancer increases with each ovulation, since damaged cells might revert malignant. However, progesterone-only contraceptives that do not consistently inhibit ovulation show the same protective effects, suggesting that not the inhibition of ovulation but the presence of progesterone confers protection (Erickson *et al*, 2013). The majority of ovarian cancer cases are thought to be sporadic (85%), but 15% are of the hereditary type, mainly through BRCA1/2 activity alteration. Women with mutations in *BRCA1/2* undergoing prophylactic salpingo-oophorectomy had a high incidence of *p53* mutations (80%) (Lee *et al*, 2007).

Origins of ovarian cancer

Often primary tubal and peritoneal cancer are grouped together with ovarian cancer, since distinguishing between the different types proves challenging (Coleman *et al*, 2013). The ovary does not have a well-defined epithelial layer like other organs, only a surface epithelium that also covers the serosa of the fallopian tubes, the uterus and the peritoneum. Furthermore, the Ovarian Surface Epithelium (OSE) arises from the coelomic epithelium (Landen *et al*, 2008), not from mullerian cells and shows mesenchymal molecular markers such as vimentin and N-cadherin and not epithelial markers such as E-cadherin and CA-125. High grade serous

ovarian tumors were believed to originate from this OSE, but extensive histopathological analysis did not show precursor lesions of these aggressive tumors. However, upon microscopic inspection of the fallopian tubes of patients that had received risk-reducing salpingo-oophorectomy, cellular dysplasia and hyperplastic lesions were observed in the distal fimbriae of the tubal epithelium (Kurman, 2013). These lesions, Tubal Intra-epithelial Carcinomas, resembling high grade serous ovarian cancer, show non-functional p53 and share expression profiles with metastasized tumors (Erickson *et al*, 2013). The current understanding is that high grade ovarian cancer often arises from the epithelial cells of the fallopian tube; these cells can then be transported to neighboring organs and form tumors (Piek *et al*, 2003).

Subtypes of ovarian cancer

Traditionally, ovarian cancer is divided into several histological subtypes: serous carcinoma (68-71%), mucinous (3%), endometrioid (9-11%) and clear cell (12-13%) carcinoma (McCluggage, 2011). The different histologic subtypes of ovarian cancer each resemble their cell type of origin: serous resembles epithelial cells from the fallopian tubes, endometrioid from the endometrium, mucinous from the cervical glands and clear cell from the vaginal rests (Romero *et al*, 2012).

Research into the different origins, mutations, growth kinetics, drug sensitivity and hence survival have led to a new system of grouping subtypes of ovarian cancer (Berns *et al*, 2012). Type I is low grade, slowly developing, usually diagnosed in early stages and arises from a benign precursor lesion. Even though *p53* and *BRCA1/2* are wild-type in this cancer type, there are often mutations in *KRAS*, *BRAF*, *PTEN* and *ERBB2* that lead to PI3K activation. The

tumors respond poorly to standard chemotherapies, only 15%-26% responds to platinum drugs, but might be sensitive to hormone treatment. If the patient is optimally debulked and no residual disease is detected after surgery, often no chemotherapy is given for type I ovarian cancers. The karyotype is normal and cells have papillary morphology. Therefore, type I cancer cells appear to grow driven by several PI3K activating mutations (Romero *et al*, 2012), and follow the typical path of benign precursor transformation to malignant tumor. Low grade serous, mucinous, endometrioid, clear cell, transitional and mixed are the histological subtypes corresponding to type I (Kurman, 2013).

Type II is high grade, usually serous and diagnosed in advanced stages. *p53* is mutated in 96% of the high grade serous carcinomas tested in the cancer genome atlas study (Cancer Genome Atlas Research Network, 2011). BRCA1/2 function is silenced in more than 40% of the tumors. Type II tumors have altered gene copy numbers and appear driven by genomic instability. High grade endometrioid but mainly serous carcinomas form type II. High grade serous carcinomas arise from the distal fibral part of the fallopian tube and are poorly differentiated, with nuclear atypia and many mitotic figures (Coleman *et al*, 2013).

Treatment of ovarian cancer

The current treatment of ovarian cancer consists of initial cytoreductive surgery. Even though surgery alone is rarely curative, a randomized trial has shown that optimal cytoreductive surgery is associated with improved progression-free and overall survival (Goodman *et al*, 1992). Ovarian cancer is a cancer where cytoreductive surgery is first-line treatment and its benefit may be due in part, to eradication of large tumors that often are chemoresistant.

Standard chemotherapy consists of a combination of platinum and Taxol. Incorporation of Taxol into first-line chemotherapy was shown to improve survival compared with non-Taxol regimens in several Phase 3 clinical trials conducted in the 1990's (Agarwal & Kaye, 2003).

More recently, several clinical trials have shown the advantage of intraperitoneal administration instead of intravenous administration of both Taxol and the platinum.

Intraperitoneal administration changes the drug kinetics, increasing the half life and the concentration near the target organs. This led to a 21.6% reduction in risk of death and a twelve-month increase in overall survival (Trimble & Alvarez, 2006).

Even so, the five-year survival rate is still only 44.6% (Siegel *et al*, 2014). As stated before, the late stage in which ovarian cancer is usually diagnosed is an important attributing factor to this low survival, even though most patients have a high level of remission after completing chemotherapy. Recurrence occurs in 70% to 90% of women with ovarian cancer and is frequently accompanied by drug resistance, complicating full remission (StatBite: Ovarian cancer: risk of recurrence by stage of diagnosis., 2009). In the setting of recurrent ovarian cancer, chemotherapy is considered palliative in nature, as no treatments have demonstrated the ability to reverse drug resistance and effectively eradicate the disease, with rare exceptions.

Advances in molecular targeted treatments for cancers have been made over the last fifteen years, especially for hematological and breast malignancies. For selected patients, specific combination therapies using chemotherapy along with small-molecule inhibitors and antibodies have proven to be more effective than chemotherapy alone (Vanneman & Dranoff, 2012). However, no such significant advances have been made for ovarian cancer, partly because the molecular basis of this cancer remains to be completely elucidated. Clinical trials

with the VEGF-A antibody bevacizumab have shown better progression-free survival, but no enhanced overall survival (Burger *et al*, 2011). BRCA seems an interesting target since cells with BRCA activity altered have already one impaired DNA repair pathway. Platinum drugs cause double strand breaks, so mutant cells have to rely on base excision repair to repair these breaks. Inhibiting this pathway with poly-ADP ribose polymerase (PARP) inhibitors while simultaneously treating with a platinum, might enhance outcome in patients with BRCA silencing (Romero *et al*, 2012).

So far, no single agent seems to improve outcome for ovarian cancer patients and trials are being designed to target several signaling pathways simultaneously.

Drug resistance in ovarian cancer

Resistance to chemotherapy is the indirect cause of death in 90% of patients with metastatic disease and one of the reasons that ovarian cancer has a low five-year survival rate. Type II high grade serous ovarian carcinoma is often chemosensitive and therefore after the first treatment with chemotherapy, a high level of response is observed. When the patient recurs, 70% of patients with ovarian cancer recur, the tumors initially respond to same combination of chemotherapy (Fung-Kee-Fung *et al*, 2007). The response rate correlates positively to the time the patient was disease free. It is thought that a sub-population of cancer cells was halted in G0 of the cell cycle during the initial treatment. Since most chemotherapies only affect rapid-dividing cells, the halted cells are not impacted. During remission, these cells start cycling again to form a new, chemo-naïve, tumor (Agarwal & Kaye, 2003).

Even so, tumor cells frequently acquire resistance to the chemotherapies they are treated with. This means that the treatment becomes ineffective, the cancer continues to progress leading eventually to the death of the patient.

An important factor involved in the acquisition of resistance is pharmacokinetics; drug metabolism is different between patients and therefore, the intended concentration of cytotoxic drugs might not reach all cells of the tumor (Szakács *et al*, 2006). The cancer cells will therefore survive and treatment will fail. Since most chemotherapies have a low therapeutic index, concentrations cannot be increased without causing lethal side effects. Even so, higher concentrations of chemotherapies have been shown to delay resistance and not prevent it (Tan *et al*, 2008).

The micro-environment of the tumor also appears to play an important role. Through interaction by signaling molecules between the cancer cells and surrounding stromal cells, the tumor cells are able to resist higher concentrations of the drugs (Coleman *et al*, 2013). For example, multiple myeloma cells are more resistant to chemotherapy in the presence of bone marrow stromal cells (McMillin *et al*, 2010). In a similar fashion, cells grown in a spheroid setting tend to be more resistant than cells grown in a monolayer (Shield *et al*, 2009).

The last and most-studied factor is the changes specific to the cancer cell itself through acquired somatic mutations and epigenetic alterations. The rapid division of cells within tumors increases the frequency with which mutations occur, even more so in cancer cells where the DNA replication machinery is affected (Szakács *et al*, 2006). If one or several of these mutations provide protection against the chemotherapy used, positive selection will cause these cells to continue proliferating and form drug-resistant tumors.

Many different mechanisms of these cell-specific changes have been described in various major processes in the cell. Replication of DNA can be affected by alterations in Nucleotide Excision Repair and MisMatch Repair, allowing the proliferation of cells that have lost their DNA integrity (Agarwal & Kaye, 2003). Tubulin mutations can decrease the effect of tubulin-targeting drugs, even though this has not been detected in the clinic. Similarly, differential expression of β -tubulin isotypes can confer resistance to tubulin-interacting drugs (Kavallaris, 2010). The increase in expression of influx and efflux pumps in the cell membrane allows the cell to pump out drugs before they can execute their cytotoxic effects. Changes in Glutathione S Transferase enzymes allow the processing and inactivation of drugs such as platinum based chemotherapies (Tan *et al*, 2008).

Besides acquired resistance, cancer cells can also have intrinsic drug resistance, since many mutations that cause cells to become malignant are involved in cell cycle and therefore provide protection against chemotherapies that target this process (Yasui *et al*, 2004). As mentioned before, certain cancer cells are stopped in G0 and are not affected by chemotherapy. Closely related is the hypothesis that tumors have a small sub-population of less-differentiated cells that are inherently chemo-resistant, called Cancer Stem Cells or tumor initiating cells (Maenhaut *et al*, 2010). These cells can withstand an insult by chemotherapy and consecutively repopulate the tumor with more differentiated cells. However, it has proven difficult to define and identify this population within a tumor. Morphologically, there are no clear differences and their presence remains difficult to demonstrate (Stewart *et al*, 2011). Understandably, much research has been done to reverse or avoid resistance but so far little progress has been made. One possible reason is the models we currently use to investigate

resistance. Much of the research carried out has been done in monolayer cell culture, but this model proves difficult to translate to clinic. Especially in drug resistance, the influence of neighboring cells seems to be of high importance. In monolayer culture cells have the possibility to anchor to the plate, whereas cells in tumors are often anchorage independent (Agarwal & Kaye, 2003). Prolonged culture of a cell line will induce changes in the cells that can change their behavior in the presence of drugs. Currently, 3D models are becoming increasingly available to imitate anchorage-independent growth and the presence of neighboring cells that can provide paracrine signaling. However, in these models only one cell type is cultured, while tumors are surrounded by several different types. Co-cultures with stromal cells have proven to affect drug resistance and might constitute a more physiological model (Maenhaut *et al*, 2010). Xenograft models have the advantage that the cancer cells are surrounded by many types of cells, even if they are of a different species (Marangoni *et al*, 2007).

Another difficulty is how cells are made drug resistant. A common method used is by exposing monolayer cell culture to stepwise-increasing drug concentrations, thereby positively selecting those mutants that are drug resistant (Parekh *et al*, 1997). However, in clinic chemotherapies are often administered not constantly but on intervals. Optimally, chemo-naive and a chemo-resistant tumors from the same patient would be compared to find which mechanisms of drug resistance are most important in clinic. However, in ovarian cancer a biopsy is normally only taken when the patient first undergoes diagnosis and not in refractory disease (Agarwal & Kaye, 2003).

The current first line treatment for ovarian cancer is a combination therapy of Taxol and carboplatin (Coleman *et al*, 2013). These two compounds act on different processes in the cell: alterations in microtubule dynamics and DNA-crosslinking, respectively. If resistance occurs after relapse, other drugs can be used targeting other processes, such as topotecan or doxorubicin (both topoisomerase inhibitors) (Bookman *et al*, 2009). Inhibitors of P-glycoprotein and Multi Resistance Proteins have not shown to be useful in clinic so far due to high toxicity. Taxol is a substrate for P-glycoprotein, but other microtubule stabilizing drugs, such as ixabepilone, less so and can therefore be useful in refractory disease (Tan *et al*, 2008). Until now, when chemoresistance is observed in clinic, no assessment is made to determine which mechanism is conferring resistance. Using specific resistance-reversing drugs that target the mechanism altered in the patient, might offer more improvement in treatment.

The focus of this thesis is the role of IGF2 signaling in ovarian cancer. We determined its effect on the response to chemotherapy and chemoresistance and if its expression was indicative of patient prognosis. Lastly, we studied how IGF2 signaling related to tumor growth.

Hypothesis

IGF2 signaling inhibition ameliorates chemoresistance while IGF2 overexpression leads to an increase in growth of ovarian cancer cell lines.

Aims

Evaluate the effect of IGF2 expression on chemoresistance and tumor growth.

- Establish epithelial ovarian cancer cell lines with reduced and increased IGF2 expression.
- Determine resistance to current chemotherapies with reduced and overexpression of IGF2.
- Establish an *in vivo* xenograft model with mice bearing tumors of both transfected and chemo-resistant cell lines.
- Examine the effect of IGF2 inhibition on tumor growth and on the response to current chemotherapies.

MATERIALS AND METHODS

Ethics statement

All animal experiments were done with the approval of the Institutional Animal Care and Use Committee (Protocol 20130604) of the Albert Einstein College of Medicine of Yeshiva University. The Institutional Animal Welfare Assurance (A3312-01) for this facility is fully accredited by the Association for the Assessment and Accreditation of Laboratory Animal Care (AAALAC) since February 22, 1983. Animals were cared for as per the Animal Welfare Act and the NIH “Guide for the Care and Use of Laboratory Animals”.

Cell lines and reagents

The ovarian carcinoma cell lines A2780 (Eva *et al*, 1982) and HEY (Buick *et al*, 1985) (kind gifts from Dr. Susan Band Horwitz), and the ovarian carcinoma cell line NIH:OVCAR8 (Hamilton *et al*, 1984) (a kind gift from Dr. David Goldman) were grown in RPMI-1640 (Life) with 10% Fetal Bovine Serum (Life) and 1% Penicillin / Streptomycin (Life) at 37C with 5% CO₂. The human promyelocytic leukemia HL60 cell line, a kind gift of Dr. Laura Barreyro (Barreyro *et al*, 2012), were grown in suspension in IMDM (Life) supplemented with 20% Fetal Bovine Serum. NIH-3T3 mouse fibroblasts (Jainchill *et al*, 1969) were grown in DMEM (Life) with 10% Newborn Calf Serum (Life) and 1% Penicillin / Streptomycin (Life). All drug resistant cell lines were generated by the authors, except HEY-Epo8 (a gift from Dr. Susan Band Horwitz) which was developed by Dr. C-P Huang Yang using epothilone B (Shahabi *et al*, 2010). The Taxol resistant cell line, HEY-T30, was developed in our laboratory by exposure of HEY cells to stepwise escalating concentrations of Taxol over a 6-month period, and are maintained in media containing Taxol (30 nM). The A2780-T15 cell line was generated similarly from A2780 using Taxol selection but in the continuous presence of 15 μ M verapamil (Sigma). A2780-B20 and HEY-B20 were selected for resistance to ixabepilone (Ixempra™ Bristol-Myers Squibb), and OVCAR8-D30 to discodermolide. Cell lines were authenticated using the Genemarker 10 kit (Promega). Resistant cell lines were matched to their sensitive lines and to published data when available. Cell lines were routinely screened for mycoplasma with MycoAlert (Lonza). Cells were cultured in drug-free media for at least 18 hours prior to experiments except A2780-T15, which was grown in the presence of 0.5 nM Taxol. Clinically formulated Taxol (Hospira) was diluted 6-fold in 5% dextrose water (Hospira) to a final concentration of 1 mg/ml for xenograft experiments. NVP-AEW541, a small molecular weight kinase inhibitor of IGF1R, was provided by Novartis Pharma AG (García-Echeverría *et al*, 2004). A monoclonal antibody to IGF1R, IMC-A12 (Cixutumumab) was provided by Imclone, a fully owned subsidiary of Eli Lilly and Company.

IGF2 gene expression analysis in clinical samples of ovarian cancer

The cBioPortal for Cancer Genomics was used to access the gene expression and clinical data from the Cancer Genome Atlas Project (TCGA) (Cancer Genome Atlas Research Network, 2011). The query was performed using All Complete Tumors of the Ovarian Serous Cystadenocarcinoma (TCGA, Nature 2011) dataset, which includes 489 cases of high-grade serous ovarian cancer. For *IGF2* mRNA Expression Z-scores, a threshold of 1.6 standard deviations above the mean defined the IGF-high group; all other cases were included in the *IGF2*-normal group.

Quantitative PCR

Cell lysates were homogenized using Qiashredder columns (Qiagen Inc., Valencia, CA) and total RNA was isolated by RNeasy Mini Kit (Qiagen). RNA concentration and purity were evaluated using a NanoDrop spectrophotometer (Fisher Thermo Scientific), showing OD 260/280 ratio range of 2.03-2.11. RNA integrity was sampled using an Agilent Bioanalyzer (Agilent Technologies), showing a RIN score range of 9.8 to 10. Complementary DNA was made by performing reverse transcription (RT) using the SuperScript® VILO™ cDNA Synthesis Kit (Life Technologies) according to manufacturer's instructions, using 1 µg total RNA for all cell lines except A2780, A2780-T15 and A2780-B20, for which 2 µg total RNA was used. Quantitative real-time PCR was performed using an Eppendorf Mastercycler® ep realplex2 using a 3-step method (95C 10 min; followed by 40 cycles of 95C for 10 sec, 60C for 20 sec, 72C for 20 sec; then for melting curve 95C 15 sec, 60C to 95C over 20 min). Each reaction utilized 1/20th of the cDNA reaction, forward and reverse primers at a final concentration of 200 nM, and PowerSYBR (Applied Biosystems, Foster City, CA) diluted in Ultrapure water (Life Technologies) to 1X final concentration in a final reaction volume of 10 µL. Exon junction-spanning primers were validated by analysis of melting curves and amplification efficiency. An mRNA expression score was calculated using the formula $2^{-\Delta Ct} * 1000$, where ΔCt is the difference in Ct (cycle threshold) between the gene of interest and the internal normalization gene, *PPIB* (peptidylprolyl isomerase B; cyclophilin B). Fold-change in relative mRNA expression was calculated using the $2^{-\Delta\Delta Ct}$ method (Huang *et al*, 2010). Genomic DNA was isolated with the AllPrep mini kit (Qiagen). Primers were designed to span an intron-exon junction and were validated by melting and efficiency curve analysis. Albumin (*ALB*) was used for internal normalization. By array comparative genomic hybridization, HEY cells were found to have two copies of the *IGF2*, *ABCB1* and *ALB* genes (data not shown). Copy number variation was determined from qPCR of genomic DNA using the $2^{-\Delta\Delta Ct}$ method and setting HEY to 2 copies (Ballester *et al*, 2004). The sequences of the oligonucleotides used in this thesis have been published and can be found in Supplemental Table S1 of chapter II.

Sequencing of β -tubulin

Complementary DNA of A2780 and A2780-T15 was made as described for reverse transcriptase qPCR. Using four primer sets spanning the whole β -tubulin mRNA, a PCR with 250 ng cDNA was run. The products were run on an agarose gel, the bands cut and the DNA extracted with a QIAquick Gel Extraction Kit (Qiagen). The DNA was submitted to the in-house DNA sequencing facility and the resulting sequences analyzed using Genomic Workbench with NM_178014 (*TUBB*) as the template. PyMOL was used to model the found mutation.

Proliferation kinetics and cytotoxicity assays

For proliferation kinetics, cells were seeded in 6-well plates. Every 24 hours, duplicate wells were counted using a Scepter Counter (Millipore). For cytotoxicity assays, cells were seeded in a 96 well plate. After 24 hours, cells were treated with serial dilutions of the indicated drug, with a fixed concentration of 1 µM NVP-AEW541 or 10 µg/ml IMC-A12 if indicated. After 72 hours of treatment, the relative cell number in each well was determined using the sulforhodamine B (SRB) assay. Cell growth was expressed as %, defined as the ratio of the optical density in the treated well compared with the control well x 100, as previously

described (Skehan *et al*, 1990). The IC₅₀ is the drug concentration corresponding to a 50% decrease in cell number calculated using the dose-effect curve.

ELISA for receptor phosphorylation and IGF2

Cells were grown in complete media for 24 hours, then serum-starved for 12 hours before stimulation for 10 minutes with recombinant IGF2 (50 ng/mL; Abcam) or insulin (50 nM; Sigma), with or without pretreatment of cells with NVP-AEW541 (1 μM) or IMC-A12 (10 μg/ml) for 2 hours. Cells were lysed using NP40-based lysis buffer with PhosSTOP (Roche) and protease inhibitor cocktail (Sigma). After protein quantitation, the DuoSet IC Human Phospho-IGF-1 R and Phospho-Insulin R (R&D systems) were used according to the manufacturer's instructions.

To determine the quantity of IGF2 in the growth medium, cells were grown until 80% confluence, washed twice with PBS and 1ml of serum-free medium was added. After 48 hours the growth medium was collected, spun down to remove cell debris and subjected to analysis. Cells were counted to adjust between samples. For IGF2 detection the IGF-II ELISA from Mediagnost was used according to the manufacturer's instructions.

Stimulation of cells with conditioned media

Cells were grown until 80% confluency and then starved for 48 hours with serum-free RPMI. The conditioned media was collected and filtered through a 0.2 μm filter. The cells to be stimulated were grown until 80% confluency and starved overnight.

Plates were washed and conditioned media was added and incubated for 10 minutes. Protein expression was then analyzed by Western blot.

Western blot analysis of protein expression

For analysis of phosphorylated and total AKT and ERK, equal amounts of protein (15 to 20 μg, depending on the experiment) were loaded in each lane on a tris-glycine gel and transferred to nitrocellulose membranes, which were blocked and incubated overnight with the indicated primary antibodies diluted 1:1000 in blocking buffer (LI-COR Biosciences), except GAPDH used at 1:5000 dilution. Primary antibodies used were: PhosphoAKT (Thr308) (Cell Signaling Technology 4056), PhosphoAKT (Ser473) (Cell Signaling Technology 4060), AKT1 (Cell Signaling Technology 2938), PhosphoERK1/2 (Thr202/Tyr204) (Cell Signaling Technology 4370), ERK 1/2 (Cell Signaling Technology 4695), GAPDH (Cell Signaling Technology 2118). Western blot for IGF2 was performed similarly, except using tris-tricine gels and anti-human IGF2 antibody 1:5000 (Abcam ab9574). After secondary antibody (1:10 000 anti-rabbit, LI-COR Biosciences 926-32211) incubation, membranes were scanned on an Odyssey infrared imaging system (LI-COR Biosciences) at 800 nm wavelength. Densitometry was done on the TIFF files measuring integrated density using ImageJ, correcting for background and normalizing to Ponceau staining of the respective lane.

Therapeutic studies in xenograft-bearing mice

Female athymic nude mice (Harlan) between 6 and 8 weeks old were injected subcutaneously with one million of the indicated cells, suspended in 100 μl OptiMem. Tumor size was measured using digital calipers and volume calculated using the formula: (length * width²) / 2. Mice were treated as described in the figure legends. Mice were euthanized by isoflurane anesthesia followed by cervical dislocation, when their xenograft reached 20 mm diameter, or

at the specified time points for xenograft analysis. Hematoxylin and eosin stained xenograft sections were evaluated by the study pathologist. Immunohistochemistry for IGF2 (Abcam ab9574) and Ki67 (Vector vp-k542) was done on formalin-fixed paraffin-embedded sections as described below and scored by the study pathologist.

***IGF2* and *IR* knockdown**

The *IGF2* and *IR*-targeting siRNA oligonucleotides were purchased from Life Technologies. Using RNAiMax Lipofectamine (Life), reverse transfection was performed according to the manufacturer's recommended protocol in 60 mm² dishes, using the experimentally determined optimal siRNA oligonucleotide concentration of 20 nM. After 24 hours of incubation in antibiotic-free OptiMEM (Invitrogen) with 10% FBS, cells were trypsinized and used for the experiments. RNA was harvested at 48 hours post transfection to confirm knockdown by RT-qPCR. For stable knockdown using the BLOCK-iT Inducible H1 Lentiviral RNAi System (Life), vectors were designed to express an shRNA targeting *IGF2*, or a non-targeting control (shScrambled). HEY-T30 cells were transfected with the plasmid directly or with lentiviral particles, then selected with Zeocin (Life). Clones of plasmid-transfected cells and lentiviral-transfected cells were screened for IGF2 knockdown. The clone with the lowest *IGF2* mRNA expression from each group was used for subsequent experiments.

***IGF2* overexpression**

Both A2780 and HEY cell lines were transfected with a vector containing *IGF2* cDNA with the three coding exons 7,8 and 9. The pHAGE-UbC-RIG vector, a kind gift of Dr. Jeffrey Chao (Wu *et al*, 2012), was digested with Not1 and BamH1 to remove the DsRed sequence. The PCR product of the *IGF2* cDNA (using the primers: cgcg GCGGCCGC ATGGGAATCCCAATGG and gcgc GGATCCCTACTTCCGATTGCTGGCC) was digested with Not1 and BamH1, cleaned up and ligated into the pHAGE-UbC-RIG vector. Competent DH5 α bacteria were transformed and grown. Colonies were picked and the insert was sequenced. The plasmid with the correct sequence was then used to transfect HEK-293 producer cells along with viral packaging protein vectors. The produced lentiviral particles were then added to the growth medium of the A2780 and HEY cells. Cells were sorted in a Fluorescence Activated Cell Sorter and only the highest Green Fluorescent Protein expressing cells were selected. As a control, the vector without removal of DsRed was transfected into the two cell lines and the populations sorted for DsRed/GFP double positive cells.

Migration Assay

To determine the ability of HL60 cells to migrate towards conditioned media, a modified Boyden chamber assay was used. Conditioned media was prepared as described above, but incubation time was 72 hours instead of 48 hours. HL60 cells were starved overnight, counted and resuspended in assay media (RPMI with 0.1% FBS). Inserts with 8 μ M pores (BD) were placed into 24-well plates and 500,000 HL60 cells in 100 μ l assay media were added on top of the membrane. Under the membrane 600 μ l of conditioned media was added. The plates were placed in the incubator for four hours.

Cells in the assay media above the membrane and in the conditioned media below the membrane were then counted and the percentage of migrated cells calculated. The percentage of cells migrated towards the conditioned media of the untransfected cell line was set to one.

Clinical Specimens

This study was reviewed and approved by the Institutional Review Boards of the Albert Einstein College of Medicine and the University of New Mexico Health Sciences Center. Formalin-fixed, paraffin embedded tumor specimens from 134 patients diagnosed with epithelial ovarian carcinoma or low malignant potential epithelial tumors, treated at the University of New Mexico Cancer Center between March 1996 and June 2006, were retrieved from the Human Tissue Repository. Specimens were obtained at the time of primary surgery. After secondary pathology review, a tissue microarray (TMA) was constructed, containing two cores from each specimen obtained at the time of primary surgery. Tissue cores were absent in 19 cases, leaving 115 cases available for evaluation. Pertinent clinical data were abstracted and a de-identified database was created. Investigators were blinded to clinical data until completion of staining and scoring.

Immunohistochemistry

Immunohistochemistry was performed using a rabbit polyclonal antibody directed at the IGF2 ligand (ab9574; Abcam). The optimal blocking and primary antibody conditions were determined using placental tissue. In brief, Target Retrieval Solution, Citrate pH 6 (Dako North America) was used for antigen retrieval, tris-buffered saline containing 5% goat serum and 2% bovine serum albumin was used for blocking, and the primary antibody was used at a 1:100 dilution with an incubation of 1 hour at room temperature. Secondary antibody and detection were performed using the DAKO Envision+ Polymer System (Dako North America), followed by counterstaining with hematoxylin. Staining of all tissue microarray slides was performed concurrently with staining of positive and negative control sections. Representative placenta sections are shown following staining with the IGF2 antibody, or with IGF2 antibody that was pre-absorbed with recombinant IGF2 (supplemental Figure S5). Representative stained ovarian tissue sections were photographed on a Zeiss Axioskop II, and images shown depict the TIFF image files without modifications, other than cropping of the size. To evaluate assay reproducibility, IGF2 immunohistochemistry was repeated on an independently constructed tissue microarray that contained distinct tissue cores from 53 of the tumor specimens comprising the study population.

A gynecologic pathologist, who was blinded to all clinical data, graded the cytoplasmic staining intensity (0 negative, 1+ weak, 2+ moderate, 3+ strong) and the percentage of tumor cells with positive staining (1-100%). The H-score is defined as the product of the staining intensity and the percentage of positive staining; the mean H-score for each tumor was determined from the corresponding tissue cores.

Cell cycle and apoptosis analysis

Cells were treated as described in the figure legends. After 16 hours, adherent and floating cells were collected. For cell cycle analysis, cells were fixed with 70% cold ethanol for 1 hour, then incubated with 20 $\mu\text{g/ml}$ propidium iodide (Sigma) and 100 $\mu\text{g/ml}$ RNase (Thermo) in PBS. For apoptosis analysis, the Violet Ratiometric Membrane Asymmetry Probe/Dead Cell Apoptosis Kit (Life) was used according to the manufacturer's protocol. A violet excitable dye 4'-N,N-diethylamino-6-(N,N,N-dodecyl-methylamino-sulfopropyl)-methyl-3-hydroxyflavone (F2N12S) was used for the detection of membrane asymmetry changes that occur during early apoptosis, resulting in a decreased ratio of 585 nm to 530 nm emission. Simultaneously,

SYTOX(R)AADvanced was used as a dead cell stain. Using unstained cells and control untreated cells, gating of quadrants was determined; live, apoptotic, and dead cells were quantified using FlowJo (Treestar).

Drug efflux analysis

Two hundred thousand HEY and HEY-T30 cells were resuspended in 1 ml warm PBS + 5% FBS. All incubation steps were done at 37C in the cell culture incubator. Verapamil (15 μ M) or NVP-AEW541 (1 μ M) was added and the samples incubated for 1 hour. Then 50 μ M of Tubulin Tracker Green reagent (Oregon Green® 488 Taxol, bis-acetate) (Life) was added and the samples incubated for 45 minutes. Cells were pelleted then resuspended in PBS + 5% FBS, with verapamil or NVP-AEW541 if indicated, and incubated for an additional 20 minutes, washed in PBS and stained with TO-PRO-3 (Life). Cells were immediately analyzed using a FACSCanto II (BD) and FlowJo; TO-PRO-3 positive cells (dead cells) were gated out and the remaining cells were graphed to determine labeled Taxol retention (Marcelletti *et al*, 2009).

Statistical analysis

For cell line experiments, numerical values (drug concentrations, combination index, mRNA levels) are expressed as the mean \pm standard error. The number of biological and technical replicates per assay are described in the figure legends. Differences between means of two groups were analyzed using the t-test. For differences between three or more groups, one-way ANOVA with the post-test indicated in the figure legends was used. For analysis of two independent variables, two-way ANOVA with a Bonferroni post-test was used. For survival analysis, the log-rank test was used. All P values are two-tailed and $P < 0.05$ was considered statistically significant.

For analysis of IGF2 expression in the ovarian tumor tissues, IGF2 expression was categorized as high or low using the median IGF2 H-score, and the Chi-square or Fisher's exact tests were used to determine the association of IGF2 expression with clinical and pathological variables. Correlation of IGF2 H-scores obtained using two independently constructed and stained tissue microarrays was assessed by Spearman Rank correlation. Survival analysis was performed to study the effect of IGF2 expression on overall and disease-free death events using the Cox proportional hazards regression. Additional adjustment for age, grade, stage, extent of cytoreduction, performance status, and chemotherapy was achieved by including these variables in the Cox models. A predictor was considered as a potential candidate for the final model if the log-rank test of equality across strata had a p-value less than 0.25 in a univariate analysis. During final multivariate Cox model building, all the potential predictors were included in the model and the Wald test was used to measure the statistical significance of hazard ratios. All the possible interactions were tested and proportional hazards (PH) assumptions were checked. No significant interactions were found and the final model was stratified on the non-proportional predictors.

**CHAPTER I: INSULIN-LIKE GROWTH FACTOR 2 EXPRESSION MODULATES
TAXOL RESISTANCE AND IS A CANDIDATE BIOMARKER FOR REDUCED
DISEASE-FREE SURVIVAL IN OVARIAN CANCER**

Gloria S. Huang, **Jurriaan Brouwer-Visser**, Marissa J. Ramirez, Christine H. Kim, Tiffany M. Hebert, Juan Lin, Hugo Arias-Pulido, Clifford R. Qualls, Eric R. Prossnitz, Gary L. Goldberg, Harriet O. Smith, and Susan Band Horwitz

Clin Cancer Res. American Association for Cancer Research; 2010 Jun 1;16(11):2999–3010.

Published OnlineFirst April 19, 2010; DOI:10.1158/1078-0432.CCR-09-3233

Cancer Therapy: Preclinical

**Clinical
Cancer
Research**

**Insulin-like Growth Factor 2 Expression Modulates Taxol
Resistance and Is a Candidate Biomarker for Reduced
Disease-Free Survival in Ovarian Cancer**

Gloria S. Huang^{1,3,5}, Jurriaan Brouwer-Visser^{1,3}, Marissa J. Ramirez³, Christine H. Kim¹, Tiffany M. Hebert², Juan Lin⁴, Hugo Arias-Pulido⁶, Clifford R. Qualls⁷, Eric R. Prossnitz⁸, Gary L. Goldberg^{1,5}, Harriet O. Smith^{1,5}, and Susan Band Horwitz^{3,5}

Abstract

Purpose: This study was undertaken to examine the role of the insulin-like growth factor (IGF) signaling pathway in the response of ovarian cancer cells to Taxol and to evaluate the significance of this pathway in human epithelial ovarian tumors.

Experimental design: The effect of Taxol treatment on AKT activation in A2780 ovarian carcinoma cells was evaluated using antibodies specific for phosphorylated AKT. To study the drug-resistant phenotype, we developed a Taxol-resistant cell line, HEY-T30, derived from HEY ovarian carcinoma cells. *IGF2* expression was measured by real-time PCR. An IGF1R inhibitor, NVP-AEW541, and *IGF2* siRNA were used to evaluate the effect of IGF pathway inhibition on proliferation and Taxol sensitivity. IGF2 protein expression was evaluated by immunohistochemistry in 115 epithelial ovarian tumors, and analyzed in relation to clinical/pathologic factors using the Chi-square or Fisher's exact tests. The influence of *IGF2* expression on survival was studied with Cox regression.

Results: Taxol-induced AKT phosphorylation required IGF1R tyrosine kinase activity and was associated with upregulation of *IGF2*. Resistant cells had higher *IGF2* expression compared with sensitive cells, and IGF pathway inhibition restored sensitivity to Taxol. High IGF2 tumor expression correlated with advanced stage ($p < 0.001$) and tumor grade ($p < 0.01$), and reduced disease-free survival ($p < 0.05$).

Conclusions: IGF2 modulates Taxol resistance, and tumor IGF2 expression is a candidate prognostic biomarker in epithelial ovarian tumors. IGF pathway inhibition sensitizes drug-resistant ovarian carcinoma cells to Taxol. Such novel findings suggest that IGF2 represents a therapeutic target in ovarian cancer, particularly in the setting of Taxol resistance.

Statement of Translational Relevance

Elucidation of biological factors underlying drug resistance is critical for developing more effective treatments for ovarian cancer. Activation of the serine-threonine kinase, AKT, which promotes cellular survival, occurs following Taxol treatment; however, the upstream signaling events have not been thoroughly investigated. In this study, we examined the role of the insulin-like growth factor (IGF) signaling pathway in the response of ovarian cancer cells to Taxol. Taxol-induced AKT phosphorylation required IGF1R activity, and was associated with upregulation of *IGF2*. Resistant cells exhibited increased *IGF2* mRNA compared with sensitive cells. IGF pathway inhibition, by IGF1R blockade or *IGF2* depletion, restored Taxol sensitivity. High IGF2 expression in ovarian tumors was associated with advanced stage and high grade; patients with high IGF2 tumor expression had reduced disease-free survival. Thus, IGF2 modulates Taxol-resistance, and its expression correlates with poor prognosis in patients. These novel findings suggest that IGF2 is a therapeutic target for ovarian cancer.

Introduction

The high mortality rate of ovarian cancer is due to treatment failure in the setting of recurrent/progressive disease that is unresponsive to chemotherapy. Elucidation of the biological factors underlying drug resistance is critical for the development of more effective treatment.

Exposure to diverse chemotherapeutic agents induces alterations in gene expression and in signaling cascades that can mediate resistance. Identifying and targeting these cell-specific adaptive responses represents a rational approach to the development of novel drug combination treatment strategies to circumvent resistance.

The widely used chemotherapeutic agent Taxol is indicated for first-line and subsequent treatment of ovarian carcinoma. Upon associating with its specific binding site on β -tubulin in the microtubule polymer, Taxol stabilizes microtubules and alters their dynamic properties, thereby perturbing their normal function in spindle assembly, cell division, motility, intracellular trafficking and signaling (Schiff *et al*, 1979; Horwitz, 1994; Rao *et al*, 1995; Parekh *et al*, 1997; Giannakakou *et al*, 2002; Jordan & Wilson, 2004). Several mechanisms of Taxol resistance have been identified, including overexpression of the transporter p-glycoprotein, alterations in tubulin, and aberrant signal transduction pathways and/or cell death pathways (Orr *et al*, 2003). Despite these discoveries, there remains a critical need for the development of effective strategies to overcome clinical Taxol-resistance.

We and others have shown that Taxol exposure can activate proliferative and anti-apoptotic signaling pathways in cancer cells. For example, cell-specific activation of ERK activity has been observed after Taxol treatment (McDaid & Horwitz, 2001). In cells that exhibit Taxol-induced ERK activation, MAPK pathway inhibitors potentiate Taxol response in vitro and in vivo (McDaid *et al*, 2005). Activation of the serine-threonine kinase, AKT, which promotes cellular survival, has also been observed following Taxol treatment of ovarian cancer cells (Mabuchi *et al*, 2002). However, the upstream signaling events that initiate Taxol-induced AKT activation have not been thoroughly investigated.

Ovarian carcinoma cells grown in tissue culture secrete insulin-like growth factor 2 (IGF2) and express its major receptor, the Type 1 IGF receptor (IGF1R), suggesting a role for autocrine/paracrine IGF2-IGF1R signaling in these cells (Gotlieb *et al*, 2006). The IGF1R is a transmembrane tyrosine kinase receptor that undergoes autophosphorylation upon binding of either IGF1 or IGF2, leading to tyrosine kinase activation. Activated IGF1R initiates an anti-apoptotic signaling cascade mediated by increased phosphatidylinositol 3-kinase (PI3K) activity, resulting in activation of the downstream anti-apoptotic effector, AKT (Dudek *et al*, 1997; Kulik *et al*, 1997). The IGF1R pathway is an attractive candidate for targeted therapy, and several small molecules and antibodies that specifically inhibit the IGF1R are undergoing clinical evaluation and may be approved for use in the clinic (Rodon *et al*, 2008).

For these reasons, the present study was undertaken, to our knowledge the first to examine the role of the IGF signaling pathway in the cellular response of ovarian cancer cells to Taxol treatment, as well as the first to measure IGF2 protein expression in a sizable cohort of patients with epithelial ovarian tumors. We report the novel finding that Taxol-induced AKT

phosphorylation occurs in an IGF1R-dependent manner, and is associated with upregulation of *IGF2* mRNA expression. Furthermore, in order to study the drug resistant phenotype, we developed a cell line model of acquired Taxol resistance and compared these cells with the parental, chemo-sensitive cell line. The Taxol-resistant cells exhibit significant upregulation of *IGF2* gene expression. IGF pathway inhibition, by IGF1R blockade or *IGF2* depletion, restores sensitivity to Taxol in these resistant cells. Furthermore, we assessed IGF2 protein expression levels by immunohistochemistry in 115 primary human epithelial ovarian tumors. High *IGF2* expression was significantly associated with invasive carcinoma and disease progression, and correlated with shortened interval to disease recurrence. Thus, IGF2 is identified for the first time to be a crucial mediator of Taxol resistance in ovarian carcinoma cells, and its expression in primary epithelial ovarian tumors is associated with poor prognostic factors for recurrence; these findings offer significant potential for clinical application.

Results

Activation of AKT by Taxol

The effect of Taxol treatment on AKT activation in A2780 cells was evaluated by immunoblot analysis. Initially, a dose response experiment was performed to evaluate a range of Taxol concentrations (1, 5, and 50 nM). The 5 nM concentration produced the largest effect on AKT phosphorylation at 24 hours (data not shown); therefore, subsequent experiments utilized this drug concentration. As shown in Figure 1, Taxol (5 nM) treatment for 24 hours resulted in increased AKT phosphorylation at the critical residues for activation, Threonine 308 and

Serine 473. The mean fold-change in phosphorylation level after Taxol treatment, compared with basal phosphorylation level, was 8.5-fold and 2-fold, for Threonine 308 and Serine 473, respectively. ERK phosphorylation was not appreciably altered by Taxol treatment in these cells (data not shown).

To determine whether Taxol-induced AKT phosphorylation is dependent on IGF1R activation, the small molecule IGF1R tyrosine kinase inhibitor NVP-AEW541 (Novartis Pharma AG, Basel, Switzerland) was used. With regard to selectivity, NVP-AEW541 is a 27-fold more potent inhibitor of the IGF1R kinase compared with inhibition of the insulin receptor kinase, over 50-fold more potent compared with inhibition of c-Kit, and over 100-fold more potent compared with inhibition of HER1, PDGFR, and Bcr-Abl (14). We evaluated a range of concentrations of NVP-AEW541 (0.1 to 10 μ M) for the ability to disrupt IGF1R signaling in ovarian carcinoma cells. NVP-AEW541 at 1 μ M effectively abrogates IGF2-induced IGF1R autophosphorylation and downstream AKT phosphorylation, and this concentration was used for subsequent experiments (Supplemental Figure S1).

Shown in Figure 1, Taxol-induced AKT phosphorylation was inhibited by concurrent treatment with the IGF1R inhibitor NVP-AEW541. Our results indicate that Taxol treatment results in increased AKT phosphorylation, and that phosphorylation of AKT due to Taxol treatment requires IGF1R tyrosine kinase activity.

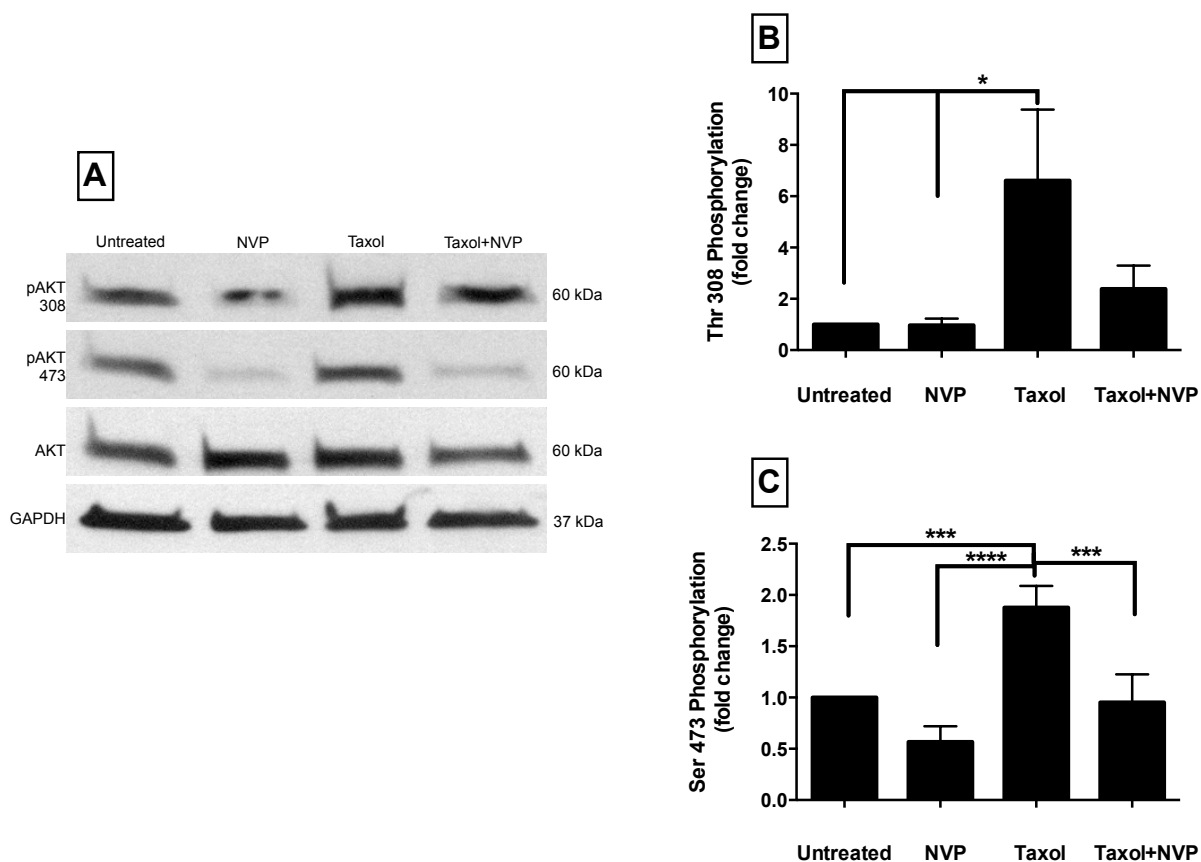


Figure 1. Effect of Taxol treatment on AKT phosphorylation

A2780 cells were maintained in complete media containing 10% fetal bovine serum and treated for 24 h with Taxol (5 nM), NVP-AEW541 (1 μ M), or both drugs concurrently. Immunoblotting was done to determine the effect of Taxol treatment on AKT phosphorylation. A, representative immunoblots are shown for phospho-AKT (pAKT; Thr308) and phospho-AKT (Ser473), along with the corresponding total AKT and glyceraldehyde-3-phosphate dehydrogenase (GAPDH) immunoblots.

B, the relative level of AKT phosphorylation at Thr308, as determined by densitometry, is shown in the graph. Columns, mean of four independent experiments; bars, SE. *, $P < 0.05$, one-way ANOVA, Dunnett post test.

C, the relative level of AKT phosphorylation at Ser473, as determined by densitometry, is shown in the graph. Columns, mean of seven independent experiments; bars, SE. **, $P < 0.01$, one-way ANOVA, Dunnett post test.

IGF2 regulation by Taxol

To investigate whether the observed IGF1R activation is mediated by autocrine signaling, the effect of Taxol treatment on the expression of *IGF1* mRNA and *IGF2* mRNA was quantified in A2780 cells. A dose response experiment was performed to evaluate the effect of different Taxol concentrations (1, 5, 20, and 50 nM) on *IGF2* mRNA levels. Concordant with the immunoblot results, Taxol 5 nM produced the greatest increase in *IGF2* mRNA expression (data not shown). Following Taxol treatment (5 nM), *IGF2* mRNA levels progressively increased over 24 hours (Figure 2A). In contrast, cells treated with baccatin III, an inactive Taxol analog which does not bind to or stabilize microtubules (He *et al*, 2000), did not alter *IGF2* mRNA levels compared with untreated cells. *IGF1* mRNA expression was unchanged after Taxol treatment (data not shown).

To evaluate whether treatment with other cytotoxic compounds induces *IGF2* mRNA expression, A2780 cells were treated for 24 hours with each of several microtubule-interacting drugs and other compounds at their approximately equipotent drug concentrations (as determined by SRB proliferation assays), and *IGF2* mRNA levels were measured (Figure 2B). Treatment with the microtubule-stabilizing agent ixabepilone (10 nM), an epothilone compound with a chemical structure distinct from Taxol, resulted in an increase in *IGF2* mRNA expression, to a similar degree as Taxol. However, treatment with discodermolide (20 nM), also a microtubule-stabilizing agent but with a more complex mechanism of action (Klein *et al*, 2005; Huang *et al*, 2006), did not significantly induce *IGF2* mRNA at this time point. Treatment with the microtubule-destabilizing agent vinblastine (5 nM) or the DNA-intercalating agent doxorubicin (50 nM) did not result in significant *IGF2* upregulation. These

findings suggest that *IGF2* upregulation by Taxol does not occur as a generalized response to cytotoxic drugs, but may require a specific interaction with microtubules that is shared between Taxol and ixabepilone.

Evaluation of paired sensitive and resistant HEY ovarian cancer cells

The Taxol resistant cell line, HEY-T30, was developed in our laboratory by repeated exposure of HEY ovarian carcinoma cells to Taxol. Like A2780 cells, HEY ovarian carcinoma cells exhibit upregulation of *IGF2* mRNA levels following Taxol treatment for 24 hours (Figure 2C). The Taxol resistant HEY-T30 cells exhibit significantly elevated *IGF2* mRNA levels compared with the parental HEY cells (Figure 2D). Under either normal growth or serum starvation conditions, constitutive IGF1R phosphorylation is observed in HEY-T30 cells whereas parental HEY cells do not exhibit constitutive IGF1R phosphorylation (Supplemental Figure S2). Cross-resistance to cisplatin, a platinum DNA-damaging chemotherapy drug, is not observed in HEY-T30 cells (Supplemental Figure S3).

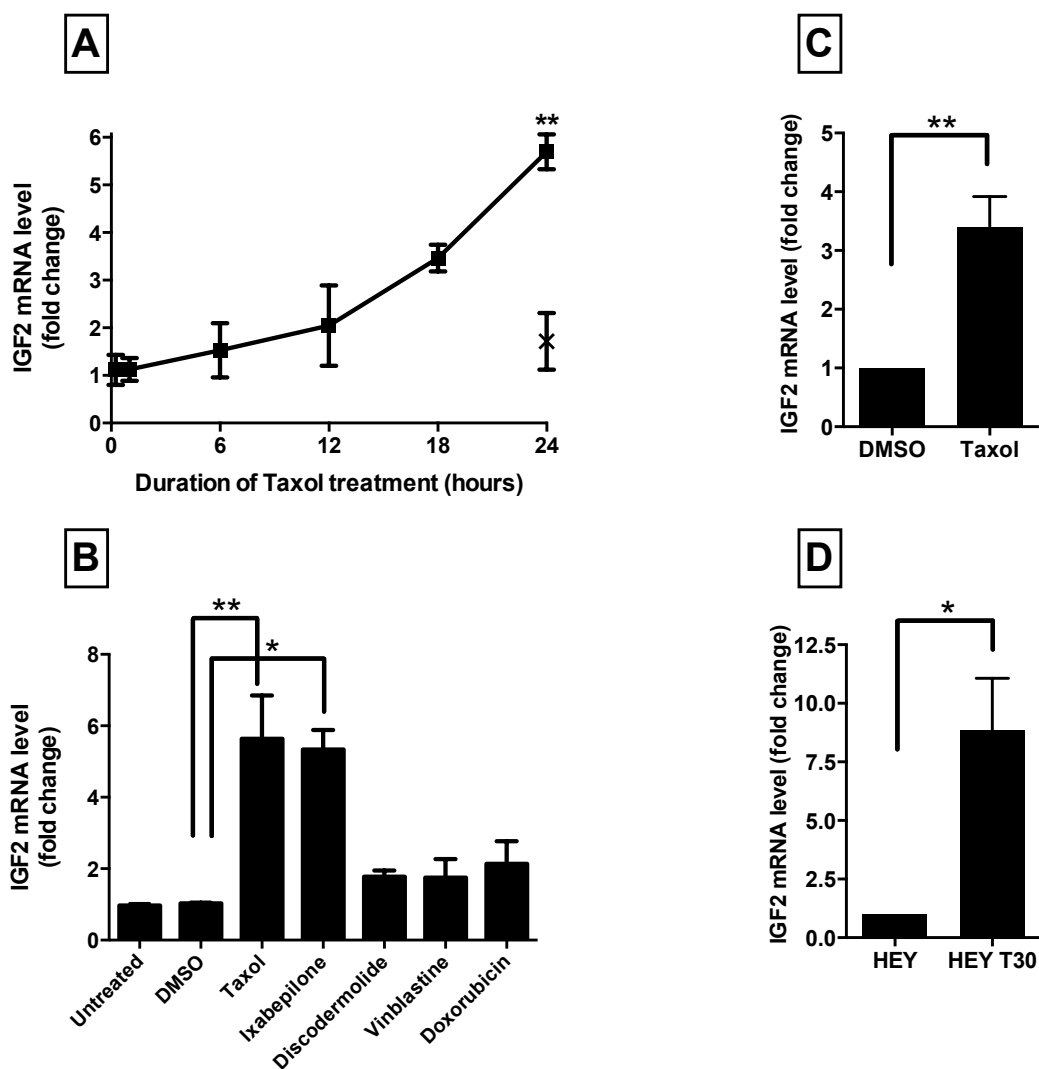


Figure 2. Taxol-induced *IGF2* mRNA expression

A, the time course of *IGF2* expression following Taxol treatment (5 nM) in A2780 cells is depicted with squares and a solid connecting line. The *IGF2* mRNA level after baccatin treatment (5 nM) for 24 h is also shown on the graph, marked by an X. Points, mean of two independent experiments, each done in triplicate; bars, SE. **, $P < 0.01$ paired two-tailed t-test. B, A2780 cells were treated for 24 h with vehicle alone (DMSO) or with cytotoxic drugs at their equipotent molar concentrations. The *IGF2* mRNA level is expressed as fold change relative to untreated cells. Columns, mean of two independent experiments, each done in triplicate; bars, SE. *, $P < 0.05$; **, $P < 0.01$, one-way ANOVA, Dunnett post test. C, HEY cells were treated with vehicle alone (DMSO) or Taxol (5 nM) for 24 h. The *IGF2* mRNA level, determined by reverse transcription quantitative real-time PCR, is expressed as fold change relative to untreated cells in complete growth medium. Columns, mean of three independent experiments, each done in triplicate; bars, SE. **, $P < 0.01$, t test.

D, *IGF2* mRNA expression in Taxol-resistant HEY-T30 cells, determined by reverse transcription quantitative real-time PCR, is expressed as fold change relative to HEY parental cells. Columns, mean of three independent experiments, each done in triplicate; bars, SE. *, $P < 0.05$, t test.

The Taxol concentration that results in 50% growth inhibition (IC_{50}) for parental and resistant cells is shown in Figure 3. We next assessed whether inhibition of IGF1R alters Taxol sensitivity in HEY and HEY-T30 cells. The growth inhibition resulting from combination drug treatment with Taxol and concurrent NVP-AEW541 was evaluated and compared with the effect of either drug alone (Figure 3). As in the previous experiment, NVP-AEW541 was used at a concentration of 1 μ M, a concentration which effectively blocks IGF1R phosphorylation. As a single agent, NVP-AEW541 (1 μ M) alone had a minimal effect on cell growth in either cell line. In the parental HEY cells, treatment with NVP-AEW541 (1 μ M) modestly potentiated the effect of Taxol. In these cells, the IC_{50} for Taxol is 2.6 nM; however in the presence of NVP-AEW541, it is 1.7 nM. The potentiation of Taxol efficacy by NVP-AEW541 in the resistant HEY-T30 cells was more dramatic. In the resistant cells, the IC_{50} for Taxol is 106 nM, while in the presence of NVP-AEW541, it decreases to 17 nM, representing a greater than 6-fold sensitization to Taxol. Thus, IGF1R inhibition was efficacious in sensitizing ovarian cancer cells to Taxol in this model of acquired drug resistance.

We have evaluated three additional ovarian carcinoma cell lines made resistant to Taxol and other microtubule-stabilizing agents (MSA) in our laboratory. As determined by SRB assay, the A2780-Tx15 cell line is 20-fold resistant to Taxol, the HEY-BMS20 cell line is 3-fold resistant to ixabepilone, and the OVCAR8-D30 cell line is 2-fold resistant to discodermolide. Each of these resistant cell lines is significantly sensitized to MSA treatment by concurrent IGF1R inhibition using 1 μ M NVP-AEW541.

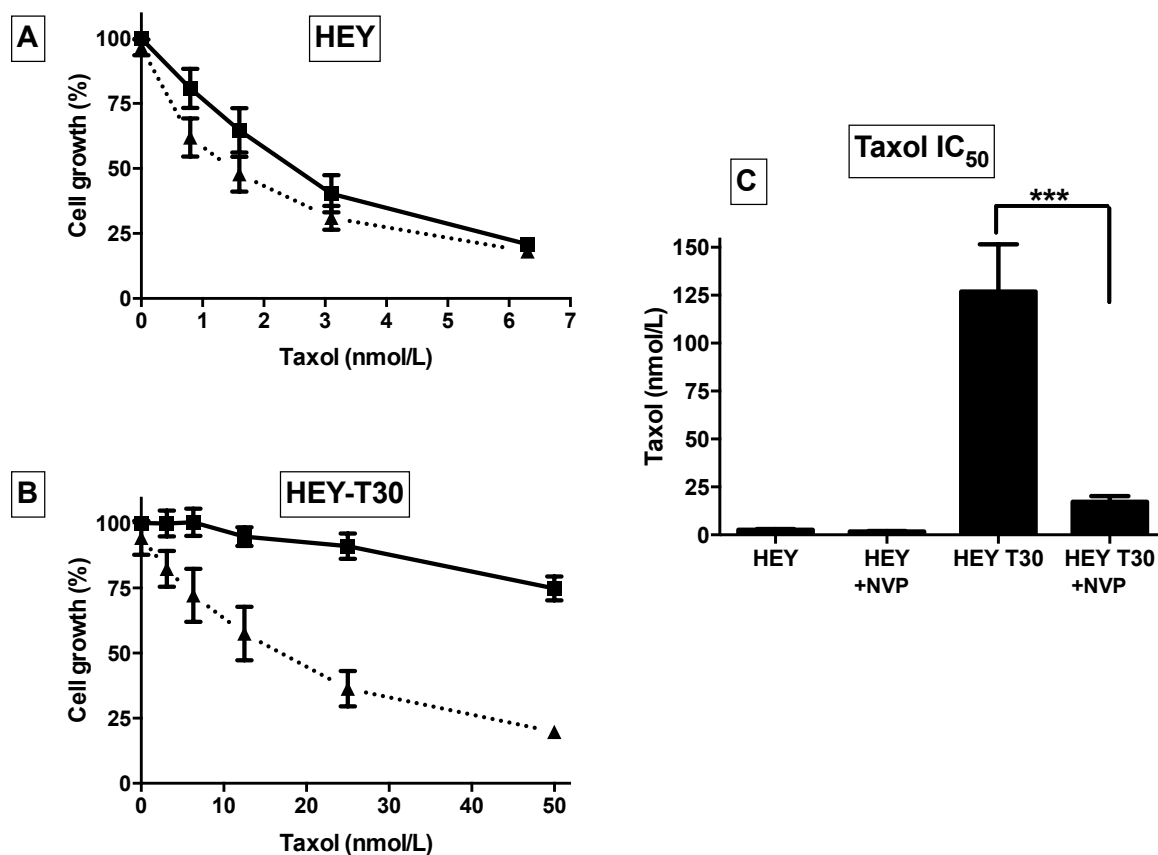


Figure 3. Potentiation of Taxol treatment by the IGF1R inhibitor NVP-AEW541

Cytotoxicity assays for HEY and HEY-T30 ovarian carcinoma cells were done using the SRB method to determine the effect of Taxol treatment alone or with concurrent NVP-AEW541. A, HEY parental cells: the cell number relative to untreated cells, expressed as cell growth (%), is plotted over a range of Taxol concentrations. Treatment with Taxol alone is depicted with squares and solid lines, compared with combination treatment with Taxol plus NVP-AEW541 1 μ M, depicted with triangles and dotted lines. The cell growth (%) resulting from NVP-AEW541 (1 μ M) alone is plotted on the Y axis (triangle). $P < 0.05$, two-way ANOVA. B, HEY-T30 resistant cells: the cell number relative to untreated cells, expressed as cell growth (%), is plotted over a range of Taxol concentrations, as in A. The cell growth (%) resulting from NVP-AEW541 (1 μ M) alone is plotted on the Y axis (triangle). $P < 0.001$, two-way ANOVA.

C, for each cell line, the IC₅₀ concentration of Taxol alone or with concurrent NVP-AEW541 (1 μ M) is plotted in the bar graph. Columns, mean of at least three independent experiments with six replicates each; bars, SE. $P < 0.0001$, one-way ANOVA, Bonferroni post test.

***IGF2* knockdown in Taxol-resistant cells**

IGF1R inhibition would be expected to block signaling transduced not only by IGF2 but also by IGF1 ligand-binding. Therefore, to determine whether inhibition of IGF2-transduced signaling alone is sufficient to sensitize ovarian cancer cells to Taxol, *IGF2* depletion by siRNA was examined. The parental HEY cells and the Taxol-resistant HEY-T30 cells were transfected with *IGF2*-siRNA or control-siRNA. As determined by real-time PCR, the efficacy of *IGF2* mRNA knockdown by *IGF2* siRNA was decreased by approximately 90% at 48 and 96 hours; immunoblotting confirmed that IGF2 protein expression was decreased by approximately 70% by *IGF2* siRNA treatment (Supplemental Figure S4). For each cell line, the proliferation and the sensitivity of the *IGF2*-depleted cells to Taxol was compared with control-siRNA transfected cells. In parental HEY cells (Figure 4A), *IGF2* depletion does not significantly affect the cell growth nor does it significantly potentiate the effect of Taxol in these cells, compared with control-siRNA transfection. In contrast, the effect of *IGF2* depletion in the resistant HEY-T30 cells is substantial (Figure 4B). Unlike IGF1R inhibition, which alone minimally affects cellular proliferation of HEY-T30 cells, *IGF2* depletion by siRNA robustly suppressed cellular proliferation. The relative cell number following *IGF2*-siRNA transfection was 27% compared with control-siRNA transfected cells, corresponding to an approximately 4-fold reduction in cell number ($p < 0.01$). Treatment of *IGF2*-depleted HEY-T30 cells using approximately the IC_{50} concentration of Taxol (100 nM) was highly efficacious. As shown in Figure 4B, IGF2-siRNA plus Taxol treatment resulted in 10% cell growth after a 72 hour incubation, compared with 45% cell growth following control-siRNA plus Taxol treatment ($p < 0.05$).

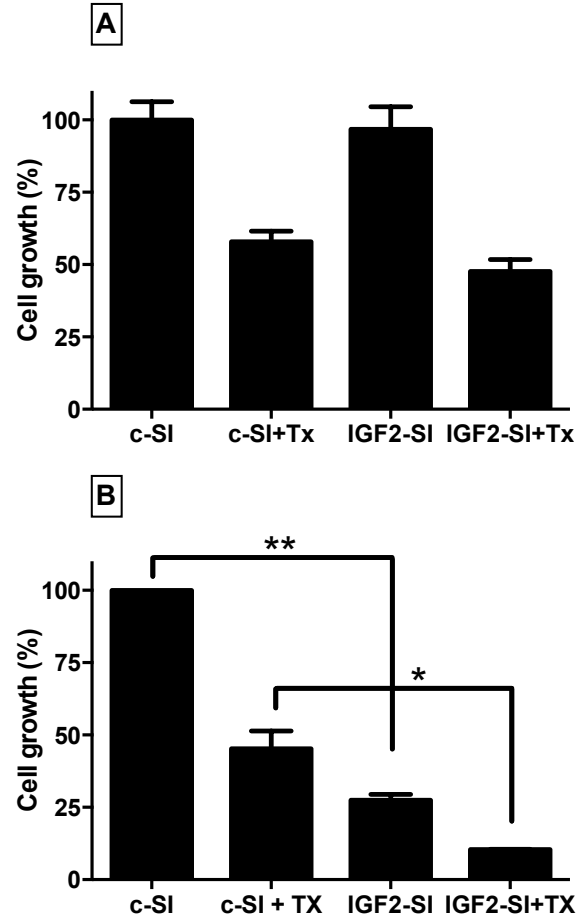


Figure 4. Effect of *IGF2* depletion by siRNA transfection in HEY and HEY-T30 cells

IGF2 siRNA transfection was used to evaluate the effect of *IGF2* depletion on cell proliferation and Taxol (Tx) sensitivity. Cells were transfected with *IGF2* siRNA (IGF2-SI) or control siRNA (c-SI). Twenty-four hours after transfection, cells were counted, reseeded, and incubated for an additional 72 h, with or without the addition of Taxol at the IC_{50} concentration of Taxol for each cell line, followed by cell counting. Cell numbers are expressed as % cell growth relative to DMSO-treated, control siRNA-transfected cells. Columns, mean of two independent experiments, each done in triplicate for HEY parental cells (A) and HEY-T30 cells (B); bars, SE. *, $p < 0.05$; **, $p < 0.01$, one-way ANOVA, Bonferroni post test.

To determine additivity, according to the definition of Bliss, $Taxol + IGF2-SI - Taxol * IGF2-SI \Rightarrow 0.55 + 0.73 - 0.55 * 0.73 = 0.88$; When treated together, the fraction affected was 0.90.

Therefore, the combination treatment of Taxol and *IGF2* knockdown with siRNA was slightly greater than additive at this concentration.

IGF2 expression in epithelial ovarian tumors

To assess the potential clinical application of these findings, IGF2 protein expression was analyzed in primary ovarian tumors. The clinical and pathologic characteristics of the study population are shown in Table 1. Thirty-six (31.3%) patients had epithelial ovarian tumors of low malignant potential (LMP) while 79 (68.7%) had invasive epithelial ovarian carcinoma (EOC). Patients with EOC were older ($p=0.001$) and were more likely to have advanced stage disease ($p<0.001$). The distribution of histologic types differed between the LMP and EOC groups ($p<0.001$). In the EOC group, serous histology (55.7%) was the most frequent histology. Mucinous histology was more frequent in the LMP group than in the EOC group (47.2% versus 13.9%).

Representative tissue sections of benign and malignant clinical specimens demonstrating a range of IGF2 protein expression, with corresponding H-scores noted in the figure legends, are shown in Figure 5. Positive and negative control sections used for quality assurance are shown in supplemental Figure S5. To assess potential batch effects and biological variation due to tissue sampling, a second tissue microarray was used that included distinct tissue cores from 53 tumors from the original study population. The correlation of IGF2 H-scores from the two independently constructed and stained tissue microarrays was high (Spearman Rank correlation, $R=0.664$).

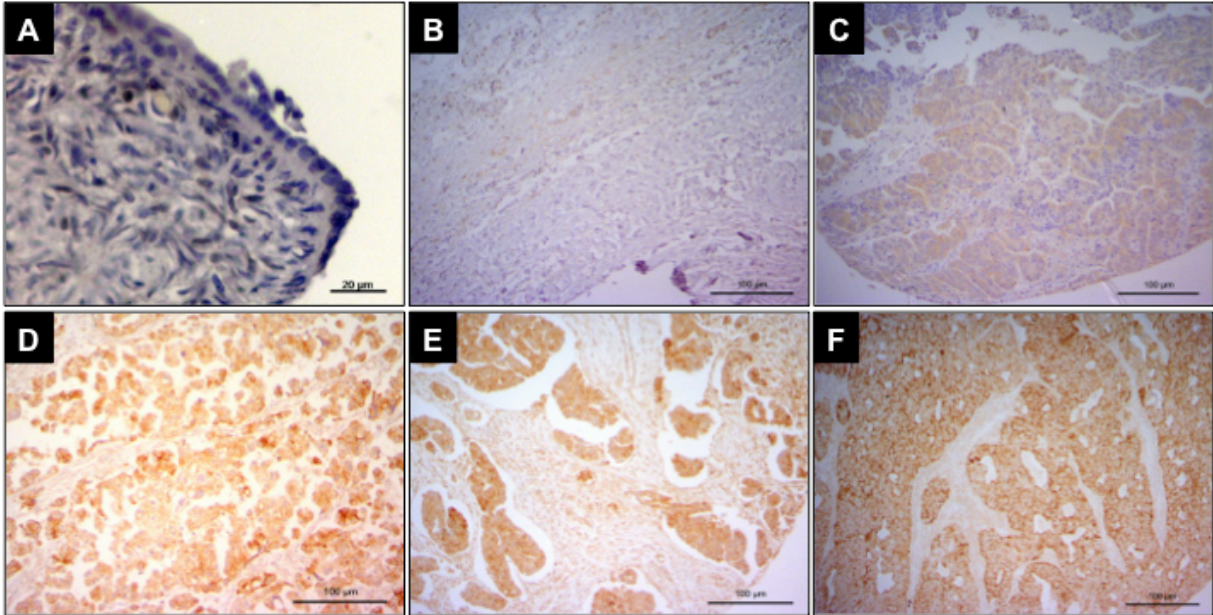


Figure 5. Representative images of IGF2 immunohistochemical staining

A, absence of staining in the surface epithelium of a normal ovary. Magnification, $\times 40$

B, extremely low staining in a stage I mucinous borderline tumor (H-score = 0.5).

Magnification, $\times 10$

C, low staining in a stage III, grade 1 serous carcinoma (H-score = 75). Magnification, $\times 10$

D, medium staining in a stage III, grade 3 serous carcinoma (H-score = 100). Magnification, $\times 10$

E, high staining in a stage III, grade 3 adenocarcinoma, not otherwise specified (H-score = 250). Magnification, $\times 10$

F, high staining in a stage III, grade 3 serous carcinoma (H-score 300). Magnification, $\times 10$

Table 1. Characteristics of the study population

Variable	LMP N	(%)	EOC N	(%)	Total N	(%)	p
Age							0.001
≤ 50 years	22	61.1	23	29.1	45	39.1	
> 50 years	14	38.9	56	70.9	70	60.9	
Race/Ethnicity							0.142
Non-Hispanic White	21	58.3	36	45.6	57	49.6	
Hispanic	11	30.6	28	35.4	39	33.9	
American Indian	2	5.6	14	17.7	16	13.9	
Black	1	2.8	1	1.3	2	1.7	
Asian	1	2.8	0	0.0	1	0.9	
FIGO Stage							<0.001
I	32	88.9	24	30.4	56	48.7	
II	2	5.6	7	8.9	9	7.8	
III	2	5.6	38	48.1	40	34.8	
IV	0	0.0	10	12.7	10	8.7	
Histology							<0.001
Serous	17	47.2	44	55.7	61	53.0	
Mucinous	17	47.2	11	13.9	28	24.3	
Endometrioid	0	0.0	6	7.6	6	5.2	
Other	2	5.6	18	22.8	20	17.4	
Grade							N/A
0	36	100.0	0	0.0	36	31.3	
1	0		12	15.2	12	10.4	
2	0		19	24.1	19	16.5	
3	0		48	60.8	48	41.7	
Total	36		79		115		

LMP, epithelial ovarian tumors of low malignant potential; EOC, invasive epithelial ovarian carcinoma; Race/ethnicity as defined by SEER coding; N/A, not applicable.

Table 2 depicts the association of IGF2 expression with selected clinical and pathologic variables. IGF2 tumor expression was not correlated with age or ethnicity. Shown in Figure 6A, IGF2 expression was significantly associated with FIGO stage, with higher expression in advanced stage tumors compared with early stage tumors ($p < 0.001$). The histological subtypes demonstrated distinct patterns of expression (Figure 6B): mucinous tumors had lower IGF2 expression compared with serous or endometrioid tumors ($p = 0.011$). Shown in Figure 6C, IGF2 expression varied significantly with tumor grade, with higher expression observed in invasive epithelial ovarian cancers compared with borderline ovarian tumors ($p = 0.003$). On univariate survival analysis (Figure 6D), high IGF2 expression was significantly associated with reduced disease-free survival ($p = 0.03$). Age ($p = 0.02$), grade ($p < 0.0001$), stage ($p < 0.0001$), extent of cytoreduction ($p < 0.0001$), and performance status ($p = 0.0002$), and chemotherapy ($p = 0.0002$), but not race or histology, were risk factors associated with disease-free survival on univariate analysis. When LMP tumors were excluded from the analysis, the association of IGF2 expression and disease-free survival was no longer statistically significant (Figure 6E). On multivariate analysis, stage ($p = 0.001$), extent of cytoreduction ($p = 0.002$), and grade ($p = 0.04$) were independently associated with disease-free survival.

With regard to overall survival, there have been 29 deaths. There have been 12 deaths (among 60 patients; 20%) in the low IGF2 group, compared with 17 deaths (among 55 patients; 31%) in the high IGF2 group; the effect of IGF2 expression on overall survival was not significant on univariate analysis ($p = 0.19$). Age ($p = 0.005$), grade ($p < 0.0001$), stage ($p < 0.0001$), extent of cytoreduction ($p < 0.0001$), performance status ($p < 0.0001$), and chemotherapy ($p = 0.009$) were

risk factors associated with overall survival on univariate analysis. For multivariate analysis, stratification by grade (LMP vs EOC) was performed, as no deaths occurred in the LMP group. On multivariate survival analysis, stage ($p=0.007$), extent of cytoreduction ($p=0.001$), and chemotherapy ($p=0.0003$) were independently associated with overall survival.

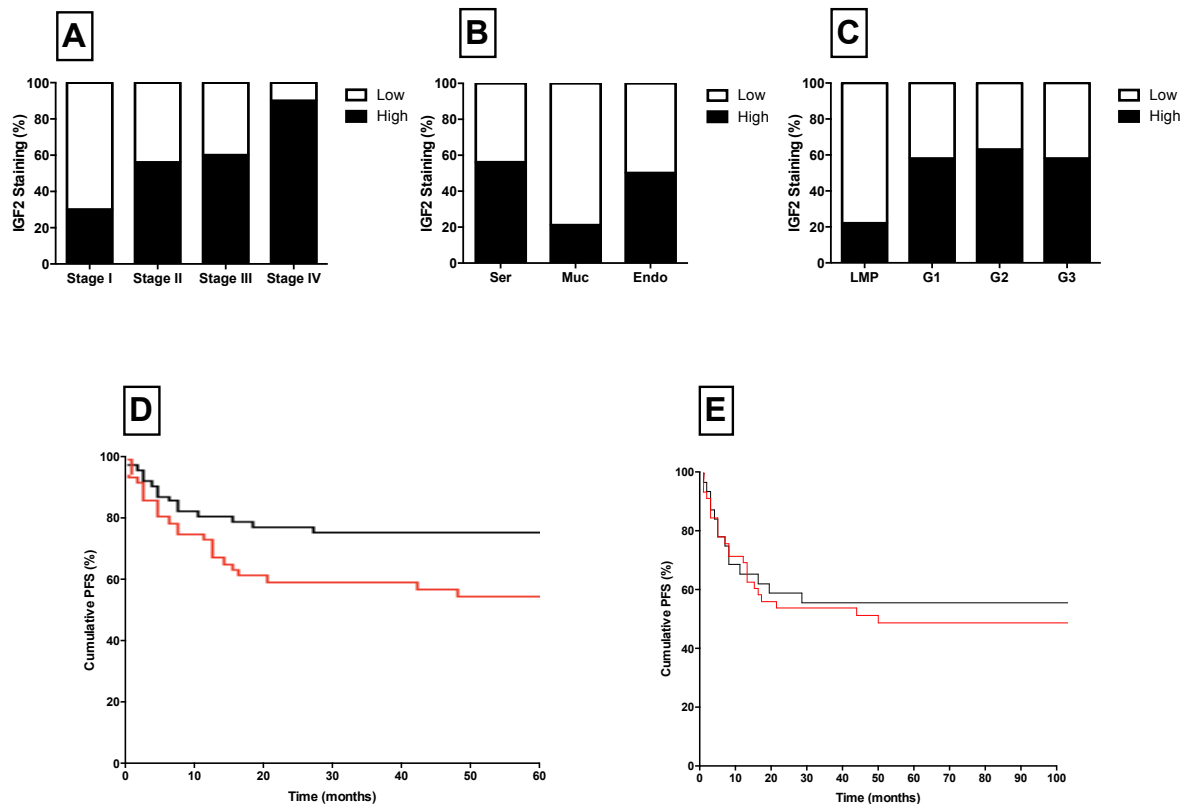


Figure 6. Correlation between IGF2 expression and clinicopathologic factors in ovarian tumors

A, IGF2 staining is correlated with FIGO stage, with higher frequency of IGF2 overexpression in advanced-stage tumors. $P < 0.001$, Fisher's exact test.

B, serous (Ser) and endometrioid (Endo) histologic types are correlated with high IGF2 staining compared with mucinous (Muc) tumors. $P = 0.011$, χ^2 test.

C, IGF2 staining is correlated with tumor grade, with LMP (borderline) tumors showing the lowest frequency of IGF2 overexpression. $P = 0.003$, Fisher's exact test.

D, patients with high IGF2 expression (red line) had a significant reduction in progression-free survival (PFS) compared with patients with low IGF2 expression (black line). $P = 0.03$, log-rank test.

E, when LMP tumors are excluded from the analysis, the association of IGF2 expression and progression-free survival is not statistically significant.

Table 2. IGF2 expression in LMP tumors and epithelial ovarian carcinoma (EOC)

Variable	LMP tumors (36)				EOC (79)				Totals (115)						
	IGF2-Low N	(%)	IGF2-High N	(%)	p	IGF2-Low N	(%)	IGF2-High N	(%)	p	IGF2-Low N	(%)	IGF2-High N	(%)	p
Age					1.000					0.873					0.335
≤ 50 years	17	60.7	5	62.5		9	28.1	14	29.8		26	43.3	19	34.5	
> 50 years	11	39.3	3	37.5		23	71.9	33	70.2		34	56.7	36	65.5	
Race/Ethnicity					0.544					0.339					0.166
Non-Hispanic White	15	53.6	6	75.0		12	37.5	24	51.1		27	45.0	30	54.6	
Hispanic	10	35.7	1	12.5		14	43.8	14	29.8		24	40.0	15	27.3	
American Indian	1	3.6	0	0.0		1	3.1	0	0.0		6	10.0	10	18.2	
Black	1	3.6	1	12.5		5	15.6	9	19.1		2	3.3	0	0.0	
Asian	1	3.6	0	0.0		0	0.0	0	0.0		1	1.7	0	0.0	
FIGO Stage					0.028					0.124					<0.001
I	27	96.4	5	62.5		12	37.5	12	25.5		39	65.0	17	30.9	
II	0	0.0	2	25.0		4	12.5	3	6.4		4	6.7	5	9.1	
III	1	3.6	1	12.5		15	46.9	23	48.9		16	26.7	24	43.6	
IV	0	0.0	0	0.0		1	3.1	9	19.1		1	1.7	9	16.4	
Histology					0.055					0.664					0.011
Serous	10	35.7	7	87.5		17	53.1	27	57.4		27	45.0	34	61.8	
Mucinous	16	57.1	1	12.5		6	18.8	5	10.6		22	36.7	6	10.9	
Endometrioid	0	0.0	0	0.0		3	9.4	3	6.4		3	5.0	3	5.5	
Other	2	7.1	0	0.0		6	18.8	12	25.5		8	13.3	12	21.8	
Tumor Grade					N/A					0.933					0.003
0	28	100	8	100.0		0	0.0	0	0.0		28	46.7	8	14.6	
1	0	0.0	0	0.0		5	15.6	7	14.9		5	8.3	7	12.7	
2	0	0.0	0	0.0		7	21.9	12	25.5		7	11.7	12	21.8	
3	0	0.0	0	0.0		20	62.5	28	59.6		20	33.3	28	50.9	
Total	28		8			32		47			60		55		

LMP, epithelial ovarian tumors of low malignant potential; EOC, invasive epithelial ovarian carcinoma; Race/ethnicity as defined by SEER coding; N/A, not applicable. IGF2-Low, H-score≤105; IGF2-High, H-score>105

Discussion

This study is the first, to our knowledge, to evaluate the role of the IGF signaling pathway in the response of ovarian carcinoma cells to Taxol. Our findings demonstrate that Taxol treatment results in upregulation of *IGF2* expression associated with activation of AKT. As shown in a cell line model of acquired drug resistance in ovarian carcinoma, Taxol-resistance is associated with elevated *IGF2* expression, while IGF1R inhibition or *IGF2* depletion restores drug sensitivity. In clinical tumor specimens, high IGF2 protein expression is significantly associated with poor prognostic factors for recurrence and death.

The pyrrolo[2,3-d]pyrimidine compound NVP-AEW541 used in this study, and the closely related compound NVP-ADW742, were the first IGF1R-specific small molecule tyrosine kinase inhibitors reported in the literature (García-Echeverría *et al*, 2004; Mitsiades *et al*, 2004). Using doses corresponding to specific inhibition of the IGF1R tyrosine kinase, we demonstrated that NVP-AEW541 effectively blocks Taxol-induced AKT phosphorylation. Although NVP-AEW541 alone did not suppress proliferation in ovarian carcinoma cells, treatment with NVP-AEW541 significantly potentiated the effect of Taxol in both sensitive and resistant cells. While the compound NVP-AEW541 is not undergoing clinical development at this time, a variety of small molecule inhibitors and monoclonal antibodies that target the IGF1R are presently undergoing evaluation in clinical trials, and it is anticipated that one or more of these compounds may be approved for use in the clinic (Rodon *et al*, 2008).

An alternate therapeutic strategy is to target the aberrantly expressed ligand, rather than its receptor. As IGF2 has been shown to bind not only the IGF1R, but also the insulin receptor isoform A and hybrid IGF1R-insulin receptors, signaling by IGF2 could potentially circumvent the IGF1R in the presence of IGF1R-specific inhibitors (Pandini *et al*, 2002; Sciacca *et al*, 2002). In the present study, the combination of IGF2 depletion and Taxol was found to be highly effective at inhibiting cell growth in the setting of acquired drug resistance. Interestingly, IGF2 depletion alone resulted in potent suppression of proliferation distinct from the minimal anti-proliferative effect of IGF1R inhibition. The potent effect of IGF2 depletion suggests possible dependency on IGF2 for proliferation in these Taxol-resistant cells.

Previously, it was reported that PI3K and AKT inhibition could enhance sensitivity to Taxol (Hu *et al*, 2002; Mabuchi *et al*, 2002; Luo *et al*, 2005). As PI3K/AKT are major downstream effectors of IGF1R activity, the concordant effects resulting from blockade at downstream targets in the IGF signaling cascade validates the findings of the present study. From a clinical perspective, significant metabolic toxicity has been encountered with direct AKT inhibition (Luo *et al*, 2005), highlighting a potential disadvantage to blockade at the downstream intracellular targets where multiple signaling pathways converge. Targeting a specific ligand-cell surface receptor may reduce these undesired effects on the physiology of normal cells.

However, targeting at the receptor level, such as IGF1R or EGFR inhibition, has been shown to promote activation of the reciprocal receptor in cancer cell lines via crosstalk mechanisms (Haluska *et al*, 2008). Thus, it is likely that optimal combination treatment strategies will require consideration of compensatory feedback signals that occur in a cell-specific manner.

In the clinic, multi-drug resistance is a hallmark of progressive ovarian cancer. In addition to Taxol, platinum compounds are widely used in the treatment of primary and recurrent ovarian cancer. Interestingly, it was recently reported that IGF1R inhibition may restore drug sensitivity in platinum-resistant ovarian cancer cells (Eckstein *et al*, 2009). Another study demonstrated activity of an IGF1R-targeting antibody in a fluorouracil-resistant colorectal carcinoma cell line (Dallas *et al*, 2009). With regard to tubulin-targeting agents, resistance to the microtubule stabilizing agent docetaxel was associated with predicted PI3K pathway activation, by gene expression profiling, in a variety of carcinoma cell lines (Potti *et al*, 2006). These studies, in conjunction with the present study, strongly support the relevance of the IGF pathway to chemotherapy resistance.

IGF2 upregulation has been implicated in carcinogenesis and disease progression in ovarian cancer. Previous studies utilized a gene expression microarray approach to identify *IGF2* mRNA to be significantly over-expressed in ovarian cancer compared with benign ovary (Sawiris *et al*, 2002; Lancaster *et al*, 2004). In addition, high *IGF2* mRNA expression was associated with advanced stage, high grade, and poor survival in a cohort of patients with serous epithelial ovarian cancer (Sayer *et al*, 2005). Interestingly, IGF2 protein levels in the serum of patients with ovarian cancer were decreased compared with unaffected women (Mor *et al*, 2005; Visintin *et al*, 2008). The present study is, to our knowledge, the first to evaluate the significance of IGF2 expression at the protein level in ovarian tumors from patients.

Consistent with the prior mRNA expression studies, high IGF2 protein expression was observed more frequently in patients with advanced stage and high-grade tumors, and was associated with clinical/pathologic predictors of worse prognosis. In the study sample,

approximately half of the tumors were serous histology, which is the most common type of epithelial ovarian cancer; however, early stage cancer, less common histological types, and LMP tumors were also present at relatively high proportions in this cohort. Based on our findings, subsequent studies should prospectively evaluate IGF2 protein expression in primary and recurrent epithelial ovarian tumors for evaluation of its utility as a potential biomarker, and to confirm its frequent overexpression in ovarian cancer. If IGF2 is found to be a useful biomarker, the standard methods used for IGF2 immunohistochemistry in this study are within the capability of many surgical pathology laboratories and therefore readily translatable to clinical application.

In summary, activation of autocrine IGF signaling occurs following Taxol treatment of ovarian carcinoma cells, and is observed in association with the acquisition of Taxol resistance.

Inhibition of the IGF signaling pathway significantly potentiates Taxol efficacy and sensitizes drug-resistant cells. In primary ovarian tumors, high IGF2 expression is strongly associated with known clinicopathologic risk factors, including stage and grade, and its overexpression is associated with reduced disease-free survival. These findings strongly support the clinical relevance of the IGF pathway in ovarian cancer, and suggest a potential therapeutic role for inhibitors of this pathway in the management of this disease.

Acknowledgements

We acknowledge the use of the Genomics Shared Resource and the Analytical Imaging Facility of the Albert Einstein Cancer Center, supported by the National Cancer Institute Cancer Center Support Grant (2P30CA013330). The authors would like to thank Drs. Charles R. Key and Mary Lipscomb, Co-Directors of the Human Tissue Repository at the University of New Mexico Hospital/Cancer Center, supported by the National Cancer Institute Cancer Center Support Grant (P30 CA118110), for providing tissue samples and clinical data. The authors appreciate helpful discussions with Drs. Chia-Ping Huang Yang and Hayley McDaid.

Supplemental Figures

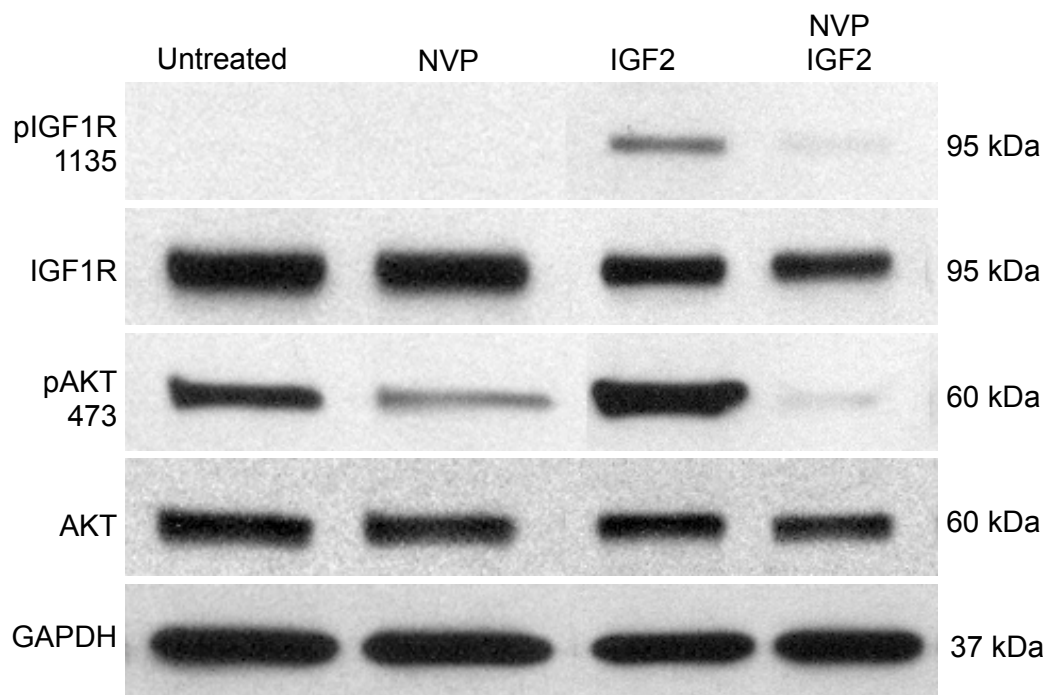


Figure S1. Inhibition of IGF1R by NVP-AEW541

A2780 cells were serum-deprived for 24 hours then treated as indicated prior to preparation of cell lysates as described in the methods. Lane 1: untreated, unstimulated cells; Lane 2: cells were treated with NVP-AEW541 (1 μ M) 45 minutes prior to harvesting; Lane 3: cells were stimulated with IGF2 (50 ng/mL) 15 minutes prior to cell lysate preparation; Lane 4: cells were treated with NVP-AEW541 (1 μ M) 45 minutes prior to harvesting and stimulated with IGF2 (50 ng/mL) 15 minutes prior to harvesting. Immunoblotting was performed as described in the methods. As shown in the representative immunoblots, NVP-AEW541 (1 μ M) abrogates IGF2-stimulated IGF1R phosphorylation and AKT phosphorylation.

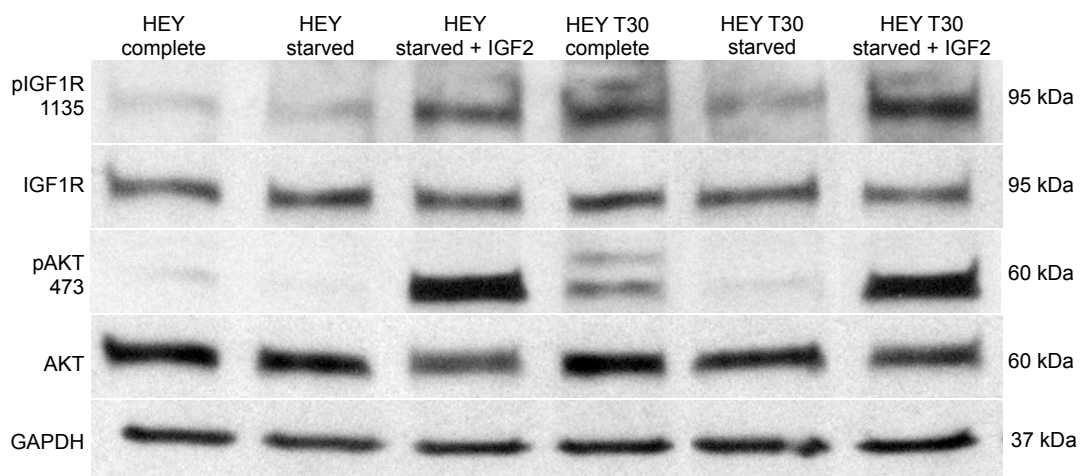


Figure S2. Constitutive IGF1R activation in HEY-T30 cells

HEY and HEY-T30 cell lysates were prepared under conditions of growth in complete media, serum-deprivation for 24 hours, or serum-deprivation followed by IGF2 (50 ng/mL) stimulation for 10 minutes prior to harvesting. Preparation of cell lysates and immunoblotting are described in the methods. As shown in the representative immunoblots, phosphorylation of IGF1R and AKT are increased in the Taxol-resistant HEY-T30 cells compared to HEY parental cells.

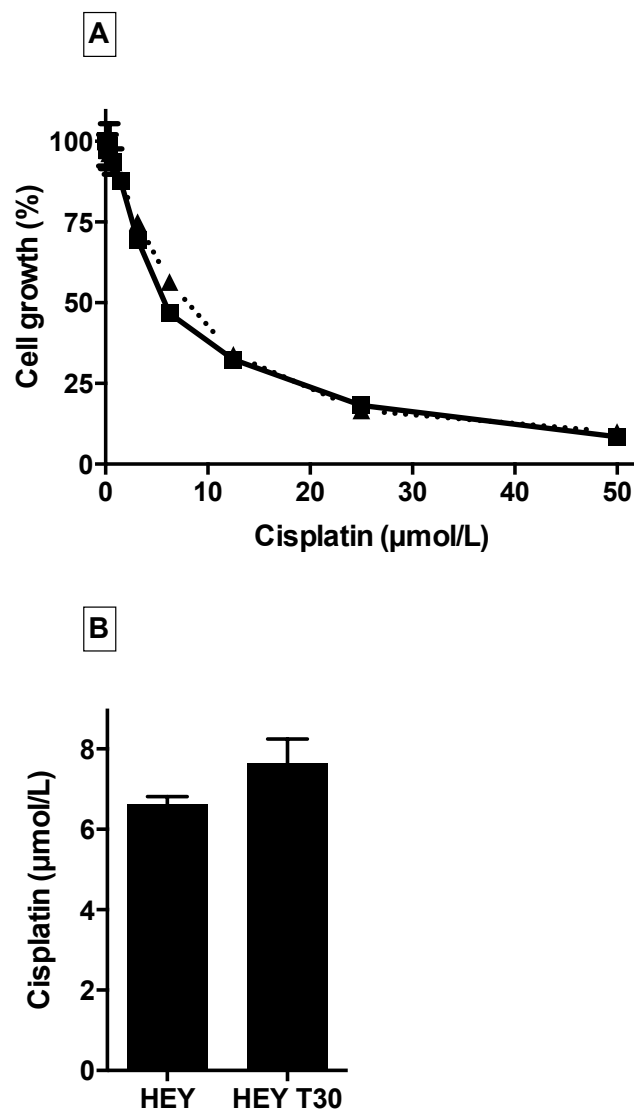


Figure S3. Evaluation of cisplatin cytotoxicity in HEY and HEY-T30 cells

A. Cytotoxicity assays were performed using the sulforhodamine B method to determine the effect of cisplatin treatment in HEY (squares; solid connecting lines) and HEY-T30 cells (triangles; dotted connecting line). The cell number relative to untreated cells, expressed as cell growth (%), is plotted over a range of cisplatin concentrations.

B. The IC₅₀ concentrations of cisplatin in HEY and HEY-T30 cells Taxol are shown in bar graph (mean \pm SE; 3 independent experiments with 6 replicates each).

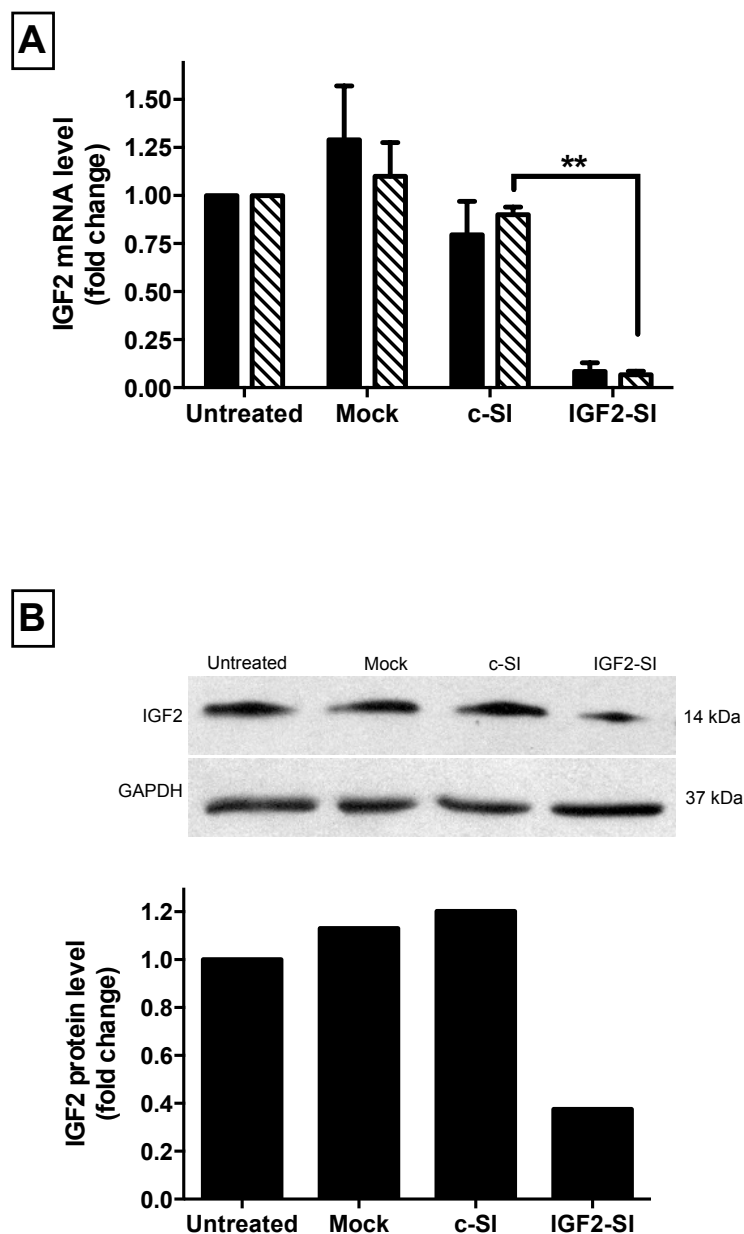


Figure S4. *IGF2* depletion by siRNA transfection in HEY-T30 cells

A. As determined by quantitative real-time PCR, *IGF2* mRNA levels at 48 hours (solid bar) and 96 hours (cross-hatched bar) are shown for mock-transfected, control siRNA-transfected, and *IGF2*-siRNA transfected HEY-T30 cells. Results are expressed as fold-change relative to untreated HEY-T30 cells (mean \pm SE; 3 independent experiments for 96 hours, **, $p < 0.01$, one-way ANOVA, Bonferroni post test).

B. The *IGF2* protein level was determined by immunoblotting. A representative experiment is shown, and the expression level determined by densitometry is shown in the accompanying bar graph.

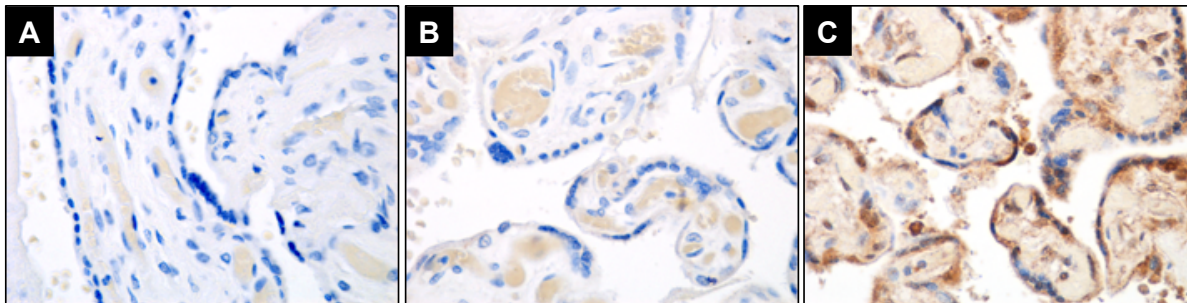


Figure S5. Quality control assays for IGF2 immunohistochemistry

A. Negative control placenta section: Primary antibody is omitted (antibody diluent is applied), followed by the identical staining procedure as used for the positive control section.

B. Negative control placenta section: The primary antibody to IGF2 (Abcam, ab9574) is pre-absorbed with recombinant IGF2 (Abcam, AB9575) at a 1:1 concentration, followed by the identical staining procedure as used for the positive control section.

C. Positive control placenta section: The primary antibody to IGF2 (Abcam, ab9574) is used at a 1:100 dilution (5 $\mu\text{g}/\text{mL}$) as described in the methods.

Positive and negative control sections are stained concurrently with experimental sections, as described in the methods.

CHAPTER II: INSULIN-LIKE GROWTH FACTOR 2 SILENCING RESTORES TAXOL SENSITIVITY IN DRUG RESISTANT OVARIAN CANCER

Jurriaan Brouwer-Visser, Jiyeon Lee, KellyAnne McCullagh, Maria J. Cossio, Yanhua Wang, Gloria S. Huang

PLoS ONE. Public Library of Science; 2014 Jun 16;9(6):e100165.

OPEN ACCESS Freely available online

 PLOS ONE

Insulin-Like Growth Factor 2 Silencing Restores Taxol Sensitivity in Drug Resistant Ovarian Cancer

Jurriaan Brouwer-Visser¹, **Jiyeon Lee**¹, **KellyAnne McCullagh**¹, **Maria J. Cossio**¹, **Yanhua Wang**², **Gloria S. Huang**^{1,3,4*}

Abstract

Drug resistance is an obstacle to the effective treatment of ovarian cancer. We and others have shown that the insulin-like growth factor (IGF) signaling pathway is a novel potential target to overcome drug resistance. The purpose of this study was to validate IGF2 as a potential therapeutic target in drug resistant ovarian cancer and to determine the efficacy of targeting IGF2 *in vivo*. An analysis of The Cancer Genome Atlas (TCGA) data in the serous ovarian cancer cohort showed that high *IGF2* mRNA expression is significantly associated with shortened interval to disease progression and death, clinical indicators of drug resistance. In a genetically diverse panel of ovarian cancer cell lines, the *IGF2* mRNA levels measured in cell lines resistant to various microtubule-stabilizing agents including Taxol were found to be significantly elevated compared to the drug sensitive cell lines. The effect of *IGF2* knockdown on Taxol resistance was investigated *in vitro* and *in vivo*. Transient *IGF2* knockdown significantly sensitized drug resistant cells to Taxol treatment. A Taxol-resistant ovarian cancer xenograft model, developed from HEY-T30 cells, exhibited extreme drug resistance, wherein the maximal tolerated dose of Taxol did not delay tumor growth in mice. Blocking the IGF1R (a transmembrane receptor that transmits signals from IGF1 and IGF2) using a monoclonal antibody did not alter the response to Taxol. However, stable *IGF2* knockdown using short-hairpin RNA in HEY-T30 effectively restored Taxol sensitivity. These findings validate IGF2 as a potential therapeutic target in drug resistant ovarian cancer and show that directly targeting IGF2 may be a preferable strategy compared with targeting IGF1R alone.

Introduction

Ovarian cancer is the leading cause of gynecologic cancer death in the United States. Since the mid-1990s, the standard treatment for ovarian cancer is surgical cytoreduction and systemic chemotherapy, usually Taxol and platinum (Vaughan *et al*, 2011). However, the majority of patients eventually succumb to recurrent, progressive disease due to resistance to chemotherapy.

In addition to its well-established roles in development and growth, aging, and carcinogenesis (Baker *et al*, 1993; Gallagher & LeRoith, 2011; Tazearslan *et al*, 2011; Pollak, 2012; Ratajczak *et al*, 2013), the insulin-like growth factor (IGF) signaling pathway has recently been implicated in drug resistance (Gotlieb *et al*, 2006; Eckstein *et al*, 2009; Huang *et al*, 2010; Ogawa *et al*, 2010; Sherman-Baust *et al*, 2011). As we previously reported, upregulation of

insulin-like growth factor 2 (IGF2) is an acute cellular response to Taxol treatment, and its expression modulates the response to Taxol in drug resistant ovarian cancer cell lines. (Huang *et al*, 2010). Since Taxol is used in the first-line treatment of ovarian cancer, we hypothesized that high IGF2 would be associated with intrinsic clinical drug resistance, manifesting as decreased time to disease progression/recurrence in patients. Supporting this hypothesis, our prior study using a tissue microarray approach indicated that high IGF2 expression in ovarian tumor tissue was indeed predictive of shortened interval to progression/recurrence.

Based on these laboratory and clinical data, we determined that IGF2 is a potential therapeutic target to ameliorate drug resistance in ovarian cancer, but to our knowledge, no prior *in vivo* validation studies have been done. Therefore, as described herein, we performed studies to evaluate if Taxol resistance could be overcome *in vivo* by targeting IGF2. We examined the impact of *IGF2* knockdown on not only Taxol's effects, but also the response to non-taxane microtubule interacting drugs, and other drugs commonly used in the treatment of ovarian cancer. To confirm the clinical relevance of our findings, an analysis of the serous ovarian cancer cohort of The Cancer Genome Atlas (TCGA) was done to evaluate the relation of *IGF2* expression and clinical outcomes.

Results

Our prior study of IGF2 protein expression using a tissue microarray of epithelial ovarian tumors indicated that high tissue expression levels of IGF2 were associated with a shortened interval to progression/recurrence (Huang *et al*, 2010). Since then, gene expression data from 489 clinically-annotated stage II-IV high-grade serous ovarian cancer samples of The Cancer

Genome Atlas project (TCGA) were made available through the cBioPortal for Cancer Genomics (Cancer Genome Atlas Research Network, 2011). Using this data portal, we tested a relationship of *IGF2* expression and intrinsic drug resistance, wherein high *IGF2* was defined as 1.6 SD above the mean, corresponding to 94-95th percentile in a normal distribution. By using this cut score, the size of the *IGF2*-high group approximates the fraction of ovarian cancer patients expected to have intrinsically drug resistant tumors, manifested by progression during or shortly after completing chemotherapy. In our analysis of the TCGA data, we indeed found that high *IGF2* mRNA expression in tumor tissue significantly correlated with a shortened interval to progression/recurrence, i.e. progression-free survival (Fig. 1A). Median progression-free survival in this group was <12 months, indicative of intrinsic drug resistance. High *IGF2* mRNA expression also correlated with significantly shortened overall survival (Fig. 1B). Multivariate analysis was not enabled by this data portal, however in our prior publication we noted an association of *IGF2* expression with higher stage and grade (Huang *et al*, 2010).

We previously showed that *IGF2* mRNA levels increase during acute Taxol treatment, and we hypothesized that upregulation of *IGF2* is associated with persistent surviving cells giving rise to drug resistant recurrent disease. To study drug resistance in the laboratory, Taxol, as well as non-taxane microtubule-stabilizing agents (MSAs), ixabepilone, discodermolide, and epothilone B, were used to develop six distinct resistant cell lines. As determined by real-time PCR, all MSA-resistant cell line models had elevated *IGF2* mRNA expression relative to their sensitive parental line (Fig 1C). Since Taxol is by far the most clinically used among these

drugs, subsequent experiments focused on the Taxol resistant cell lines HEY-T30 and A2780-T15.

We evaluated the drug resistant cell lines for other mechanisms of Taxol resistance (Duan *et al*, 2004; Stordal *et al*, 2012). HEY-T30 has *ABCB1* mRNA over expression (Fig. 1D) associated with genomic amplification of *ABCB1* (Fig. 1E), while HEY has no copy number change of *ABCB1*. These findings were confirmed by array comparative genomic hybridization (data not shown). A2780-T15 was selected in the presence of verapamil and does not overexpress *ABCB1* (Fig.1D), and neither A2780-T15 nor A2780 has DNA copy number change of *ABCB1* (Fig. 1E). We found no significant correlation between *IGF2* and *ABCB1* expression in our panel of cell lines (Fig. S3). DNA sequencing revealed that A2780-T15 has a mutation (Glycine at position 360 is changed to an Aspartic acid) in the Taxol-binding pocket of β -tubulin (Fig. S1A and S1B), while HEY-T30 does not have a mutation in β -tubulin.

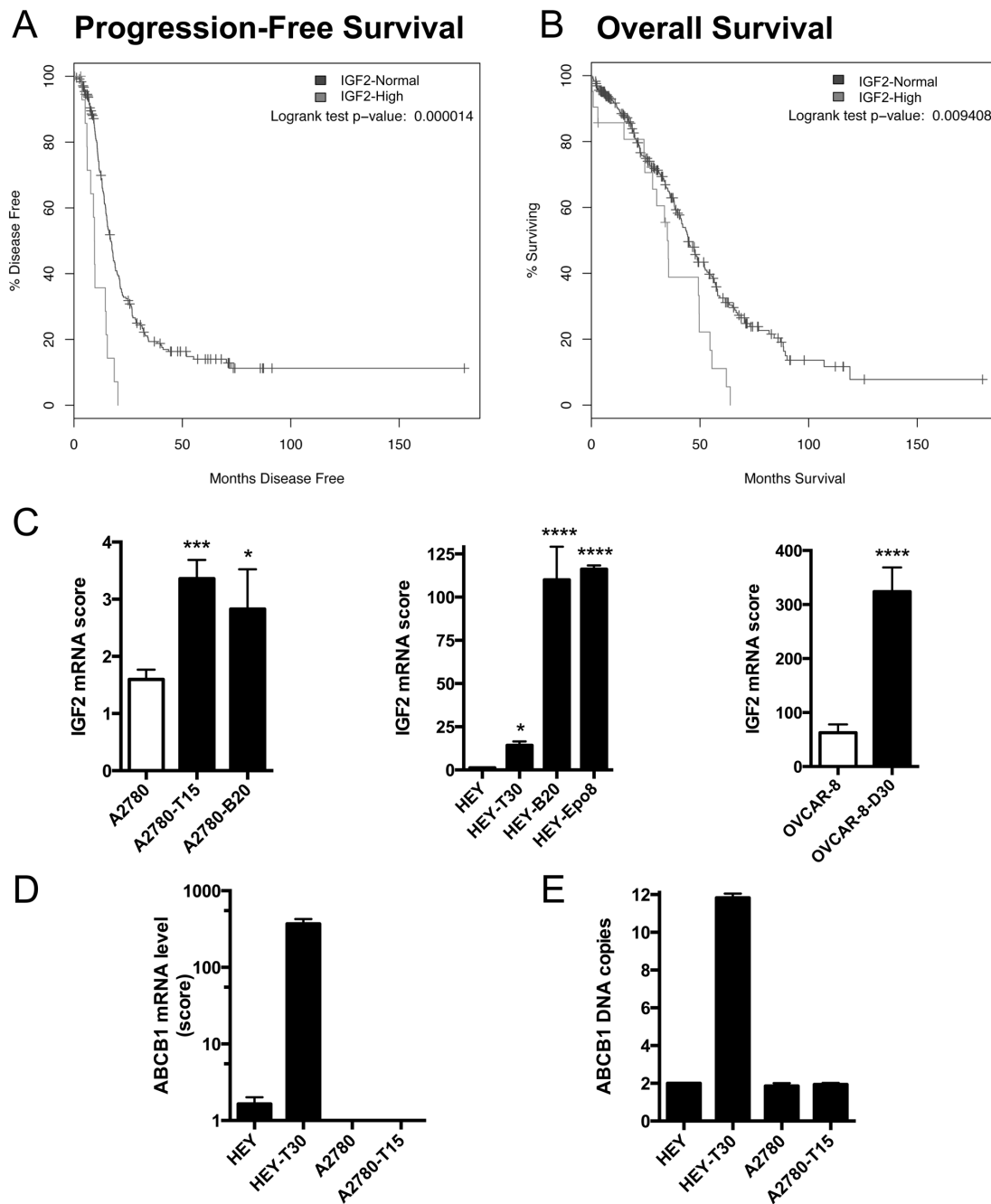


Figure 1

IGF2 expression and ovarian cancer survival

Using the cBioPortal for Cancer Genomics to analyze the data from the Cancer Genome Atlas study of ovarian serous cystadenocarcinoma, we compared the progression-free survival and overall survival in patients with high tumor levels of *IGF2* mRNA (greater than 1.6 standard deviations above the mean; gray line) and those with normal tumor levels of *IGF2* mRNA (all

other patients; black line). Patients with high *IGF2* mRNA levels had significantly shortened progression-free survival (A) and overall survival (B).

(C) **IGF2 expression in sensitive and resistant cell lines.** By RT-qPCR, we measured the IGF2 mRNA level in six drug resistant ovarian carcinoma cell lines and their three cell lines of origin. All drug resistant cell lines have significantly higher IGF2 mRNA expression compared to their sensitive cell line of origin. Bars show the mean \pm SEM of IGF2 mRNA expression score for at least two independent experiments for each cell line, each done in triplicate, and the symbol above the bar indicates the statistical significance comparing that resistant cell line with its parental counterpart; * $p < 0.05$, *** $p < 0.001$, **** $p < 0.0001$ by One-way ANOVA with Bonferroni posttest.

(D) ***ABCB1* expression.** *ABCB1* mRNA expression levels were measured by RT-qPCR in HEY, HEY-T30, A2780 and A2780-T15. HEY-T30 has higher *ABCB1* mRNA expression compared to the other cell lines. Bars show the mean \pm SEM of *ABCB1* mRNA expression score for at least four independent experiments for each cell line, each done in triplicate,

(E) ***ABCB1* DNA copy number.** By qPCR performed on genomic DNA, HEY-T30 has a six-fold increase in *ABCB1* DNA copy number indicating gene amplification. Bars show the mean \pm SEM of two independent experiments, each done in triplicate.

HEY-T30 proliferated similarly in Taxol-free media or media containing low concentrations of Taxol (≤ 30 nM) (Fig. 2A). A2780-T15 proliferated much more slowly in Taxol-free media than in media containing Taxol (≤ 15 nM) (Fig. 2B), suggesting possible Taxol dependent-growth associated with its β -tubulin mutation. When low-dose Taxol was present, A2780-T15 proliferated at a similar rate as A2780. The resistant cell lines showed cross-resistance to ixabepilone, an MSA that shares a common β -tubulin binding site with Taxol. Expanded profiling of HEY-T30 (Fig. 2C, left panel) showed resistance to the microtubule-destabilizing drug vinblastine and resistance to doxorubicin, but similar sensitivity to cisplatin, compared to parental HEY. A2780-T15 (Fig. 2C, right panel) was cross-resistant to both doxorubicin and CDDP, but was more sensitive to vinblastine. Hypersensitivity to microtubule-destabilizing drugs has been observed previously in another drug resistant cell line harboring a β -tubulin mutation that was associated with dependency on microtubule-stabilizing drugs for proliferation (He *et al*, 2001).

A critical step in translating laboratory findings into potential therapies for patients is to conduct *in vivo* testing using animal models. Since A2780-T15 cells were dependent on Taxol for their growth but HEY-T30 were not, we evaluated HEY-T30 as a xenograft model for *in vivo* testing of therapeutic strategies targeting drug resistance. We administered Taxol using the previously determined maximum-tolerated dose (MTD; cumulative dose of 100 mg/kg) (Huang *et al*, 2006) to evaluate drug resistance *in vivo*. Parental HEY xenograft growth was effectively suppressed by Taxol, indicating sensitivity to Taxol (Fig. 2D). In contrast, Taxol failed to inhibit HEY-T30 xenograft growth compared to vehicle (5% dextrose in water; D5W) treatment, indicating drug resistance (Fig. 2E).

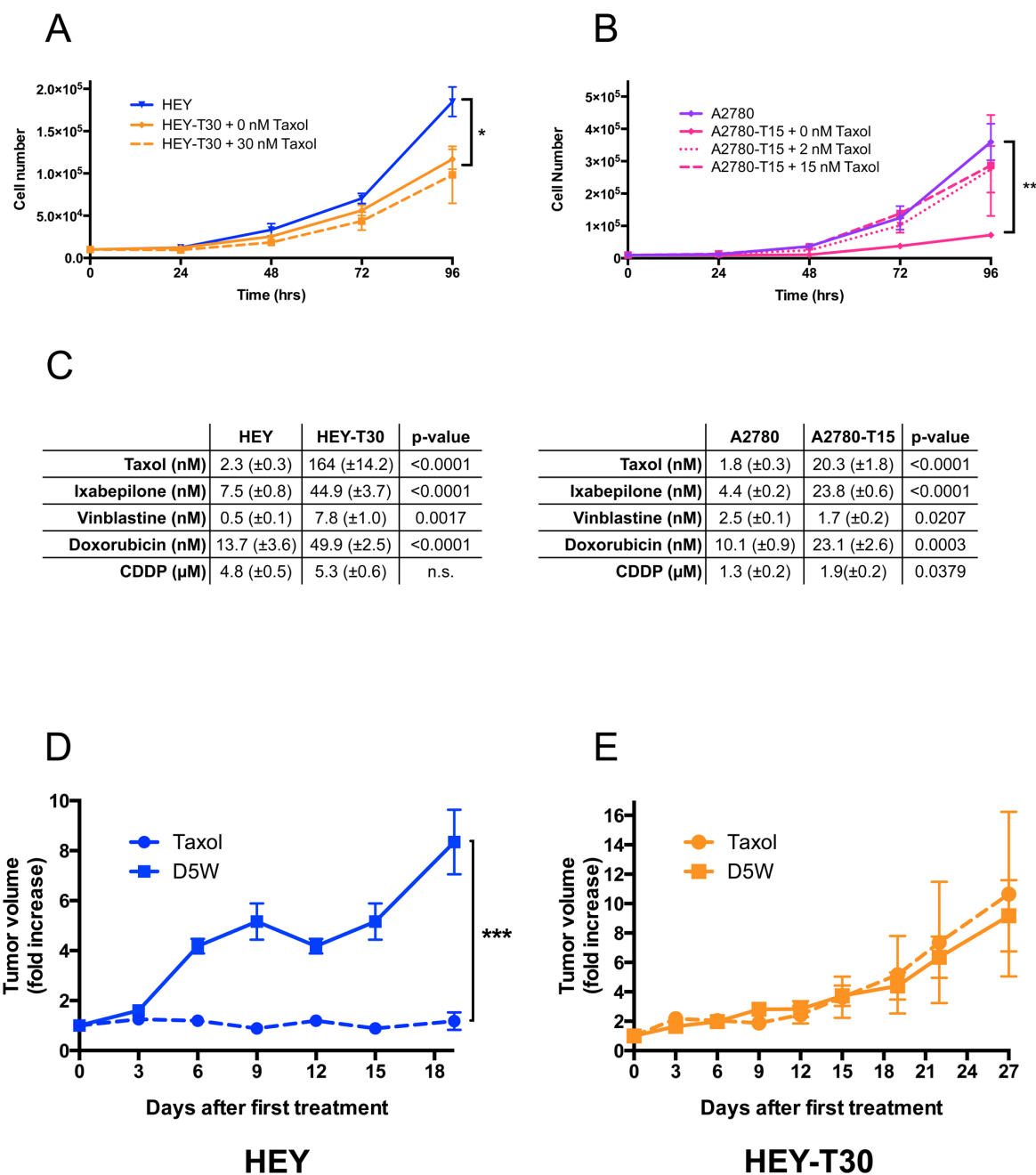


Figure 2

Proliferation kinetics of cell lines.

Cells were grown in complete media with the indicated concentration of Taxol in 6-well dishes, and cells from duplicate wells counted every 24 hours. (A) HEY-T30 cells in the presence or absence of 30 nM Taxol proliferate more slowly than HEY cells ($p < 0.05$, Repeated Measures Two-way ANOVA, Bonferroni posttest). (B) A2780-T15 in the presence of 2 nM and 15 nM Taxol grow similarly to A2780. However, in the absence of Taxol, A2780-T15

proliferates more slowly, suggesting Taxol dependence ($p < 0.01$, Two-way ANOVA, Bonferroni posttest). Each growth curve represents the mean of at least two independent experiments performed with duplicates, each point is represented as the mean \pm SEM.

(C) IC₅₀'s of chemotherapeutic drugs in sensitive and resistant cell lines. In 96-well plates, cells were treated with serial dilutions of the indicated drugs and the concentration of 50% proliferation inhibition (IC₅₀) determined using the SRB cytotoxicity assay. HEY-T30 are cross-resistant to ixabepilone and to vinblastine. There is modest cross-resistance to doxorubicin but not to CDDP. A2780-T15 are cross-resistant to ixabepilone, and modestly cross-resistant to doxorubicin and CDDP, but more sensitive to vinblastine. Data are presented as the mean \pm SEM of at least three independent experiments performed with six replicates. P-values calculated by unpaired t-test.

(D,E) Comparison of HEY-T30 and HEY xenograft response to Taxol. Following subcutaneous injection of HEY-T30 or HEY cells, mice were divided into treatment groups of 6 animals each. When the average xenograft volume reached 120 mm³, Taxol treatment was administered at the maximal tolerated dose (MTD) of 20 mg/kg intraperitoneally every three days for five treatments (treatment days: 0, 3, 6, 9, 12), resulting in a cumulative dose of 100 mg/kg. Control animals received intraperitoneal injections of the diluent (5% dextrose in water; D5W) according to the same schedule. Tumors were measured every three days, and mean tumor volumes \pm SEM for each group shown at each time point. HEY xenografts responded to Taxol treatment, which potently suppressed tumor growth (Fig. 2D; dashed blue line). HEY-T30 xenografts did not respond to Taxol treatment (Fig. 2E; dashed orange line) and grew at a similar rate as vehicle-treated HEY-T30 xenografts. HEY Taxol vs HEY D5W on day 19, $p < 0.001$; unpaired t-test.

To strategize how to target IGF2-mediated drug resistance, we examined receptor expression and activation in the drug resistant and sensitive cell lines. Previously published studies indicated that IGF2-binding induces autophosphorylation of IGF1R and the insulin receptor isoform A, IR-A (Beauchamp *et al*, 2010; Greenall *et al*, 2013), resulting in receptor activation and downstream signaling to effector molecules such as AKT. In addition, high IR-A/IGF1R expression was associated with resistance to anti-IGF1R therapies, as signaling through IR-A can circumvent dependency on IGF1R (Ulanet *et al*, 2010). We determined that *IGF1R* mRNA expression was higher in HEY and HEY-T30, compared with A2780 and A2780-T15, without significant differences between the paired sensitive and resistant lines (Fig. 3A). As shown in Fig. 3B, *IR-A* levels were lower in HEY and HEY-T30 compared to A2780 and A2780-T15. Real time PCR data was also analyzed with correction for differences in amplification efficiency between primer sets (Table S1), with similar findings. By Western blot, IGF1R and IR protein expression corresponded to mRNA levels (data not shown). Thus, HEY and HEY-T30 had lower IR-A/IGF1R ratios than A2780 and A2780-T15.

Receptor activation and downstream signaling induced by IGF2 was evaluated.

Phosphorylation of IGF1R increased over 5-fold after IGF2 or insulin stimulation in HEY-T30 (Fig. 3C upper panel). Much smaller changes (<1.5-fold) were observed in IR phosphorylation compared to IGF1R phosphorylation levels after IGF2 or insulin stimulation of HEY-T30 (Fig. 3C lower panel). Downstream, we observed increased phosphorylation of AKT at serine 473 and threonine 308 after IGF2 or insulin stimulation, but no changes in ERK phosphorylation (Fig. 3D). Equal protein loading was confirmed by both Ponceau staining of the membrane and incubation with a GAPDH antibody. IGF2-stimulated phosphorylation of IGF1R and

AKT were potently inhibited by either the small molecule IGF1R inhibitor NVP-AEW541 or the anti-IGF1R monoclonal antibody IMC-A12.

Compared to HEY and HEY-T30, A2780 and A2780-T15 had significantly higher *IR-A* expression (Fig. 3B). In A2780-T15, IGF2 or insulin stimulation significantly increased phosphorylation of both IGF1R and IR (Fig. 3E). NVP-AEW541 inhibited phosphorylation of IGF1R and IR. IMC-A12 inhibited IGF2-induced IGF1R phosphorylation, while having minimal effect on IGF2-induced IR phosphorylation, indicating specificity for IGF1R. Downstream, NVP-AEW541 inhibited IGF2-mediated AKT and ERK phosphorylation, while IMC-A12 did not (Fig. 3F).

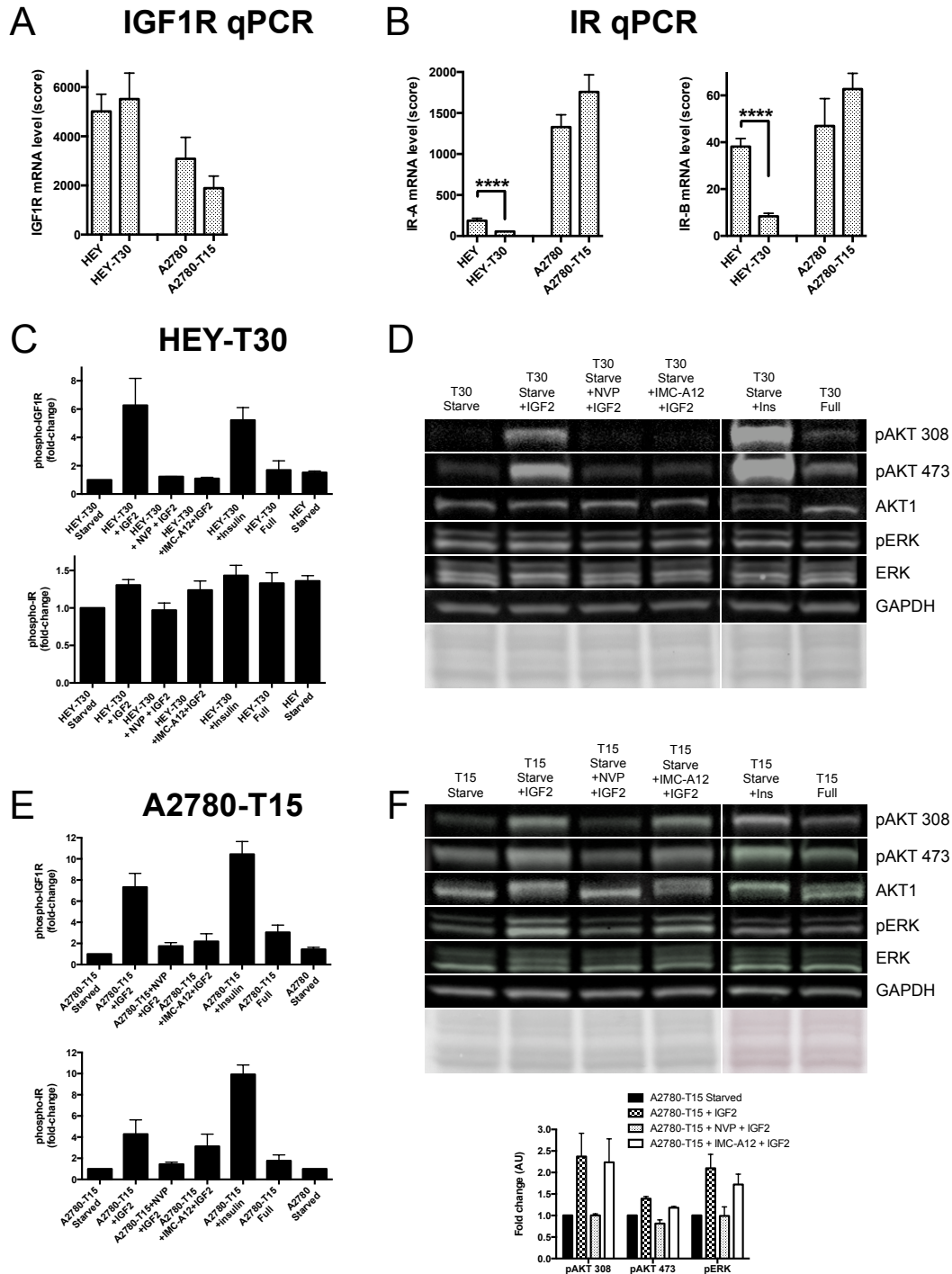


Figure 3

(A) *IGF1R* mRNA of sensitive and resistant cell lines. Measured by RT-qPCR (n=5 independent experiments each done in triplicate), *IGF1R* mRNA levels are similar when resistant cell lines are compared to their parental cell lines of origin. Bars show the mean \pm SEM.

(B) **IR mRNA of sensitive and resistant cell lines.** Measured by RT-qPCR (n=5 independent experiments each done in triplicate) *IR-A* and *IR-B* mRNA levels in HEY-T30 are significantly decreased when compared to HEY, while similar levels are observed when comparing A2780-T15 to A2780. Bars show the mean \pm SEM, **** $p < 0.0001$; unpaired t-test.

(C) **Phospho-IGF1R and phospho-IR ELISA in HEY-T30.** Cells were starved overnight, incubated with 1 μ M NVP-AEW541 or 10 μ g/ml IMC-A12 for 2 hours, stimulated with 50 ng/ml IGF2 or 50 nM insulin for 10 minutes, lysed, and levels of phosphorylated IGF1R and IR determined by ELISA. Both IGF2 and insulin caused 5- to 6-fold-change increased levels of phospho-IGF1R that could be suppressed by NVP-AEW541 or IMC-A12. The changes in phospho-IR after stimulation with IGF2 or insulin were much smaller (fold-change < 1.5). Bars depict mean \pm SEM fold-change phosphorylation levels of at least two independent experiments, each done in duplicate.

(D) **Phospho-AKT and phospho-ERK Western blot.** Cell lysates prepared as described in (C) were used for immunoblotting using phosphorylation-specific AKT and ERK antibodies. IGF2-induced AKT phosphorylation at threonine 308 and serine 473 was suppressed by NVP-AEW541 and IMC-A12, while total AKT was unchanged. No effect was seen on phospho-ERK levels. One representative experiment of two independent experiments is shown. Equal protein loading was confirmed by Ponceau staining and GAPDH immunoblotting.

(E) **Phospho-IGF1R and phospho-IR ELISA in A2780-T15.** Cells were prepared similarly to (C). IGF2 and insulin caused 7-fold and 10-fold increased levels of phospho-IGF1R, respectively, and this could be suppressed by NVP-AEW541 or IMC-A12. Levels of phospho-IR after IGF2 or insulin stimulation also increased, 4-fold and 9-fold, respectively. Suppression of phospho-IR with NVP-AEW541 was more effective than with IMC-A12, at these concentrations. Bars depict mean fold-change phosphorylation levels \pm SEM of at least two independent experiments, each done in duplicate.

(F) **Phospho-AKT and phospho-ERK Western blot.** IGF2-induced AKT and ERK phosphorylation was suppressed by NVP-AEW541 but not by IMC-A12. One representative experiment of two independent experiments is shown. Quantitation by densitometry is shown in the accompanying graph, where bars depict the mean expression \pm SEM (from two independent experiments) of each of the indicated phospho-proteins, normalized to starved unstimulated cells.

Previously, we showed that IGF pathway inhibition overcame IGF2-mediated Taxol resistance in tissue culture (Huang *et al*, 2010). To validate this finding *in vivo*, the effect of IGF pathway inhibition on Taxol resistance was evaluated HEY-T30 xenografts. Since NVP-AEW541 is not being clinically developed, we used IMC-A12 to specifically target IGF1R *in vivo*, using a validated regimen that inhibits IGF1R phosphorylation and reduces IGF1R protein levels in subcutaneous xenografts (Wu *et al*, 2005). As shown in Fig. 4A, IMC-A12 alone or in combination with Taxol did not reduce tumor growth compared to vehicle or Taxol treatment. Concordant with the *in vivo* findings, SRB cytotoxicity assays showed no change in the sensitivity to Taxol in the presence of IMC-A12 compared to Taxol alone (Fig. 4B). In contrast, NVP-AEW541 sensitized HEY-T30 to Taxol, as previously shown (Fig. 3 in (Huang *et al*, 2010)), NVP-AEW541 also sensitized A2780-T15 to Taxol (Fig. 4C), although to a lesser degree compared to the effect in HEY-T30. Neither IMC-A12 alone nor NVP-AEW541 alone reduced cell survival or proliferation. We explored if the differential ability of NVP-AEW541 and IMC-A12 to sensitize cells to Taxol was due to IR. As shown in supplemental figure S2C, IGF1R inhibition using IMC-A12 did not appear to affect Taxol sensitivity in HEY-T30 even after *IR* knockdown (hatched bars). The efficiency of *IR* knockdown (Fig. S2A) ranged from 71-83% for *IR-A* and 73-76% for *IR-B*.

Since concurrent targeting of *IR* and IGF1R did not recapitulate the Taxol-sensitizing effect observed with NVP-AEW541, we also tested whether NVP-AEW541 altered drug efflux. As a result of ABCB1-mediated drug efflux, HEY-T30 retain less labeled Taxol compared to HEY, while treatment with the p-glycoprotein inhibitor verapamil increases drug retention (Fig. 4D; left panel). In contrast, treatment with NVP-AEW541 at the 1 μ M concentration used for

cytotoxicity assays and signaling studies did not affect retention of labeled Taxol (Fig. 4D; right panel). Therefore, NVP-AEW541 at the concentrations used for cytotoxicity and signaling assays did not modulate drug efflux.

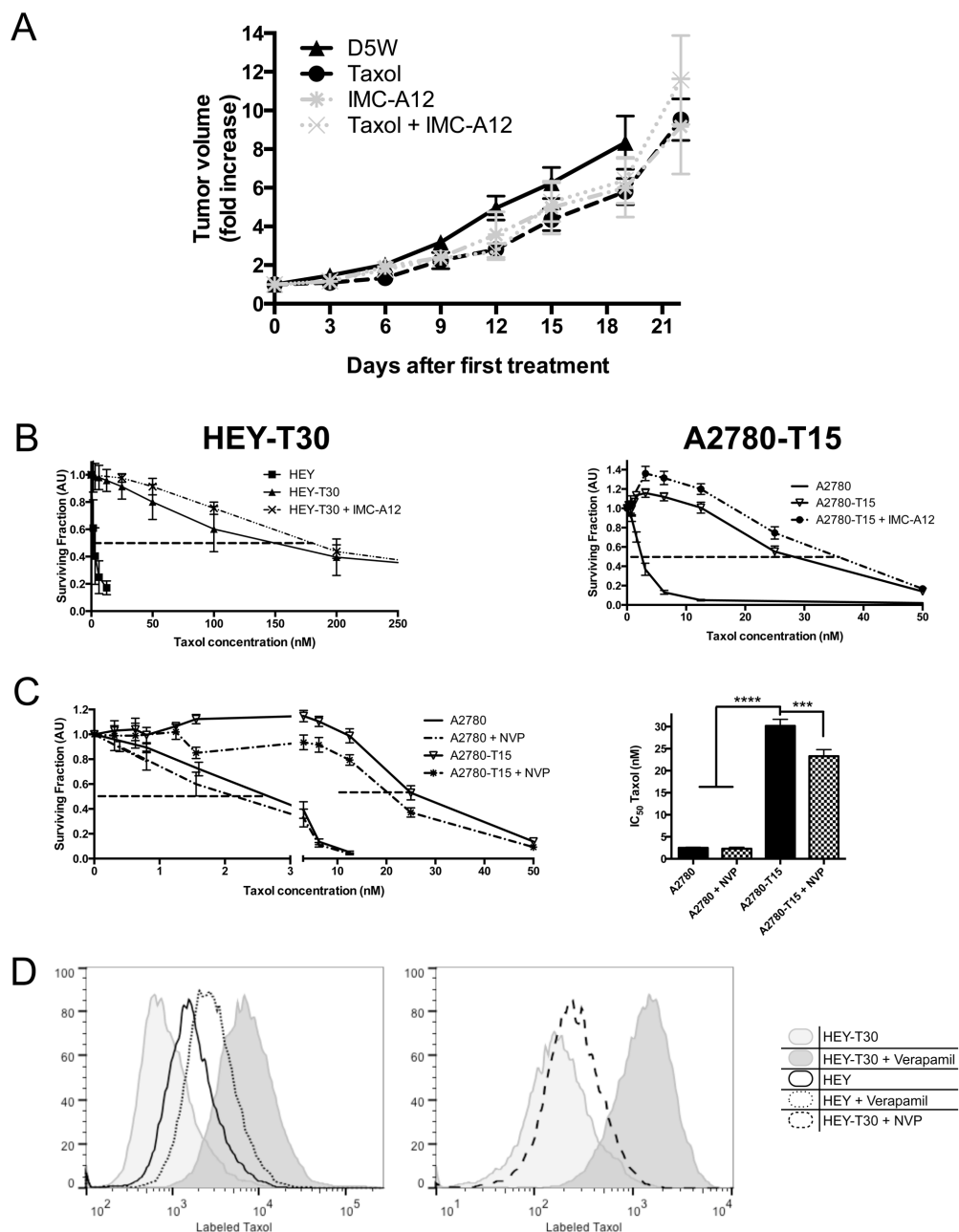


Figure 4

(A) Combination treatment using Taxol and IMC-A12 in mice with HEY-T30 xenografts. HEY-T30 xenografts were grown as described in Figure 2D, then treated with Taxol (black circles), according to the same dose/schedule described in Figure 2D, or with IMC-A12 (intraperitoneal injection of 40 mg/kg three times per week, grey *), or with combination treatment of Taxol and IMC-A12 (grey x). Data points show the mean tumor volume \pm SEM for each treatment group (n=8 animals per group). No significant differences in tumor volume

were observed with IMC-A12 or combined Taxol/IMC-A12 treatment compared to D5W or Taxol alone. This experiment was repeated a second independent time with similar results.

(B) Effect of IMC-A12 on Taxol sensitivity, evaluated by SRB cytotoxicity assay. In 96-well plates, cells were treated with serial dilutions of Taxol alone (solid lines) or together with a fixed dose of 10 $\mu\text{g/ml}$ IMC-A12 (dashed lines). Dose response curves show the mean of the surviving fraction $\pm\text{SEM}$ of cells relative to untreated cells at the indicated Taxol concentrations ($n=7$ independent experiments, each done in six replicates). No significant Taxol sensitization was observed in the presence of IMC-A12.

(C) Effect of NVP-AEW541 on Taxol sensitivity, evaluated by SRB cytotoxicity assay. In 96-well plates, cells were treated with serial dilutions of Taxol alone (solid lines) or together with a fixed dose of 1 μM NVP-AEW541 (dashed lines). Dose response curves show the mean $\pm\text{SEM}$ of the surviving fraction of cells relative to untreated cells at the indicated Taxol concentrations. The bar graphs depict the IC_{50} of Taxol for the indicated cell lines and drug treatments, and show the mean $\pm\text{SEM}$ calculated from at least four independent experiments (each with six technical replicates) per cell line. NVP-AEW541 sensitizes A2780-T15 to Taxol. *** $p < 0.001$, **** $p < 0.0001$; One-way ANOVA with Bonferroni posttest.

(D) ABCB1 (p-glycoprotein) function in HEY and HEY-T30 in the presence and absence of NVP-AEW541. Cells were incubated with labeled Taxol (Oregon Green® 488 Taxol, bis-acetate) in the presence or absence of NVP-AEW541 or verapamil. The ABCB1-overexpressing HEY-T30 cells (light gray shaded graph) retain less labeled Taxol than HEY cells (unfilled black outline). Verapamil, a known p-glycoprotein inhibitor, markedly increases the retention of labeled Taxol in HEY-T30 cells (and to a lesser degree in HEY cells), as demonstrated by the rightward shift of the peaks. Shown in the right panel with the dashed black line, treatment with 1 μM NVP-AEW541 does not appear to affect retention of labeled Taxol in HEY-T30 cells. Two independent experiments were done with similar results.

Our prior data suggested that directly targeting IGF2 would be an efficacious approach to restoring Taxol sensitivity (Huang *et al*, 2010). First using several siRNA sequences to *IGF2* (siIGF2), we evaluated the effect of *IGF2* knockdown in HEY-T30 and A2780-T15.

Transfection with each of the unique siIGF2 significantly reduced *IGF2* mRNA levels compared to siCTRL (Fig. S2D). We previously observed that *IGF2* knockdown decreased proliferation in HEY-T30 (Fig. 4B in (Huang *et al*, 2010)). Using two other *IGF2*-targeting siRNA sequences, we confirmed an anti-proliferative effect of *IGF2* knockdown, although the effect size varied. In A2780-T15, *IGF2* knockdown similarly decreased proliferation. In both Taxol resistant models, *IGF2* knockdown significantly sensitized cells to Taxol treatment compared to control knock down cells (Fig. 5A). *ABCB1* expression was not altered by *IGF2* knockdown in HEY-T30 (data not shown).

We next tested whether stable knockdown of *IGF2* mRNA could restore sensitivity to Taxol in drug resistant cells and xenografts. The stable *IGF2* knockdown cell lines, HEY-T30 shIGF2-p or HEY-T30-shIGF2-v had greater than 70% decrease in *IGF2* mRNA compared to HEY-T30 or HEY-T30 shScrambled (Fig. 5B). With regard to protein expression and processing of IGF2, the 21 kDa pre-pro-protein is cleaved into a 15 kDa pro-protein that undergoes several modifications to produce the mature 7 kDa peptide (Lee *et al*, 1994) . By Western blot, we confirmed a significant decrease in the 15 kDa pro-IGF2 in HEY-T30 shIGF2-p and shIGF2-v compared to HEY-T30 shScrambled (Fig. S2E). We did not detect altered levels of the 7 kDa peptide, which is known to be rapidly secreted from the cell (Duguay *et al*, 1998), and the levels of IGF2 in the conditioned media were below the sensitivity of the ELISA. Unlike the decrease in proliferation after transient knockdown with siRNA, proliferation rates of the

stable knockdown cell lines were not significantly altered. The doubling times for HEY-T30 shIGF2-p and shIGF2-v were slightly (non-significantly) longer compared to their cell line of origin, HEY-T30 (Fig. S4). This is likely due to the stable selection process favoring expansion of clonal populations able to overcome the anti proliferative effect of *IGF2* knockdown through compensatory pathways. The reason that HEY-T30 themselves have a longer doubling time than HEY cells is unclear but appears to be independent of *IGF2* expression.

Cytotoxicity assays showed that HEY-T30 shIGF2-p and shIGF2-v were significantly more sensitive to Taxol than HEY-T30 shScrambled or untransfected HEY-T30 (Fig. 5C); HEY-T30 shIGF2-p and shIGF2-v were approximately 10-fold and 6-fold more sensitive, respectively, to Taxol than HEY-T30 shScrambled; $p < 0.01$ for both comparisons. In addition, both *IGF2* knockdown cell lines were significantly sensitized to the microtubule-interacting drugs ixabepilone and vinblastine (Fig. 5C). There was slight sensitization to doxorubicin (1.6 fold sensitization for either shIGF2-p or shIGF2-v compared to shScrambled; $p < 0.05$ for both comparisons, but no change in sensitivity to cisplatin. Given the profound effect of *IGF2* knockdown to sensitize cells in tissue culture, we evaluated the effect of *IGF2* knockdown in vivo in xenograft experiments. Concordant with tissue culture doubling times, the in vivo tumor growth prior to treatment initiation was similar between HEY-T30 shIGF2-p and HEY-T30 shScrambled (Supplemental Fig. S5). However, their response to Taxol differed significantly. The growth of *IGF2* knockdown xenografts (HEY-T30 shIGF2-p) was significantly suppressed by Taxol similar to the effect observed in sensitive HEY xenografts,

while control knockdown xenografts (HEY-T30 shScrambled) remained resistant to Taxol similar to the untransfected HEY-T30 xenografts (Fig. 5D). Two independent experiments were done with concordant findings and the combined data is shown. Thus, *IGF2* knockdown restored the efficacy of Taxol in this in vivo model of drug resistant human ovarian cancer, consistent with the effect observed in tissue culture. Although the final mean tumor volume in the vehicle control groups differed slightly (shIGF2-p D5W being larger than shScrambled D5W), this difference was not statistically significant at any time points when analyzing either of the 2 independent experiments separately or their combined data. Immunohistochemical analysis of IGF2 protein expression was done in HEY-T30 shIGF2-p xenografts compared to HEY-T30 shScrambled xenografts to confirm that stable knockdown is maintained in vivo (Fig. 5E-F).

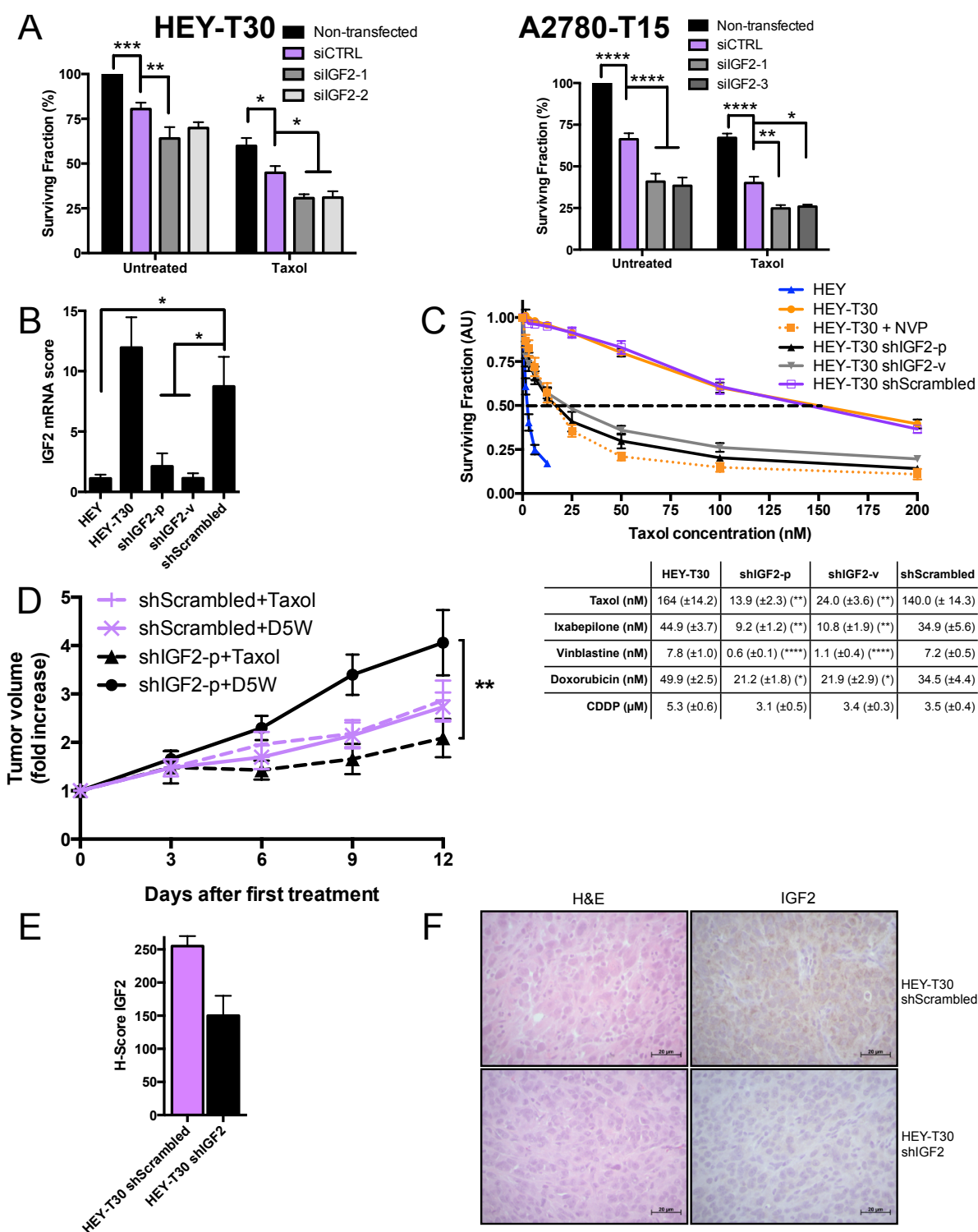


Figure 5

(A) Taxol sensitivity after *IGF2* knockdown by siRNA. HEY-T30 and A2780-T15 cells were transfected with control non-targeting siRNA (siCTRL) or siRNAs targeting *IGF2*

(siIGF2-1, siIGF2-2, siIGF2-3), and treated with DMSO or Taxol at the approximate IC_{50} (100 nM for HEY-T30 and 15 nM for A2780-T15). The surviving fraction was reduced after *IGF2* siRNA transfection compared to control siRNA transfection. The effect of Taxol was significantly enhanced in both HEY-T30 and A2780-T15 by *IGF2* siRNA transfection compared with control siRNA transfection. Bars represent the mean of four independent experiments (each in duplicate) \pm SEM; * $p < 0.05$, ** $p < 0.01$, *** $p < 0.001$, **** $p < 0.0001$; Two-way ANOVA with Bonferroni posttest.

(B) *IGF2* mRNA after stable knockdown with shRNA. HEY-T30 cells were transfected with shRNA targeting *IGF2* by plasmid transfection (shIGF2-p) or lentiviral infection (shIGF2-v), or with a control vector containing the scrambled version of the *IGF2* targeting sequence (shScrambled). Clonal stably-transfected cell lines were used for all experiments. *IGF2* mRNA levels are depicted in bars \pm SEM. The shIGF2-p and shIGF2-v cell lines have low *IGF2* mRNA levels similar to HEY, whereas HEY-T30 and shScrambled cell lines had several-fold higher mRNA expression levels. ($n > 6$ independent experiments, each done in triplicate) * $p < 0.05$; One-way ANOVA with Bonferroni posttest.

(C) Cytotoxicity assays in cell lines with *IGF2* shRNA. The indicated cell lines were treated with serial dilutions of Taxol, and sensitivity to Taxol determined by the sulforhodamine B assay. The dose-response curves are shown on the left, with the mean \pm SEM of the surviving fraction of cells relative to untreated cells shown at the indicated Taxol concentrations. The mean IC_{50} values \pm SEM for the indicated cell lines and drugs are shown in the table below. HEY T30 shIGF2-p and HEY-T30 shIGF2-v were significantly more sensitive to Taxol, ixabepilone, and vinblastine compared to control transfected HEY-T30 (shScrambled) or untransfected HEY-T30. The efficacy of *IGF2* knockdown at restoring sensitivity to Taxol was similar to NVP-AEW541 treatment. Only 1.6 fold sensitization to doxorubicin and no effect on cisplatin sensitivity were observed in shIGF2 lines compared to shScrambled or untransfected HEY-T30. Asterisks denote the statistical significance when comparing the IC_{50} for the indicated shIGF2 cell line versus shScrambled, where * $p < 0.05$, ** $p < 0.01$, **** $p < 0.0001$; Two-way ANOVA with Bonferroni posttest. ($n = 5$ independent experiments each done in six replicates)

(D) Xenograft growth with Taxol treatment of HEY-T30 shIGF2-p and HEY-T30 shScrambled. Female athymic nude mice were subcutaneously injected with 1 million HEY-T30 shScrambled or HEY-T30 shIGF2-p cells and tumors were allowed to grow to an average volume of 120 mm³. Mice were then treated with either D5W (vehicle) or Taxol at the MTD (described in 2D). Tumors were measured every three days, and data points show the mean tumor volume \pm SEM for each group at each time point. Two independent experiments were done for a total of 8-10 animals per group. shIGF2-p xenografts responded to Taxol treatment (triangle, dashed black line) and showed significantly tumor growth suppression compared to treatment with D5W (circle, solid black line); at day 12, ** $p < 0.01$ for shIGF2-p Taxol vs shIGF2-p D5W; One-way ANOVA with Bonferroni posttest. In contrast, HEY-T30 shScrambled xenografts did not respond to Taxol (+, dashed purple line) and continued growing at a similar rate as the vehicle-treated HEY-T30 shScrambled group (x, solid purple line). No significant difference in tumor size was observed between D5W-treated shIGF2-p

and shScrambled xenografts at day 12. Representative tumor xenografts were excised on day 13 after treatment for further analysis.

(E, F) IGF2 immunohistochemical staining of xenografts. Excised tumor xenografts (n=2 animals per group) on day 13 after treatment initiation were formalin-fixed, paraffin embedded and sections stained with hematoxylin and eosin or with an anti-human IGF2 antibody.

Staining was evaluated by the pathologist blinded to the groups and the mean of H-scores \pm SEM calculated and graphed (E). (F) Shows representative HEY-T30 shScrambled and HEY-T30 shIGF2 xenograft sections stained with hematoxylin and eosin (H&E) or with anti-IGF2 antibody (right panels). HEY-T30 shIGF2-p xenografts showed lower IGF2 expression when compared to HEY-T30 shScrambled.

Binding of Taxol to its target on β -tubulin can lead to aberrant mitosis, G2/M arrest, and apoptotic cell death in a dose-dependent, cell-specific manner. To explore the mechanism by which *IGF2* knockdown sensitizes cells to Taxol, we examined the cell fates following Taxol treatment of HEY-T30 shIGF2-p compared with HEY-T30 shScrambled. In Taxol sensitive cells, G2/M arrest peaks after 16 to 18 hours of Taxol treatment at concentrations >12 nM (Torres & Horwitz, 1998). At this time point, Taxol concentrations up to 250 nM did not induce G2/M arrest in HEY-T30. Very high concentrations at or above 375 nM Taxol were required to induce G2/M arrest (Fig. 6A). In contrast, HEY-T30 shIGF2-p, but not HEY-T30 shScrambled, arrested in G2/M when treated with much lower concentrations of Taxol (50 nM) (Fig. 6B). At this same time point, apoptosis analysis using a plasma membrane asymmetry probe (F2N12S, (Hope-Roberts *et al*, 2011)) showed an increase in the early apoptotic population following Taxol treatment in HEY-T30 shIGF2-p but not HEY-T30 shScrambled (Fig. 6C). These data indicate that *IGF2* knockdown sensitizes HEY-T30 to Taxol by significantly lowering the drug concentration required to block progression through mitosis and to induce apoptosis.

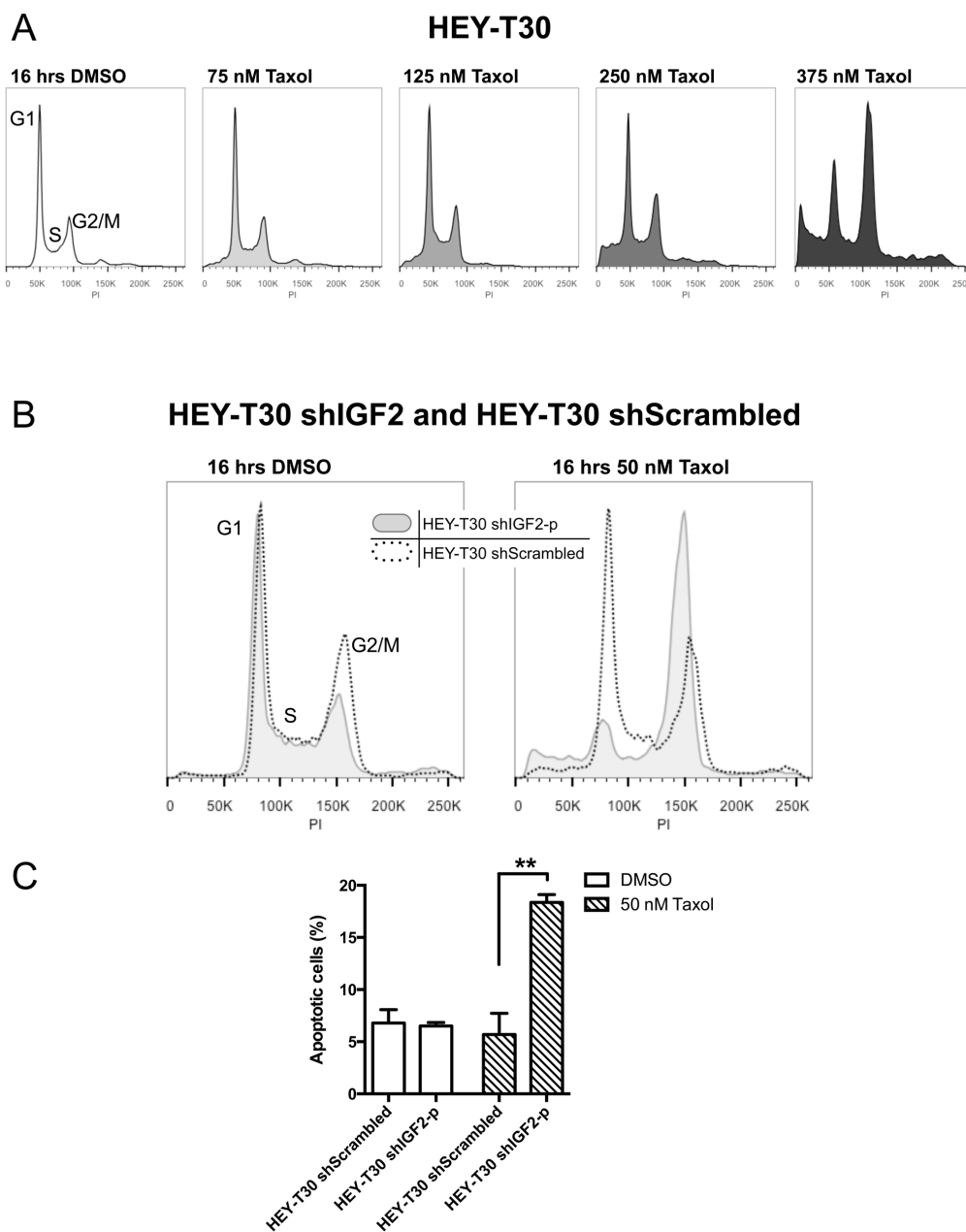


Figure 6

Taxol-induced G2/M arrest. (A) HEY-T30 cells were treated for 16 hours with the indicated concentrations of Taxol, and DNA content analyzed by flow cytometry. In HEY-T30 cells, G2/M arrest occurred after Taxol treatment at 375 nM but not lower concentrations. (B) shows HEY-T30 shIGF2-p (gray shaded) and HEY-T30 shScrambled (black dotted line) treated with DMSO or with Taxol (50 nM) for 16 hours. The HEY-T30 shIGF2-p cells showed G2/M arrest in response to Taxol while HEY-T30 shScrambled cells did not, at this Taxol concentration. Data from one experiment, of two independent experiments, are shown.

(C) **Apoptosis analysis.** Similar to (B), cells were treated with Taxol (50 nM) for 16 hours, harvested and stained with F2N12S (membrane asymmetry marker) and Sytox (dead cell marker), and analyzed by flow cytometry. Cell populations were gated in quadrants for quantitation, where the early apoptotic cell population is delineated by their decreased 585 nm/530 nm ratio due to loss of membrane asymmetry compared to non-apoptotic cells, and are Sytox-negative. Taxol treatment of HEY-T30 shIGF2-p cells resulted in a higher percentage of apoptotic cells compared to treatment with vehicle (DMSO), and Taxol-induced apoptosis was significantly enhanced in HEY-T30 shIGF2 cells compared to HEY-T30 shScrambled, at this time point. ** $p < 0.01$; One-way ANOVA with Bonferroni posttest. The bars show the mean \pm SEM of two independent experiments.

Discussion

In this study, we have shown for the first time *in vivo* that IGF2 depletion may be an effective strategy to overcome drug resistance to Taxol. In ovarian cancer patients, high IGF2 expression in tumor tissue is associated with clinically evident drug resistance, as we have now shown in two independent cohorts. Based on the laboratory data described in this paper and previously published data, we propose that IGF2 is a risk factor for disease recurrence and death due to its relationship with resistance to microtubule targeting agents such as Taxol, a drug which is used in first line and recurrence treatment for ovarian cancer. In this manuscript, we have now shown that *IGF2* knockdown restores Taxol sensitivity in well-characterized laboratory models of acquired drug resistance.

To reflect the diverse genetic alterations in drug resistant ovarian carcinoma cells (Duan *et al*, 2004; Stordal *et al*, 2012), six distinct resistant cell lines were profiled and compared to their respective chemosensitive cell lines. All of the drug resistant cell lines had significantly increased *IGF2* expression compared to the chemosensitive cell line. Since Taxol is by far the most widely used microtubule-stabilizing agent in clinical use, we focused on the Taxol resistant cell lines for further characterization. Other known mechanisms of Taxol resistance were present in these cell lines, including amplification of *ABCB1* (p-glycoprotein) in the HEY-T30 cells and a *de novo* β -tubulin mutation in the A2780-T15 cells. Despite the multiple genomic alterations in each of these cell lines, our data shows that IGF2 appears to be a significant modulator of their response to Taxol.

Evaluation of different therapeutic strategies revealed that selective inhibition of IGF1R, a major receptor for IGF2, was not sufficient to restore sensitivity to Taxol. Our previous data

showed that the small molecule tyrosine kinase inhibitor NVP-AEW541 sensitized drug resistant cells to Taxol; however, we found that in our cell line models, this molecule is not selective for IGF1R, but also inhibits IR. While we specifically excluded p-glycoprotein modulation by NVP-AEW541, we did not perform additional experiments to screen for off-target effects, as this data was previously published (García-Echeverría *et al*, 2004).

Combining *IR* knockdown with selective IGF1R blockade did not recapitulate the effect of NVP-AEW541. The lack of efficacy of combined *IR* knockdown/IGF1R blockade has not been fully elucidated but could be due to residual *IR* signaling activity (e.g. due to incomplete *IR* depletion), or IGF2 signaling through alternate, as yet to be determined receptors. Due to the ability of IGF1R, *IR*, and hybrid receptors to mediate IGF2 signaling (Ulanet *et al*, 2010; Garofalo *et al*, 2011), we hypothesized that directly targeting the ligand, IGF2, might be a more viable option in clinical development. Therefore, we evaluated the effect of *IGF2* depletion via transient or stable knockdown. The proliferation rate in tissue culture and the tumor growth kinetics *in vivo* were similar for stable *IGF2* knockdown or control knockdown. Based on tissue culture experiments wherein transient *IGF2* knockdown significantly decreased proliferation and cell viability, one might expect that *IGF2* knockdown alone would decrease tumor growth of these cells *in vivo*. However, the selection process for stable shIGF2 clones in tissue culture is inherently biased toward selection of transfected cells that retain clonogenic potential. That is, only cells that have developed compensatory mechanisms to overcome the anti-proliferative effect of *IGF2* knockdown would have been selected for further expansion and subsequently used for the *in vivo* experiments. The significant increase in sensitivity to Taxol in tissue culture was seen after either transient or stable *IGF2*

knockdown, and translated to restoration of therapeutic efficacy of Taxol treatment of drug resistant xenografts following *IGF2* knockdown.

These data provide a critical foundation for developing rational therapeutic strategies to overcome drug resistance by targeting IGF2. In ongoing laboratory studies, we intend to address some additional knowledge gaps. First, Taxol is typically used in combination with platinum agents in the first-line setting, and with both platinum and non-platinum agents in the recurrent setting. In the current study, we focused specifically on Taxol resistance and used well-defined laboratory models of Taxol resistance to avoid confounding the results with platinum-resistance mechanisms or platinum-induced genomic alterations. This proof-of-principle study, demonstrating that IGF2 modulation overcomes multiple Taxol resistance mechanisms, now forms the basis for preclinical testing of IGF2 targeting agents in combination with standard combination ovarian cancer treatment regimens. One example of such an agent is BC-821, a therapeutic vector that expresses diphtheria toxin A under the regulation of an *IGF2* fetal promoter (Amit & Hochberg, 2010). In our subsequent translational studies, we plan to evaluate this IGF2 targeting agent, and others, in combination with Taxol/platinum using prospectively collected primary and recurrent patient-derived xenografts including orthotopic models.

In summary, *IGF2* knockdown, but not selective IGF1R inhibition, effectively reverses drug resistance in a Taxol-resistant human ovarian carcinoma xenograft model. The significant association of *IGF2* upregulation with drug resistance is observed in genetically diverse cell lines, and its knockdown restores sensitivity to both microtubule-stabilizing and destabilizing

agents. Therefore, we suggest that our findings could be applicable to the general problem of resistance to microtubule-targeting chemotherapeutic agents. The clinical relevance of our findings is supported by the validation of IGF2 as a poor prognostic factor for early recurrence and death in ovarian cancer patients. Thus, we have identified IGF2 to be a promising therapeutic target for overcoming drug resistance in ovarian cancer, and further translational studies are merited to bring this fundamental discovery to the clinic.

Disclosure: The authors declare no conflicts of interest.

Acknowledgements

Grant support was provided by the National Cancer Institute-National Institute of Child Health and Human Development (K12 HD00849) and the American Congress of Obstetricians and Gynecologists through the Reproductive Scientist Development Program award to G.S.H.. We acknowledge the use of the Albert Einstein Cancer Center Shared Resources (Flow Cytometry Core, Histology and Comparative Pathology Core), supported by the National Cancer Institute Cancer Center Support grant P30CA013330. We thank Dr. Susan Band Horwitz for helpful discussions.

Supplemental Figures

Table S1. Sequences of primers and oligonucleotides

Target	Forward	Reverse	Efficiency	Amplicon Size (bp)	Accession Number
<i>IGF2</i> mRNA	ACCGTGCTTCCGGACAAC	TGGACTGCTTCCAGGTGTCA	102.5%	73	NM_000612.4
<i>IGF2</i> gDNA	GGTGCTAACACGGCTCTCTC	CGGAAACAGCACTCCTCAAC	92.1%	100	NM_000612.4
<i>ABCB1</i> mRNA	GTCAGTGTCTGTGGCAAAGATAC	TGCTGCCAAGACCTCTTCAGCTACT	102%	100	NM_000927.3
<i>ABCB1</i> gDNA	TTGAAGGAAAAGCAAATCTTCC	TTGTCAAGCCAATTTGAATAGC	103.6%	98	NM_000927.3
<i>PPIB</i> mRNA	AAGTCACCGTCAAGGTGTATTTT	GATCACCCGGCCTACATCTTC	91.4%	62	NM_000942.4
<i>ALB</i> gDNA	TCCTGACCAAGCTTAACCAAGTAT	CCAAAAAGGGTATGCTAAATGG	98.8%	117	NM_000477
<i>IGF1R</i>	TGAAAGTGACGTCTGCATTTT	GGTACCGGTGCCAGGTTATG	94%	92	NM_000875.3
<i>IR-B</i>	TGAAGGAGCTGGAGGAGTCCTCG	CCTAGGGTCTCGGCACCAGTG	115%	110	NM_000208.2
<i>IR-A</i>	CGTCCCCAGGCCATCTCGG	GCTGGTCGAGGAAGTGTGGGG	117.5%	103	NM_001079817.1

Target	Forward	Reverse
<i>IGF2</i> siRNA #1	AAGGUGAGAAGCACCAGCAUCGACU	AAGGUGAGAAGCACCAGCAUCGACU
<i>IGF2</i> siRNA #2	UCGCCUCGUGCUGCAUUGCUGCUUA	UAAGCAGCAAUGCAGCAGGAGCGA
<i>IGF2</i> siRNA #3	CGUGGCAUCGUUGAGGAGUGCUGUU	AACAGCACUCCUCAACGAUGCCACG
<i>IR</i> siRNA	CUAGUCCUGCAGAGGAUUU	AAAUCCUCUGCAGGACUAG
<i>IGF2</i> shRNA	CACCGCGTGGCATCGTTGAGGAGTGCTGTTGAAAACAG CACTCCTCAACGATGCCACG	AAAACGTGGCATCGTTGAGGAGTGCTGTTTTCGAAC AGCACTCCTCAACGATGCCACG
Scrambled shRNA	CACCGGGTGTCTGTGTCGCATGTAGTGTACGAATACACTA CATGCGACACGAGCACCC	AAAAGGGTGTCTGTGTCGCATGTAGTGTATTCGTACA CTACATGCGACACGAGCACCC

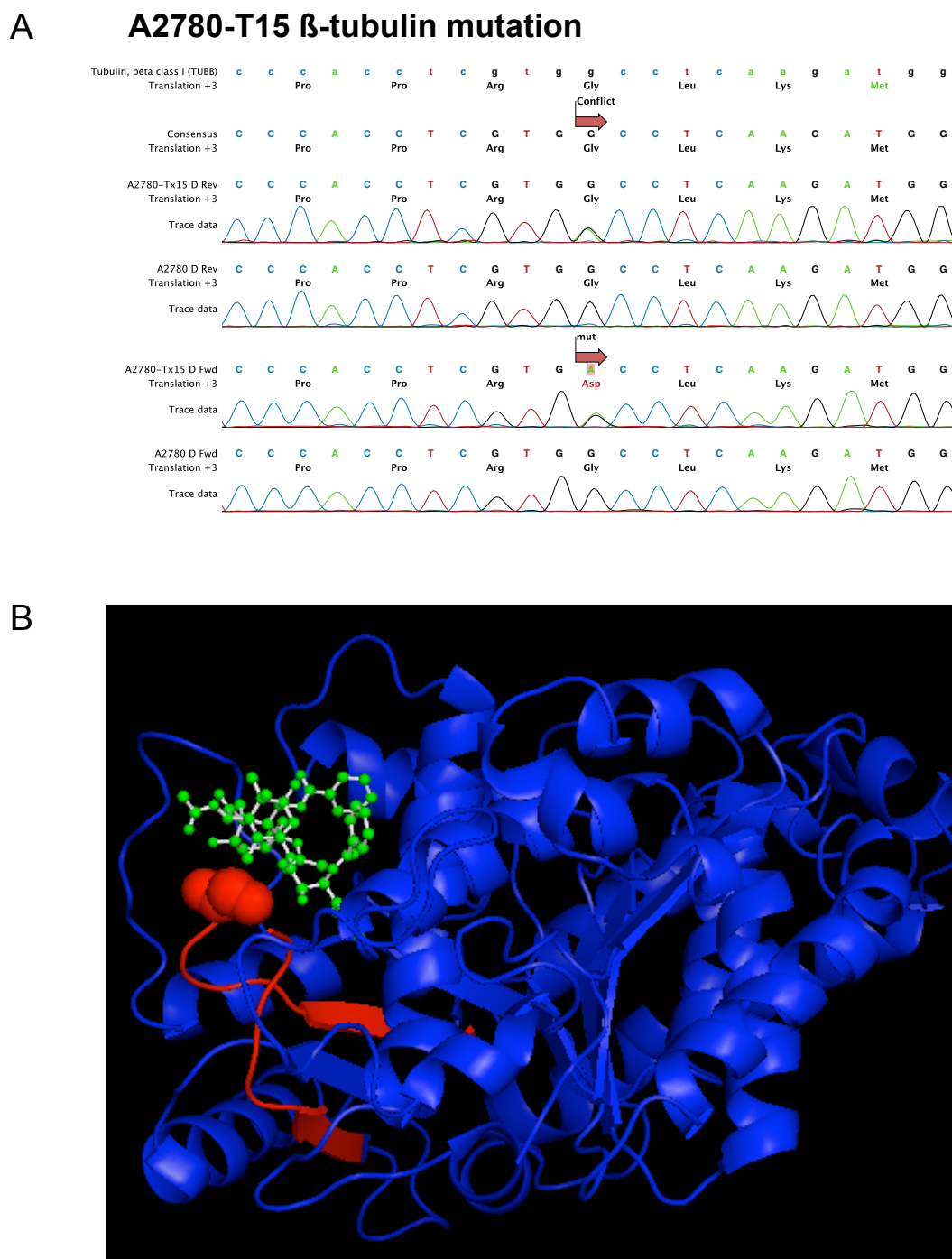


Figure S1. A2780-T15 β -tubulin mutation

(A) Sequencing data from A2780-T15 show a heterozygous mutation in β -tubulin leading to G360D. (B) This amino acid (red globes) is located in the Taxol-binding pocket of β -tubulin (blue). Taxol is depicted in green. This mutation was not found in HEY-T30. Image made with PyMOL.

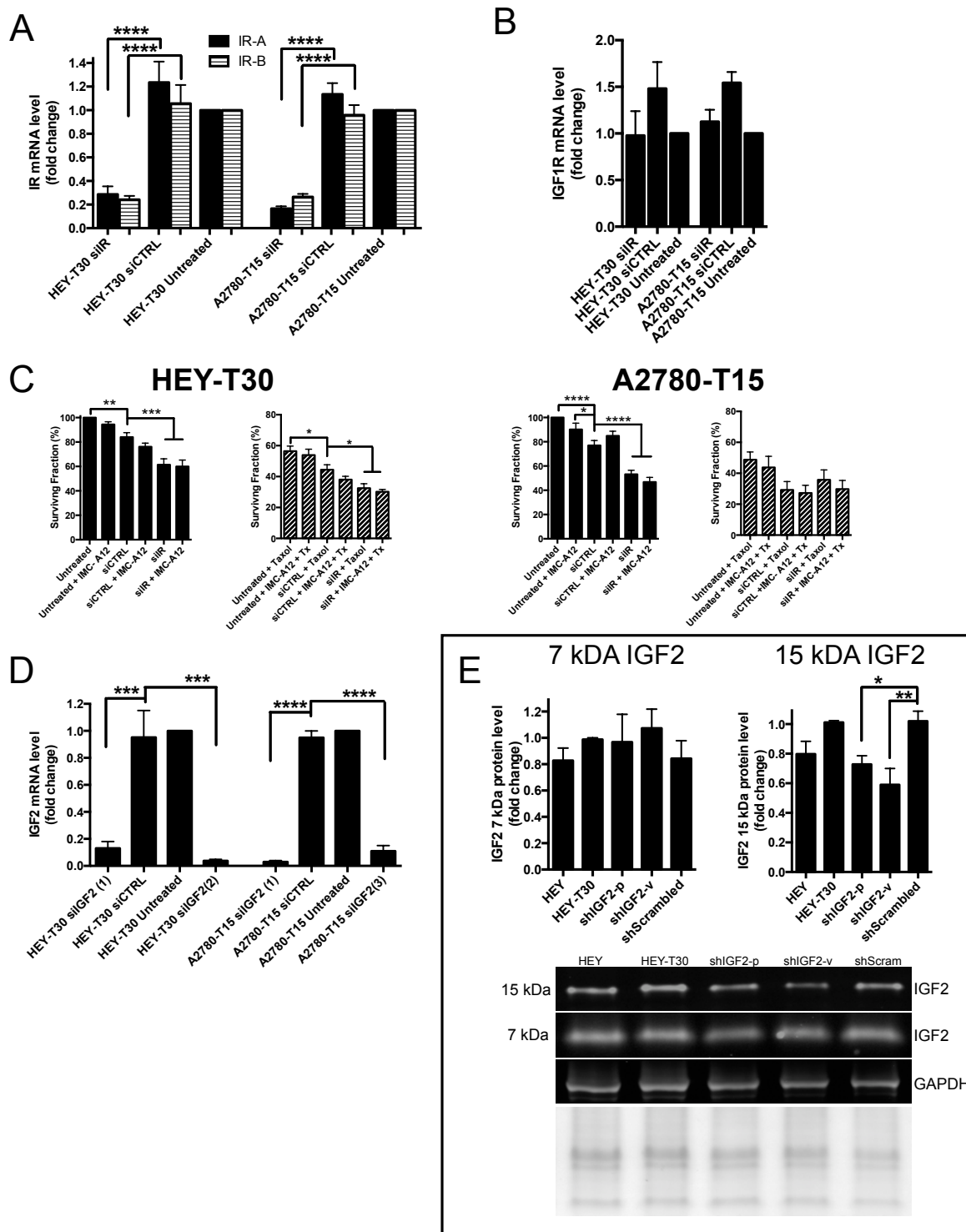


Figure S2. Knockdown by siRNA and shRNA

(A) *IR-A* and *IR-B* mRNA expression, and (B) *IGF1R* mRNA expression, quantified by reverse transcriptase quantitative PCR, 48 hours after transfection of HEY-T30 and A2780-

T15 with IR-targeting siRNA (siIR) or control non-targeting siRNA (siCTRL). The *IR* siRNA transfection significantly reduced *IR-A* and *IR-B* mRNA levels compared to untransfected (Untreated) or control siRNA (siCTRL) without any significant effect on *IGF1R* mRNA. Bars show the mean \pm SEM of at least 3 independent experiments, each done in triplicate.

(C) Effect of *IR* siRNA transfection on Taxol sensitivity. HEY-T30 and A2780-T15 cells were transfected with control non-targeting siRNA (siCTRL) or siRNA targeting *IR* (siIR), then treated 24 hours later with diluent only (DMSO; solid bars) or Taxol (100 nM for HEY-T30; 22.5 nM for A2780-T15; hatched bars). Seventy-two hours later cells were counted, and surviving fraction calculated as the % cell number relative to untransfected cells treated with diluent only (Untreated; left bar); bars show the mean \pm SEM of four independent experiments, each done in duplicate. The surviving fraction was significantly reduced following *IR* siRNA transfection compared to control siRNA in both cell lines. Shown in the hatched bars, the effect of Taxol treatment on HEY-T30 but not A2780-T15 was enhanced in cells transfected with *IR* siRNA compared with cells transfected with control siRNA. IMC-A12 did not affect the surviving fraction or the response to Taxol in either HEY-T30 or A2780-T15, whether the cells were untransfected, *IGF2* siRNA or control siRNA transfected. * $p < 0.05$, ** $p < 0.01$, *** $p < 0.001$, **** $p < 0.0001$; One-way ANOVA with Bonferroni posttest.

(D) *IGF2* mRNA expression, quantified by reverse transcriptase quantitative PCR, 48 hours after transfection of HEY-T30 and A2780-T15 cells with *IGF2*-targeting siRNA oligonucleotides (siIGF2(1), siIGF2(2), siIGF2(3)) or control non-targeting siRNA (siCTRL). All *IGF2* siRNA transfections resulted in at least 80% reduction in *IGF2* mRNA compared to the untransfected (Untreated) or control siRNA (siCTRL) transfected cell lines. Bars show the mean \pm SEM of at least 3 independent experiments, each done in triplicate.

(E) *IGF2* Western blot. The HEY-T30 shIGF2-p and shIGF2-v cell lines showed a significant decrease in the 15 kDa pro-IGF2 protein compared to HEY-T30, but not in the mature 7 kDa peptide, as determined by densitometry using ImageJ, with normalization to Ponceau staining of protein. A representative blot is shown from four independent experiments, bars show the mean \pm SEM.

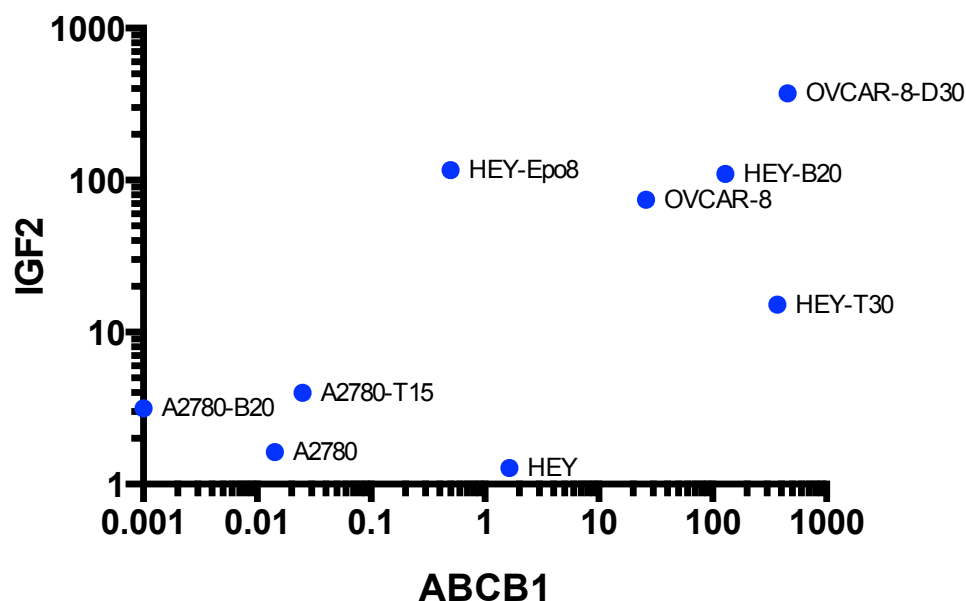


Figure S3. Correlation between *IGF2* and *ABCB1* mRNA

A correlation analysis and graphical representation of reverse transcriptase qPCR data of *IGF2* and *ABCB1* mRNA. *IGF2* mRNA scores of cell lines described in Fig. 1C were used. For *ABCB1* mRNA scores were used of cell lines described in Fig. 1D while HEY-B20 (n=8), HEY-Epo8 (n=2), A2780-B20 (n=2), OVCAR-8 (n=5) and OVCAR-8-D30 (n=5) were determined similarly by qPCR, where n=number of independent experiments each performed with 3 technical replicates per experiment. The mRNA scores were plotted and correlation calculated. The correlation was not significant ($r=0.6167$; $p=0.0857$; Spearman correlation).

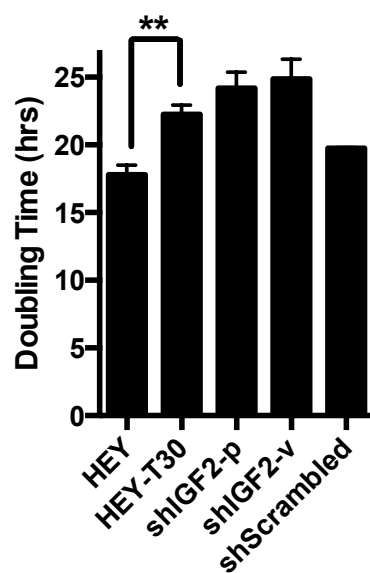


Figure S4. Cell doubling time

Cells were grown in subconfluent monolayers using 6-well dishes, and duplicate wells trypsinized for counting every 24 hours for 96 hours using a Millipore Scepter. Cell doubling time was calculated; bars show the mean \pm SEM doubling time in hours of at least two independent experiments. The shIGF2-p and shIGF2-v cell lines had a non-significantly longer doubling time than HEY-T30 cells, which in itself had a significant longer doubling time than HEY cells (One-way ANOVA, ** $p < 0.01$).

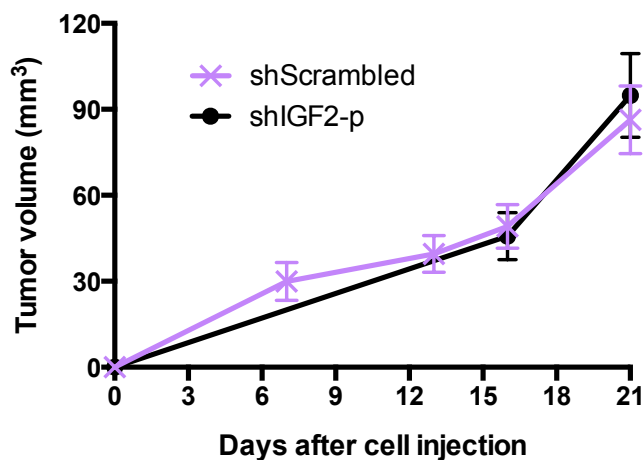


Figure S5. Xenograft growth curve of animals from D5W group until first treatment.

Female athymic nude mice were subcutaneously injected with 1 million HEY-T30 shScrambled or HEY-T30 shIGF2-p cells and tumors were allowed to grow to an average volume of 120 mm³. Data points show the mean tumor volume \pm SEM for each group at each time point. Two independent experiments were done for a total of 8-10 animals per group. HEY-T30 shIGF2-p xenografts (circle, solid black line); HEY-T30 shScrambled (x, solid purple line). No significant difference in tumor size was observed between shIGF2-p and shScrambled xenografts before treatment started (See Fig. 5D).

**CHAPTER III: OVEREXPRESSION OF INSULIN-LIKE GROWTH FACTOR 2 IN
AN OVARIAN CANCER CELL LINE LEADS TO INCREASED XENOGRAFT
GROWTH AND NEUTROPHIL INFILTRATION**

Jurriaan Brouwer-Visser, Jiyeon Lee, Maria J. Cossio, Shijun Mi, Suzan K. Chao and Gloria S. Huang

This manuscript has not been submitted yet. As such, the introduction and discussion for this publication will be a shortened version of the text written for the general introduction and discussion of this thesis.

Objectives

Our broad objective is to elucidate the mechanisms by which IGF2 alters patient outcome and sensitivity to chemotherapy. We have seen that IGF2 knockdown can lead to sensitization of resistant cells and we propose to further describe how directly modulating IGF2 affects the phenotype of cells and xenografts.

Aims

- Evaluate if overexpression of IGF2 in HEY cells causes resistance to Taxol.
- Evaluate if the conditioned media of IGF2 overexpressing HEY and A2780 cells can stimulate non-transfected cells.
- Evaluate if IGF2 overexpression in HEY and A2780 cells affects xenograft growth in mice.

Results

Phenotype of *IGF2* overexpression in HEY cells

HEY cells were transfected with a construct containing *IGF2* gene. Reverse transcriptase qPCR of the sorted mass population showed a several thousand-fold increase in *IGF2* mRNA of HEY-IGF2 cells. *ABCB1* (p-glycoprotein) mRNA showed an increase in both HEY-EV and HEY-IGF2 as well (Fig. 1A). We have previously noted that *ABCB1* expression varies greatly under different conditions in HEY cells and suspect the increase to be a result of transfection and cell sorting. Western blot analysis of the IGF2 protein showed an increase in the 21 kDa preproprotein, but not in the proprotein or the mature IGF2, possibly due to insufficient processing of the preproprotein or due to rapid secretion of the mature protein from the cell. Analysis of the HEY-IGF2 media by ELISA, which detects the different intermediary and mature forms of the IGF2 protein, showed increased levels of IGF2 protein in the media (Fig. 1B). Transfection of HEY cells with *IGF2* led to an increase of IGF2 on the mRNA, protein and secreted protein level. IGF2 can bind the IGF1 receptor, Insulin receptor or hybrid receptor to signal to downstream PI3K/AKT or MAPK pathways. Western blot analysis showed that the HEY-IGF2 cells have higher AKT phosphorylation when compared to the untransfected and empty vector-transfected HEY cells. ERK phosphorylation was unaffected by *IGF2* overexpression, likely because the *BRAF* mutation of HEY cells make that pathway less sensitive to external stimulation. Low total levels of IGF1R in HEY cells make detection of its phosphorylation by Western blot difficult, therefore we opted to use a sandwich ELISA

assay. Similar to AKT phosphorylation, tyrosine phosphorylation of IGF1R was increased in HEY-IGF2 cells, indicating increased activation of that receptor (Fig. 1C).

Both HEY-IGF2 and HEY-EV cell lines were more resistant to Taxol treatment as compared to untransfected cell lines, as determined by cytotoxicity assays, while resistance to ixabepilone was only slightly altered. Taxol is an excellent substrate of the p-glycoprotein transporter (ABCB1), while ixabepilone less so. Co-incubation of cells with verapamil, a known inhibitor of ABCB1, sensitized HEY-EV and HEY-IGF2 to Taxol, suggesting its resistance to be at least partly due to expression of ABCB1 (Fig. 1D). There are few differences described for the mechanisms of action of Taxol and ixabepilone. Both bind at the same site of β -tubulin site and show competitive binding inhibition. Besides less affinity for the p-glycoprotein, it is thought that ixabepilone can overcome resistance to Taxol caused by increased expression of the β III isotype of β -tubulin, by preferentially binding to this subtype (Dumontet *et al*, 2009). Stimulation of the survival/proliferation pathway of PI3K/AKT can lead to decreased doubling times of the cells (the time necessary to double the number of cells). We have previously shown that knocking down *IGF2* by siRNA increased the doubling time of Taxol-resistant HEY-T30 cells. Both under normal (10%) and low (1%) serum conditions HEY-IGF2 cells did not proliferate at a different speed than untransfected and HEY-EV cells. We suspect that adaptation and compensation mechanisms avoid any noticeable differences in doubling time (Fig. 1E).

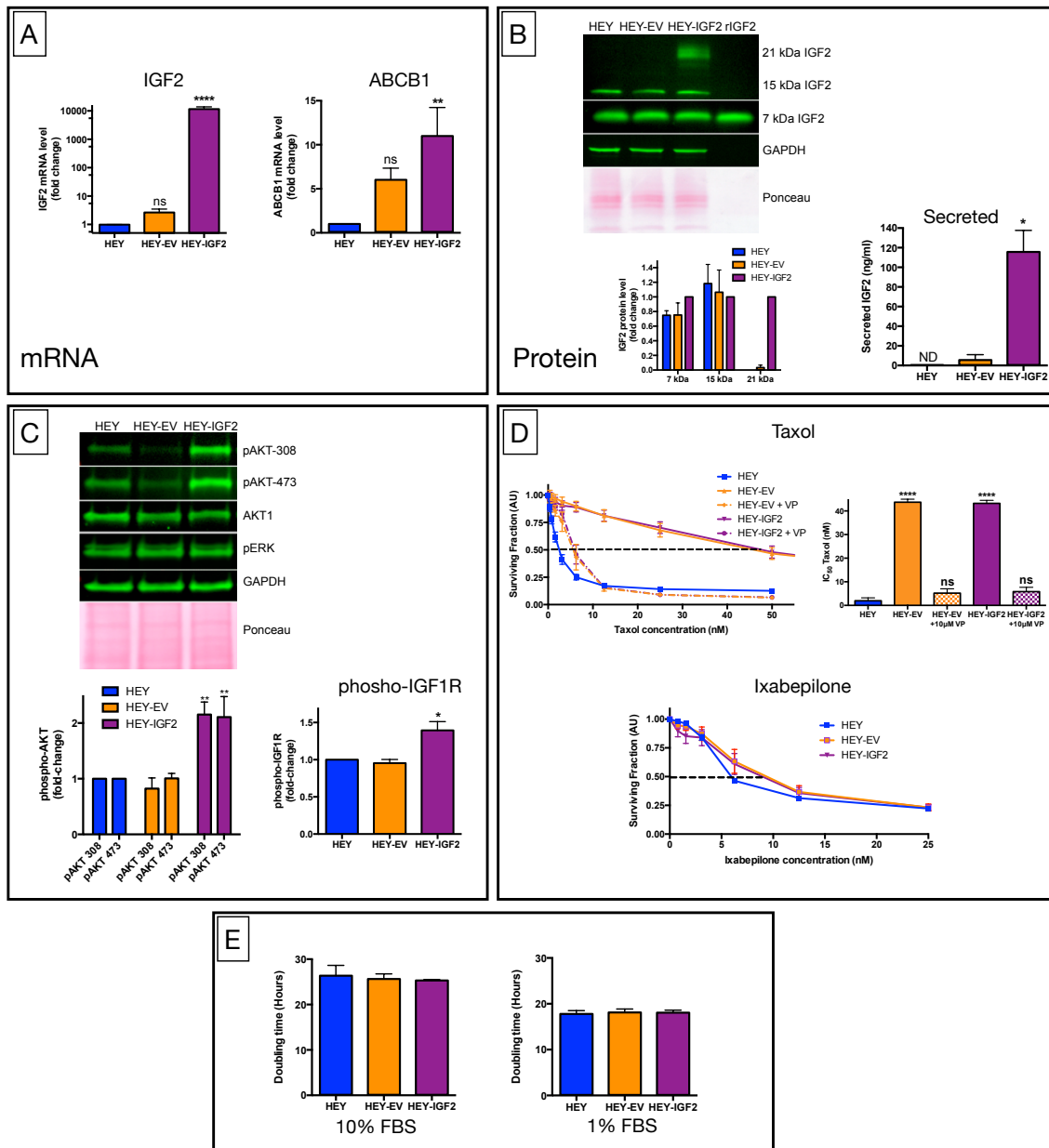


Figure 1

A
Reverse Transcriptase qPCR of HEY cells transfected with *IGF2* or with the empty vector. After FACS sorting of GFP-positive cells, RNA lysates were prepared and reverse transcribed. *IGF2* and *ABCB1* mRNA were determined by qPCR. HEY-IGF2 cells have a several thousand-fold increase in *IGF2* mRNA and a several fold-increase in *ABCB1* mRNA. Average \pm SEM, n=12 for *IGF2* and n=4 for *ABCB1*, each sample in triplicate. **** p<0.0001, ** p<0.01, ns is Non Significant, by one-way ANOVA with a Bonferroni post-test.

B

Western blot and ELISA of transfected cells. Cells were lysed, separated on a tris-tricine gel and the membrane incubated with an IGF2 antibody. HEY-IGF2 showed the presence of a heavier preproprotein of 21 kDa, but no difference in the mature 7 kDa IGF2. Representative Western blot shown, bar graph shows the quantification of three independent experiments. Secreted IGF2 was measured by ELISA. Five hundred thousand cells were seeded, washed after 24 hours and 1 ml of serum-free media was added. Cells were incubated for 48 hours, the conditioned media was then harvested and the cells counted. IGF2 was then quantified by ELISA using a standard curve. Average \pm SEM, n=2, each sample in duplicate, *p<0.05, by one-way ANOVA with a Bonferroni post-test.

C

Phosphorylation changes in transfected cells. Cells were starved overnight and subsequently lysed. Proteins were separated on a tris-glycine gel and the membrane probed with the antibodies shown. Bar graph shows the quantification of three independent experiments \pm SEM, ** p<0.01 by one-way ANOVA with a Bonferroni post-test. Using the same lysates, a sandwich ELISA was performed to determine relative phosphorylation levels of IGF1R. (Average \pm SEM, n=4, each sample in duplicate) * p<0.05 by one-way ANOVA with a Bonferroni post-test.

D

Cytotoxicity assays of transfected HEY cell lines. Cells were seeded in 96-well plates and treated the next day with decreasing concentrations of Taxol (top) and ixabepilone (bottom). For co-incubation with verapamil, media was changed to have a fixed concentration of 10 μ M. After 72 hours cells were fixed and stained with sulforhodamine B and read on a plate reader. Curves show the surviving fraction of cells at each concentration and the bars shows the calculated IC₅₀, by curve fitting. HEY-IGF2 and HEY-EV showed increased resistance to Taxol compared to HEY. This resistance was reversed by co-incubation with verapamil, a compound known to inhibit p-glycoprotein (ABCB1). Average \pm SEM, n=7 for Taxol and n=3 for Taxol + 10 μ M verapamil, each sample with six replicates, **** p>0.0001, by one-way ANOVA with a Bonferroni post-test. Both transfected cell lines showed only slight resistance to ixabepilone in comparison to the untransfected cell line.

E

Doubling time of transfected cells.

Ten thousand cells per 6-well well were seeded in either RPMI with 10% FBS (left, average \pm SEM, n=7) or 1% FBS (right, average \pm SEM, n=3). After 24 hours and 96 hours two wells were counted and the doubling time calculated. No statistical differences were observed between the three cell lines under the two conditions tested.

IGF2 conditioned media stimulates HEY cells

Since we showed that *IGF2* overexpression led to increased IGF2 protein in the media, we determined if this media was able to stimulate untransfected cell lines. As expected, HEY cells had AKT readily phosphorylated by stimulation with the conditioned media of HEY-IGF2 cells and not by conditioned media of HEY or HEY-EV cells (Fig. 2A). When the same conditioned media was used to stimulate A2780 ovarian cancer cells, no stimulation was observed of either AKT or ERK (Fig. 2B). A2780 cells have an inactivating *PTEN* mutation that leaves AKT constitutively activated; we suspect that the relatively low concentration of IGF2 in the conditioned media of HEY-IGF2 cells is not enough to further stimulate these cells. As a control, we transfected and sorted A2780 cells similarly to HEY-IGF2. The conditioned media of these transfected A2780-IGF2 cells was able to stimulate HEY cells very strongly (Fig. 2C). Again, the conditioned media of A2780-IGF2 cells was unable to further stimulate A2780 cells (Fig. 2D), indicating that the inability of conditioned media to stimulate A2780 cells, was a cell line-specific.

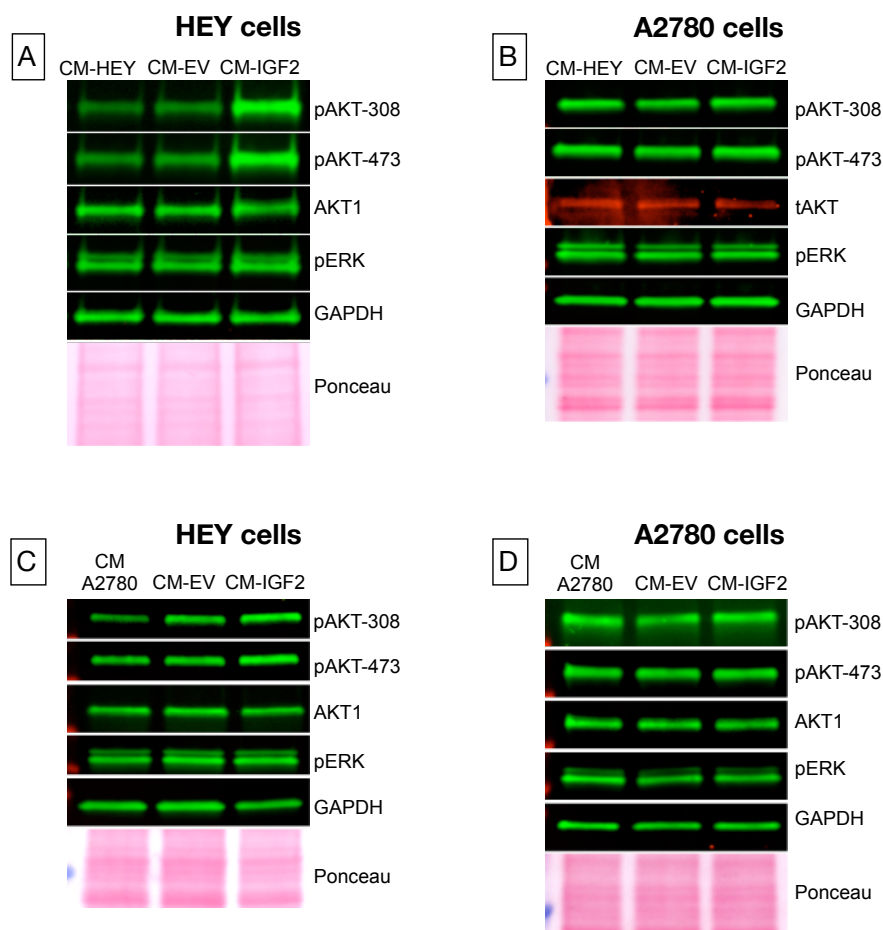


Figure 2

A

HEY-IGF2 conditioned media stimulation of HEY cells. Transfected cells were cultured in serum-free media for 48 hours; this conditioned media was then used to stimulate starved HEY cells for 10 minutes after which cells were harvested and lysed. The lysates were separated on a tris-glycine gel and the membrane blotted with the antibodies shown. The conditioned media of HEY-IGF2 increased AKT phosphorylation and not ERK phosphorylation of untransfected HEY cells (n=2).

B

In a similar fashion, A2780 cells were treated with HEY-IGF2 conditioned media. No change in phosphorylation of either AKT or ERK is seen. (n=2)

C

A2780-IGF2 conditioned media stimulation of HEY cells. The conditioned media of A2780-IGF2, prepared similarly to A), increased AKT phosphorylation of HEY cells slightly but did not show any response in A2780 cells (D) (n=2).

HEY-IGF2 xenografts have an increased growth rate

We did not observe any change in the proliferation rate of the HEY-IGF2 cells when compared to HEY-EV *in vitro* cell culture. Since it was clear that *IGF2* was being overexpressed, we hypothesized that in xenografts we might observe different growth kinetics. Nude mice were injected subcutaneously with one million of either HEY-IGF2 or HEY-EV cells. Tumor growth was recorded twice weekly. As soon as tumors were measurable, HEY-IGF2 tumors had a significant increased growth rate. HEY-IGF2 xenografts reached the maximum allowed size several days before the HEY-EV (Fig. 3A). We repeated this experiment with different dilutions of cells in 50% matrigel. The matrigel allowed the tumors to grow faster, but the same increase in growth of HEY-IGF2 xenografts compared to HEY-EV xenografts was observed with the three tested dilutions (10,000; 100,000; 1,000,000 injected cells) (Fig. 3B). Thus, similar findings were observed between xenografts injected with and without matrigel. When the first animal of a group reached the maximum allowed tumor size, the experiment for that dilution was ended and the tumors excised. The tumors were weighed and at each dilution the HEY-IGF2 tumors were heavier (Fig. 3C). To determine if the increase in tumor size was due to increased proliferation, we made sections of the tumors and stained them with Ki67, a nuclear marker only observed in cells that are actively going through the cell cycle. In HEY-IGF2 xenografts a higher percentage of nuclei stained positively for Ki67 than in HEY-EV xenografts at the three tested dilutions (Fig. 3D). A pathologist analyzed the hematoxylin and eosin sections of all tumors to determine if any morphological differences were observed between the xenografts of the two transfected cell lines. Unexpectedly, a significant increase in

the infiltration of cells with a neutrophilic appearance was observed in HEY-IGF2 xenografts when compared to HEY-EV xenografts (Fig. 3E).

Tumor growth experiments were also carried out with A2780-IGF2 and A2780-EV cells.

Similar to our observation in cell culture, no difference was observed between the growth rates of the two cell lines *in vivo* (Fig. 3F). The experiment was repeated with two dilutions in matrigel, but no difference in tumor weight was observed (Fig. 3G). The pathologist also quantified infiltrating neutrophils in A2780-IGF2 and A2780-EV xenograft sections. Very few infiltrating neutrophils were observed in either group, suggesting that overexpression of IGF2 alone was not enough to increase tumor growth or neutrophilic infiltration in A2780 xenografts (Fig. 3H).

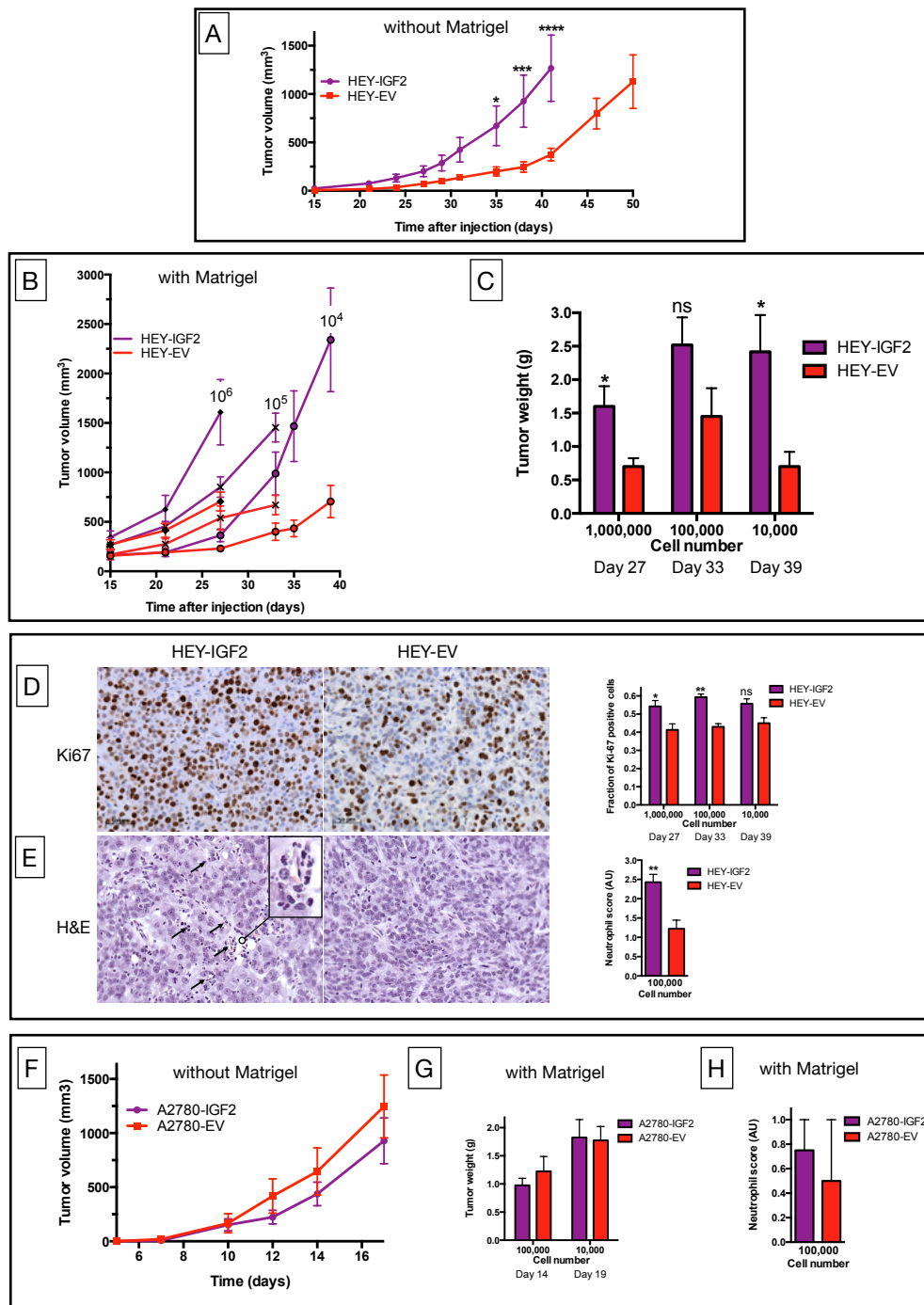


Figure 3

A
Xenograft growth of HEY-IGF2 and HEY-EV. Nude mice were injected subcutaneously with one million HEY-IGF2 or HEY-EV cells. Of the ten HEY-IGF2-injected mice, nine

developed tumors. Of the ten HEY-EV-injected mice, seven developed tumors. HEY-IGF2 xenografts (purple line) grew significantly faster than HEY-EV xenografts (red line). Average \pm SEM, * $p > 0.05$, *** $p > 0.001$, **** $p > 0.0001$, by repeated measures two-way ANOVA with a Bonferroni post-test.

B

Injection of different dilutions of cells in matrigel. Nude mice were injected with either 10,000 (○, n=6); 100,000 (×, n=5) or 1,000,000 (●, n=6) cells diluted in 50% matrigel and tumor growth was monitored. At all three dilutions HEY-IGF2 xenografts (purple lines) grew more quickly.

C

Tumor weight of each dilution at the termination of the experiment. The tumors were excised and weighed at day 27 after injection for 1,000,000 cells; day 33 for 100,000 cells; day 39 10,000 cells. HEY-IG2 tumors were heavier at each dilution tested. Average \pm SEM, * $p > 0.05$, ns = non-significant by two-tailed t-test.

D

Ki67 staining of xenografts. Tumor sections of each tumor of B) were stained with the Ki67 antibody; positive (brown) and negative (blue) nuclei were counted using Volocity software. HEY-IGF2 xenografts had a higher fraction of Ki67-positive nuclei, indicative of increased proliferation. Left photo, example of HEY-IGF2 tumor; right, HEY-EV. Average \pm SEM, * $p > 0.05$, ** $p > 0.01$, ns = non-significant by two-tailed t-test.

E

H&E staining of xenografts. Tumor sections of mice injected with 100,000 cells were stained with hematoxylin/eosin and analyzed by a pathologist. HEY-IGF2 xenograft sections (left photo) showed an increase in cells with a neutrophilic appearance (arrows, inset) in comparison to HEY-EV (right). Neutrophilic infiltration of the sections was quantified by a pathologist (right). Average \pm SEM, ** $p > 0.01$, by two-tailed t-test.

F

Xenograft growth of A2780-IGF2 and A2780-EV.

Similar to A) nude mice were injected with one million A2780-EV or A2780-IGF2 cells. Unlike HEY-IGF2, A2780-IGF2 xenografts did not show an increased growth rate (nine animals were injected for both groups, nine tumors developed from A2780-IGF2 and seven from A2780-EV). Average \pm SEM.

G

Tumor weight of each dilution at the termination of the experiment.

Similar to B) and C), either 100,000 or 10,000 A2780-IGF2 or A2780-EV cells were diluted in 50% matrigel and injected into nude mice. At the termination of the experiment (day 14 after

injection for 100,000 cells, day 19 for 10,000 cells), tumors were excised and weighed. No difference in tumor weight was observed at either dilution between the two groups (Average \pm SEM, n=4 for each dilution and each group).

H

Neutrophil infiltration in A2780-IGF2 xenografts. Similar to E) the pathologist quantified neutrophilic infiltration using H&E sections of A2780-IGF2 and A2780-EV xenografts. Very few infiltrating neutrophils were observed and there was no significant difference between the two groups. Average \pm SEM, n=4 for each group.

HEY-IGF2 conditioned media stimulates and attracts HL60 cells

Since xenografts showed differences in the involvement of mouse immune cells between HEY-IGF2 and HEY-EV, we wanted to confirm that human IGF2 stimulated mouse cells similar to human cells, considering similarity is 89% between the two species (Fig. 4A). When the mouse fibroblast cell line NIH-3T3 was stimulated with recombinant human IGF2 a clear activation of both AKT and ERK was observed by Western blot (Fig. 4B). Using the conditioned media of the HEY-IGF2 cells to stimulate the NIH-3T3 cells, phosphorylation of AKT at Threonine 308 increased, but not at Serine 473 or of ERK, likely due the lower concentration of IGF2 in the conditioned media as compared to the recombinant IGF2 (Fig. 4C). The IGF2 secreted by the HEY-IGF2 xenografts can clearly have effects on the surrounding mouse cells.

We hypothesized that the increase in secreted IGF2 of HEY-IGF2 xenografts could increase the infiltration of neutrophils in the tumor. To test this we used the human HL60 cell line, a precursor neutrophilic cell line from a patient with acute promyelocytic leukemia. HL60 cells were readily stimulated by both recombinant IGF2 and insulin and showed increased phosphorylation of IGF1R, AKT and ERK. The conditioned media of HEY-IGF2 had similar effects on HL60 stimulation, suggesting HEY-IGF2 cells could stimulate neutrophilic HL60 cells. This could be reversed by adding either the IGF2 antibody DX-2647 or the IGF1R antibody IMC-A12. ERK phosphorylation was not decreased by either antibody, suggesting other proteins present in the conditioned media also stimulated the ERK pathway (Fig 4D).

Since neutrophils appeared to be infiltrating the xenografts, we determined if HL60 cells migrate quicker towards the conditioned media of HEY-IGF2 when compared to HEY-EV. For this we set up a Boyden chamber assay with a membrane with 8 μm pores and let the HL60 cells migrate from the top through the membrane towards the conditioned media at the bottom for four hours. Significantly more HL60 cells migrated towards the HEY-IGF2 conditioned media than towards the conditioned media of HEY or HEY-EV cells. This effect could be reversed by adding either DX-2647 or IMC-A12 to the conditioned media, suggesting the IGF2 from the conditioned media is capable of attracting neutrophils (Fig. 4E). However, adding recombinant human IGF2 alone to the assay media did not induce significant more migration than just assay media, suggesting that mature IGF2 protein alone is not enough to induce more migration of HL60 cells.

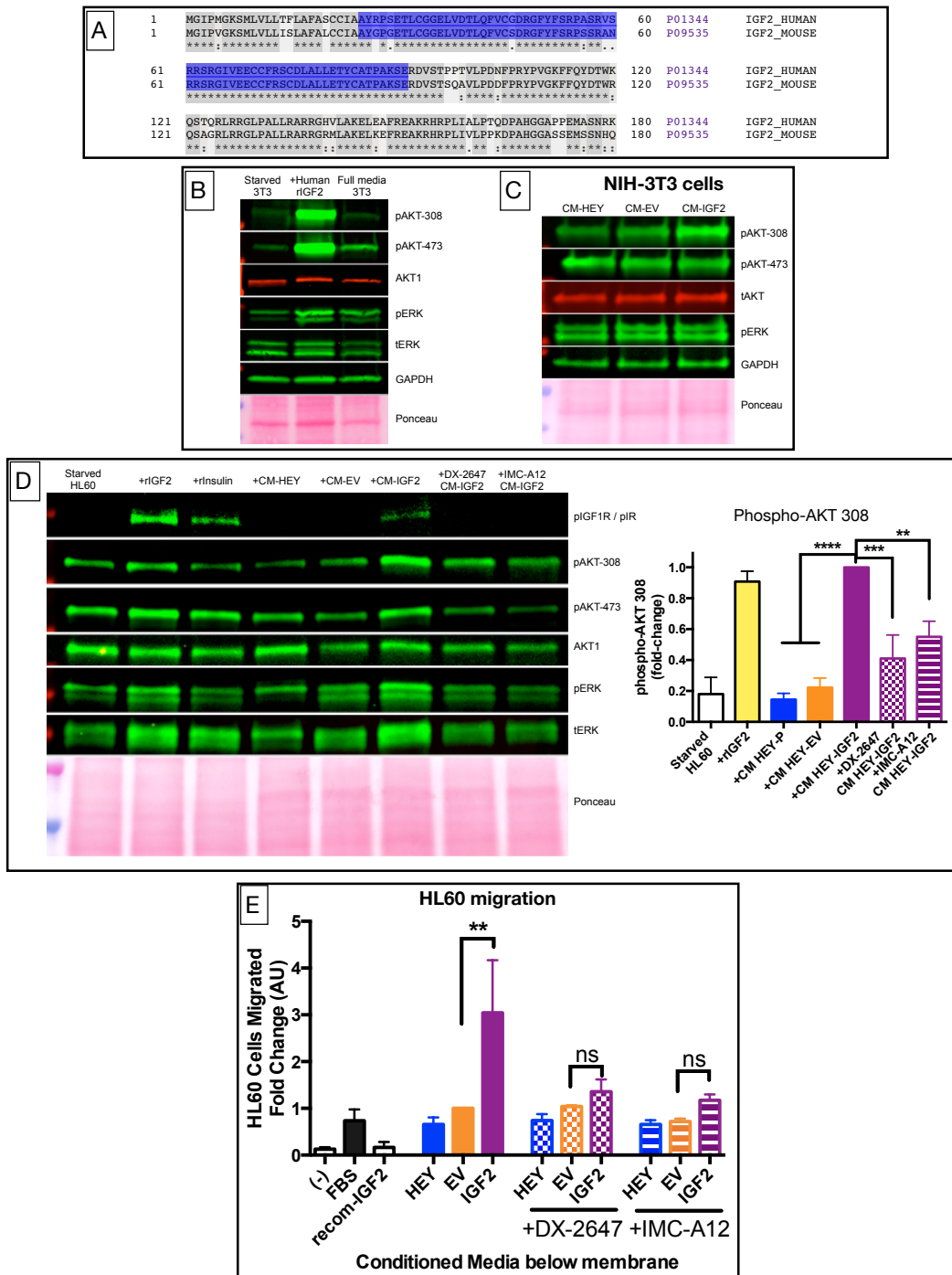


Figure 4

A
Comparison of amino acid sequence of human IGF2 and mouse Igf2. The amino acid sequences of human IGF2 (top) and mouse Igf2 (bottom) show a 89% similarity as determined

by Uniprot alignment. In blue is the mature IGF2 residues, gray shading and asterisks (*) indicate shared residues, colon (:) and period (.) indicate some similarity between residues.

B

Recombinant human IGF2 stimulation of mouse NIH-3T3 fibroblasts. NIH-3T3 cells were starved overnight and then stimulated with IGF2 50 ng/ml for 10 minutes. Cells were harvested, separated on a tris-glycine gel and the membrane blotted with the indicated antibodies. The human IGF2 was capable of stimulating mouse fibroblasts through both AKT and ERK phosphorylation. (n=2)

C

HEY-IGF2 conditioned media stimulation of NIH-3T3. Similar to B), Western blot of lysates of NIH-3T3 cells stimulated for 10 minutes with the conditioned media of transfected HEY cells. The conditioned media of HEY-IGF2 stimulates AKT phosphorylation on Threonine 308, but not on Serine 473. (n=2)

D

Precursor neutrophilic HL60 cells stimulation by HEY-IGF2 conditioned media. Human HL60 cells were starved overnight and then stimulated for 10 minutes with 50 ng/ml recombinant IGF2, 50 nM insulin or conditioned media from either HEY, HEY-EV or HEY IGF2 cells. Phosphorylation of the IGF1R/IR receptor along with AKT was observed with IGF2, insulin and HEY-IGF2 conditioned media. Phosphorylation of IGF1R and AKT was inhibited by concurrent treatment with the IGF2 antibody DX-2647 (10 nM) or the IGF1R antibody IMC-A12 (10 µg/ml). ERK phosphorylation was not inhibited, suggesting its activation was not only caused by IGF2. To the right, quantification of phospho-AKT 308 of at least three independent experiments. Average ±SEM, ** p<0.01, *** p<0.0001, **** p>0.0001 by one-way ANOVA with a Bonferroni post-test.

E

HL60 migration towards HEY-IGF2 conditioned media.

Conditioned media was prepared by incubating HEY cell lines for 72 hours in serum-free media. Overnight-starved HL60 cells (500,000 cells per well) were allowed to migrate for four hours across a membrane with 8 µm pores towards the conditioned media in a Boyden chamber assay. Cells present in the bottom conditioned media and the ones left in the top assay media were then counted. Significantly more HL60 cells migrated across the membrane if the attractant was HEY-IGF2 conditioned media when compared to HEY or HEY-EV media. This increase was attenuated by adding IMC-A12 (10 µg/ml) or DX-2647 (10 nM) to the HEY-IGF2 conditioned media. Recombinant human IGF2 (recom-IGF2, 50 ng/ml) alone could not replicate this increase. Averages of at least three independent experiments, average ±SEM, ** p<0.01 by one-way ANOVA with Bonferroni post-test.

GENERAL DISCUSSION

In this thesis we have further elucidated the role of IGF2 in ovarian cancer with three separate observations: a) Taxol treatment of ovarian cancer cells induces upregulation of *IGF2* and patients whose tumor sections stain more strongly for IGF2 have a worse prognosis; b) Three different ovarian cancer cell lines show upregulated *IGF2* in their chemoresistant counterparts and knocking down *IGF2* mRNA sensitizes these cell lines to their chemotherapies *in vitro* and *in vivo*; c) Overexpression of *IGF2* in HEY cells leads to an increased growth rate in xenografts, and attracts neutrophils *in vivo* and *in vitro*. Taken together, these results suggest a role for IGF2 in ovarian cancer.

At the genomic level, expression of *IGF2* is already exquisitely regulated: five promoters, 6 variants, maternal imprinting and extensive miRNA interactions give rise to two isoforms of the preproprotein (Mineo *et al*, 2000; Li *et al*, 2011). Then again on a protein level, processing consists of several steps, giving rise to a number of intermediary forms before finally reaching its 7.5 kDa mature protein. It is becoming increasingly clear that each form of the protein has physiological functions, not just the mature form (Greenall *et al*, 2013).

Once the protein in any of its forms is secreted from the cell, it is regulated on a macrostructural level by means of forming secondary and ternary structures with IGF-binding proteins and the Acid-Labile Subunit (Fukuda *et al*, 2006; Beauchamp *et al*, 2010). Finally, its ability to signal is determined by the receptors present on the cell membrane: binding to the IGF2 receptor does not result in survival/proliferation signaling, while binding to the IGF1,

insulin and their hybrid receptor does. The number of each of these receptors available on the membrane at any time is another level of regulation of IGF2 signaling (Holthuisen, 2003). This extensive control allows for a great variety of roles in physiological processes. Under non-pathological conditions IGF2's main function is in development, where it is essential for normal growth of the animal. In adults, IGF2 levels are low and the majority is produced in the liver (Ekstrom *et al*, 1995). However, as we and many others have shown, in cancer IGF2 has a role similar to that of an oncogene. In ovarian cancer its overexpression leads to a worse prognosis and it is the most common gene with a copy number increase in colorectal cancer (Sayer *et al*, 2005; Cancer Genome Atlas Network & Getz, 2012; Lui & Baron, 2013). This is not completely unexpected, as its signaling axis involves the PI3K/AKT and the MAPK pathways, long considered to be essential drivers of tumor growth (Livingstone, 2013). For all that we know of IGF2's function, many more questions remain to be answered and a complete understanding of its role in cancer is not understood.

In this thesis we have been able to determine that IGF2 is involved in the response to commonly-used chemotherapies in ovarian cancer. Treatment with Taxol rapidly increased *IGF2* mRNA in cell lines, while cell lines made resistant to either Taxol, ixabepilone, epothilone B or discodermolide all showed significantly increased basal levels of *IGF2* mRNA. Apparently the cells respond to the chemotherapeutic treatment by increasing the PI3K/AKT survival pathway through upregulation of *IGF2*. This suggests one reason why patients with ovarian tumors that express high *IGF2* have a worse prognosis: the tumor cells are better prepared to withstand treatment with cytostatic drugs. This is further supported by the fact that knocking down *IGF2* sensitizes the HEY-T30 to Taxol treatment both *in vitro* and

in vivo. Standard of care for ovarian cancer patients calls for only one cytoreductive surgery, normally before chemotherapy starts (Romero *et al*, 2012). On certain occasions, gynecologic oncologists can decide to do a second surgery after the disease recurs (Rawahi *et al*, 2013). We are currently collecting samples from ovarian cancer patients before and after chemotherapy and analyzing any possible differences in the IGF-axis. This will allow us to determine if IGF2 is important in the acquisition of chemoresistance. We also hypothesize that this analysis will give us predictive power as to how the patient might respond to chemotherapy.

On the other hand, overexpression of *IGF2* by itself was enough to increase the growth rate of xenografts of HEY cells. We observed two clear morphological differences between the HEY-EV and HEY-IGF2 xenografts: HEY-IGF2 xenografts had 1) more Ki67-positive staining cells, indicating increased proliferation, and 2) more neutrophilic cells infiltrating the tumors. The increase in proliferation was expected although not observed in cell culture. Since IGF2 stimulates the AKT and MAPK survival/proliferation pathways, it is expected that more IGF2 increases cellular proliferation (Marangoni *et al*, 2007). We showed that temporarily knocking down *IGF2* leads to a decrease in proliferation of resistant HEY-T30 and A2780-T15 cells, but constitutive knockdown of *IGF2* in HEY-T30 did not decrease proliferation compared to untransfected HEY-T30 cells. Similarly, constitutive overexpression of *IGF2* did not make HEY cells proliferate more rapidly. When cells are transfected, care is taken to isolate only the cells that were successfully transfected, albeit by FACS (HEY-IGF2) or by incubation with antibiotics (HEY-T30 shIGF2). These isolated populations are then grown up and used for further experiments. This has as a side effect that cell populations have an inherent bias towards cells that survive and proliferate better under standard cell culture conditions. This

gives the cells ample opportunity to adapt and compensate for either *IGF2* knockdown or overexpression. Another unwanted side effect of cell transfection, especially in HEY cells, is the upregulation of the p-glycoprotein (*ABCB1*), a drug efflux transporter that is involved in drug-resistance (Agarwal & Kaye, 2003). Even though we observed *ABCB1* upregulation in Taxol-resistant HEY-T30 cells, we were able to prove that knocking down only *IGF2*, sensitized the cells and xenografts to Taxol. This is encouraging since the development of *ABCB1* inhibitors has been disappointing because of little progression-free survival advantage and high toxicity (Zinzi *et al*, 2014). Xenografts of HEY-IGF2 cells grew faster than HEY-EV with or without matrigel at all injected cell numbers tested. It is interesting to note that even though *IGF2* is overexpressed several thousand times, it is not outside of physiological ranges. Our lab is currently developing a project with patient samples of carcinosarcoma of the uterus and high levels of *IGF2* mRNA are detected in the tumors of these patients as well (unpublished data).

As described, the *IGF2*-overexpressing construct contains only the three protein-coding exons and not the other 6 exons. So even though the whole preproprotein is expressed from the construct, isoform 2 is not, and any other transcription regulation by the other exons is also lost. Not much is known on how IGF2 function might be altered by isoform 2 and the non-coding exons, and this area invites future investigation.

One surprising observation we made was the increased infiltration of neutrophils in the HEY-IGF2 xenografts when compared to HEY-EV xenografts. Little has been described about the interaction of IGF2 signaling and the immune system. Ganitumab (AMG974), a humanized monoclonal antibody against IGF1R similar to IMC-A12, when used to treat nude mice led to

a significant decrease in neutrophils in the blood as determined by flow cytometry (Moody *et al*, 2014). Since this antibody inhibits IGF1R signaling and *IGF2* overexpression increases IGF1R signaling, our observation of increased neutrophils in tumor tissue is reasonable. Neutrophils have been described to aid in metastasis and tumor development (Swierczak *et al*, 2014; Wang *et al*, 2014). Through chemokines secreted by the tumor, such as CXCL1/2, neutrophils, which have the receptor CXCR2, are recruited and aid tumor cells in metastasis and in chemoresistance (Acharyya *et al*, 2012). Other suggested functions of attracted neutrophils include tumor angiogenesis, extravasation and increased invasiveness (Gregory & Houghton, 2011). Different immunologic cells have been more widely described to be involved in tumor progression. Tumor-associated macrophages are attracted to the tumor through the secretion of certain chemokines, such as Colony-Stimulating Factor (CSF), by the tumor cells. Macrophages have the CSF-receptor and migrate towards hypoxic areas in the tumor. They then can assist the tumor through several means: through the secretion of angiogenic factors, they increase blood vessel formation; through the production of proteases, they induce invasion of the tumor cells into the surrounding stromal tissue; and through the production of growth factors, they increase the intravasation of the tumor cells into the circulation. Among the growth factors that have been described to form part of these processes are VEGF, EGF and TGF- β (Pollard, 2004). It is important to note that another ovarian cancer cell line (A2780) transfected with exactly the same vectors did not show the same effects as the HEY-IGF2 cells. The tumors did not grow more quickly and did not show neutrophil infiltration. Along with this observation goes the fact that even though conditioned media of HEY-IGF2 cells attracted more neutrophilic HL60 cells, recombinant IGF2 protein had no

effect. This suggests that mature IGF2 alone is not enough to cause the observed effects. *IGF2* overexpression in HEY cells could possibly lead to secretion of other factors that attract neutrophils, or the processing of the IGF2 protein in the HEY-IGF2 cells might explain this difference. The exact mechanism as to how the neutrophils are attracted to *IGF2*-overexpressing HEY and not to A2780 cells and what their role is in our tumor model, still needs further investigation. HL60 cells were less attracted towards conditioned media when the IGF1R antibody IMC-A12 was added, suggesting the necessity of IGF2 stimulation of the IGF1R for neutrophil attraction. However, IGF1R showed to be of little importance in our Taxol-resistant HEY-T30 model, as no difference in sensitivity and tumor growth was observed when mice were treated with IMC-A12. Even though HEY-T30 cells overexpress *IGF2*, through multiple rounds of selection they have acquired several mechanisms of drug resistance, such as the ABCB1 overexpression described in this thesis. The *IGF2*-overexpressing HEY xenograft is a completely distinct model that is engineered to only overexpress *IGF2*. Until now we are unable to tell which model relates more to patients in the clinic and therefore studying both models gives additional insights. Future xenograft experiments with HEY-IGF2 and IMC-A12 will determine the role of IGF2 in neutrophil attraction, while experiments with tumor tissue from patients will aid in determining which of our observations are more relevant in the clinic.

Even though we can say with high confidence that IGF2 has a substantial role in the development of certain tumors and affects treatment, how to translate this to the clinical situation is more complicated. Extensive development has been done on the inhibition of IGF2's main receptor, the IGF1R, through antibodies and small molecules. Several companies

were able to start clinical trials of these drugs, but none have shown much promise in phase II trials (Abou-Alfa *et al*, 2014; Philip *et al*, 2014). Complications are multiple. Patients that receive these medications are usually not tested for specific activation of the IGF-axis, so both patients whose tumors depend on IGF-signaling and those that do not receive the same experimental treatment, diluting any benefit the antibodies or small-molecule inhibitors might have.

IGF2 can also signal through the two isoforms of the insulin receptor and the hybrid IR-A/IGF1R receptor (Greenall *et al*, 2013). If the IGF1R is inhibited it is likely that the tumor cells will quickly compensate through either the insulin receptor or the hybrid receptor. Even though co-inhibition of the insulin receptor and the IGF1R would resolve this compensation, IR-B signaling is essential for the metabolic stasis of the cell and the patient would suffer from diabetes-like symptoms if this signaling was lost (Yee, 2012). This problem was also seen with small-molecule inhibitors that target the ATP-binding site of IGF1R, such as NVP-AEW541.

Because the high similarity between the insulin receptor and IGF1R, IGF1R inhibition unavoidably led to inhibition of IR as well, resulting in high toxicities (Arcaro, 2013).

IGF2 targeting would avoid these problems, especially since non-pathological functions of IGF2 in adults seem to be of low importance (Chao & D'Amore, 2008). As explained previously, IGF2 appears in several ways: in different intermediaries of processing and in different secondary and ternary structures. The humanized antibody for IGF2 used in this thesis (DX-2647), binds to the different intermediaries of IGF2, but is unable to bind to IGF2 when it forms a secondary structure with IGF-binding proteins or a ternary structure with the Acid-Labile Subunit (Dransfield *et al*, 2010). This antibody would only be effective if the

tumor secreted large quantities of IGF2 in a paracrine fashion, without IGF2 being able to form these structures.

A more complete understanding of IGF2, i.e. which size of protein and transcription from which promoters are most important for tumors, will allow development of more precise therapeutics.

CONCLUSIONS

From the data presented here we can conclude that IGF2 has an important role in the growth and the response to treatment of ovarian tumors. We also see the possibility of using IGF2 signaling as a target for developing new treatment for ovarian cancer. To accomplish that, we will focus on the use of patient samples to develop models to test new drug combinations. This is essential as we have shown that IGF2 signaling is closely involved with the tumor micro-environment. Since we have also shown that chemotherapy affects IGF2 signaling, we will determine signaling differences in chemo-naïve and recurrent tumor samples from the same patient. Finally, as we and others have shown, IGF2 is predictive of patient outcome and as such we will continue to investigate how IGF2 can be used to optimize treatment for patients.

REFERENCES

- Abou-Alfa GK, Capanu M, O'Reilly EM, Ma J, Chou JF, Gansukh B, Shia J, Kalin M, Katz S, Abad L, Reidy-Lagunes DL, Kelsen DP, Chen HX, Saltz LB (2014) A phase II study of cixutumumab (IMC-A12, NSC742460) in advanced hepatocellular carcinoma. *J Hepatol* **60**: 319–324 doi:10.1016/j.jhep.2013.09.008.
- Acharyya S, Oskarsson T, Vanharanta S, Malladi S, Kim J, Morris PG, Manova-Todorova K, Leversha M, Hogg N, Seshan VE, Norton L, Brogi E, Massagué J (2012) A CXCL1 paracrine network links cancer chemoresistance and metastasis. *Cell* **150**: 165–178 doi:10.1016/j.cell.2012.04.042.
- Agarwal R, Kaye SB (2003) Ovarian cancer: strategies for overcoming resistance to chemotherapy. *Nat Rev Cancer* **3**: 502–516 doi:10.1038/nrc1123.
- Amit D, Hochberg A (2010) Development of targeted therapy for bladder cancer mediated by a double promoter plasmid expressing diphtheria toxin under the control of H19 and IGF2-P4 regulatory sequences. *J Transl Med* **8**: 134 doi:10.1186/1479-5876-8-134.
- Amit D, Tamir S, Hochberg A (2013) Development of targeted therapy for a broad spectrum of solid tumors mediated by a double promoter plasmid expressing diphtheria toxin under the control of IGF2-P4 and IGF2-P3 regulatory sequences. *Int J Clin Exp Med* **6**: 110–118.
- Andersen MR, Goff BA, Lowe KA, Scholler N, Bergan L, Drescher CW, Paley P, Urban N (2008) Combining a symptoms index with CA 125 to improve detection of ovarian cancer. *Cancer* **113**: 484–489 doi:10.1002/cncr.23577.
- Arcaro A (2013) Targeting the insulin-like growth factor-1 receptor in human cancer. *Front Pharmacol* **4**: 30 doi:10.3389/fphar.2013.00030.
- Baker J, Liu JP, Robertson EJ, Efstratiadis A (1993) Role of insulin-like growth factors in embryonic and postnatal growth. *Cell* **75**: 73–82.
- Ballester M, Castelló A, Ibáñez E, Sánchez A, Folch JM (2004) Real-time quantitative PCR-based system for determining transgene copy number in transgenic animals. *BioTechniques* **37**: 610–613.
- Barreyro L, Will B, Bartholdy B, Zhou L, Todorova TI, Stanley RF, Ben-Neriah S, Montagna C, Parekh S, Pellagatti A, Boulwood J, Paietta E, Ketterling RP, Cripe L, Fernandez HF, Greenberg PL, Tallman MS, Steidl C, Mitsiades CS, Verma A, Steidl U (2012) Overexpression of IL-1 receptor accessory protein in stem and progenitor cells and outcome correlation in AML and MDS. *Blood* **120**: 1290–1298 doi:10.1182/blood-2012-01-404699.

Bast RC, Spriggs DR (2011) More than a biomarker: CA125 may contribute to ovarian cancer pathogenesis. *Gynecol Oncol* **121**: 429–430 doi:10.1016/j.ygyno.2011.04.032.

Beauchamp M-C, Yasmeeen A, Knafo A, Gotlieb WH (2010) Targeting insulin and insulin-like growth factor pathways in epithelial ovarian cancer. *J Oncol* **2010**: 257058 doi:10.1155/2010/257058.

Belfiore A, Frasca F, Pandini G, Sciacca L, Vigneri R (2009) Insulin receptor isoforms and insulin receptor/insulin-like growth factor receptor hybrids in physiology and disease. *Endocr Rev* **30**: 586–623 doi:10.1210/er.2008-0047.

Beltran PJ, Calzone FJ, Mitchell P, Chung Y-A, Cajulis E, Moody G, Belmontes B, Li C-M, Vonderfecht S, Velculescu VE, Yang G, Qi J, Slamon DJ, Konecny GE (2014) Ganitumab (AMG 479) inhibits IGF-II-dependent ovarian cancer growth and potentiates platinum-based chemotherapy. *Clin Cancer Res* **20**: 2947–2958 doi:10.1158/1078-0432.CCR-13-3448.

Berns EMJJ, Berns EMJJ, Bowtell DD, Bowtell DD (2012) The changing view of high-grade serous ovarian cancer. *Cancer Res* **72**: 2701–2704 doi:10.1158/0008-5472.CAN-11-3911.

Bookman MA, Brady MF, McGuire WP, Harper PG, Alberts DS, Friedlander M, Colombo N, Fowler JM, Argenta PA, De Geest K, Mutch DG, Burger RA, Swart AM, Trimble EL, Accario-Winslow C, Roth LM (2009) Evaluation of new platinum-based treatment regimens in advanced-stage ovarian cancer: a Phase III Trial of the Gynecologic Cancer Intergroup. *J Clin Oncol* **27**: 1419–1425 doi:10.1200/JCO.2008.19.1684.

Brouwer-Visser J, Lee J, McCullagh K, Cossio MJ, Wang Y, Huang GS (2014) Insulin-Like Growth Factor 2 Silencing Restores Taxol Sensitivity in Drug Resistant Ovarian Cancer. *PLoS ONE* **9**: e100165 doi:10.1371/journal.pone.0100165.

Bruchim I, Sarfstein R, Werner H (2014) The IGF Hormonal Network in Endometrial Cancer: Functions, Regulation, and Targeting Approaches. *Front Endocrinol* **5**: 76 doi:10.3389/fendo.2014.00076.

Buick RN, Pullano R, Trent JM (1985) Comparative properties of five human ovarian adenocarcinoma cell lines. *Cancer Res* **45**: 3668–3676.

Burger RA, Brady MF, Bookman MA, Fleming GF, Monk BJ, Huang H, Mannel RS, Homesley HD, Fowler J, Greer BE, Boente M, Birrer MJ, Liang SX, Gynecologic Oncology Group (2011) Incorporation of bevacizumab in the primary treatment of ovarian cancer. *N Engl J Med* **365**: 2473–2483 doi:10.1056/NEJMoa1104390.

Cancer Genome Atlas Network, Getz G (2012) Comprehensive molecular characterization of human colon and rectal cancer. *Nature* **487**: 330–337 doi:10.1038/nature11252.

Cancer Genome Atlas Research Network (2011) Integrated genomic analyses of ovarian carcinoma. *Nature* **474**: 609–615 doi:10.1038/nature10166.

Chao W, D'Amore PA (2008) IGF2: epigenetic regulation and role in development and disease. *Cytokine Growth Factor Rev* **19**: 111–120 doi:10.1016/j.cytogfr.2008.01.005.

Coleman RL, Monk BJ, Sood AK, Herzog TJ (2013) Latest research and treatment of advanced-stage epithelial ovarian cancer. *Nat Rev Clin Oncol* **10**: 211–224 doi:10.1038/nrclinonc.2013.5.

Cui H, Cruz-Correa M, Giardiello FM, Hutcheon DF, Kafonek DR, Brandenburg S, Wu Y, He X, Powe NR, Feinberg AP (2003) Loss of IGF2 imprinting: a potential marker of colorectal cancer risk. *Science* **299**: 1753–1755 doi:10.1126/science.1080902.

Dai Y, Wang Z, Li J, Gu X, Zheng M, Zhou J, Ye X, Yao J, Cui I, Hu Y, Cui H (2007) Imprinting Status of IGF2 in Cord Blood Cells of Han Chinese Newborns. *International Journal of Molecular Sciences* 2007, Vol 8, Pages 273-283 **8**: 273–283 doi:10.3390/i8040273.

Dallas NA, Xia L, Fan F, Gray MJ, Gaur P, van Buren G, Samuel S, Kim MP, Lim SJ, Ellis LM (2009) Chemoresistant colorectal cancer cells, the cancer stem cell phenotype, and increased sensitivity to insulin-like growth factor-I receptor inhibition. *Cancer Res* **69**: 1951–1957 doi:10.1158/0008-5472.CAN-08-2023.

DEIS-MINSAL Defunciones por Tumores Malignos según Sexo, Chile 1997-2011.
www.deis.cl

Dransfield DT, Cohen EH, Chang Q, Sparrow LG, Bentley JD, Dolezal O, Xiao X, Peat TS, Newman J, Pilling PA, Phan T, Priebe I, Brierley GV, Kastrapeli N, Kopacz K, Martik D, Wassaf D, Rank D, Conley G, Huang Y, Adams TE, Cosgrove L (2010) A Human Monoclonal Antibody against Insulin-Like Growth Factor-II Blocks the Growth of Human Hepatocellular Carcinoma Cell Lines In vitro and In vivo. *Mol Cancer Ther* **9**: 1809–1819 doi:10.1158/1535-7163.MCT-09-1134.

Duan Z, Brakora KA, Seiden MV (2004) Inhibition of ABCB1 (MDR1) and ABCB4 (MDR3) expression by small interfering RNA and reversal of paclitaxel resistance in human ovarian cancer cells. *Mol Cancer Ther* **3**: 833–838.

Dudek H, Datta SR, Franke TF, Birnbaum MJ, Yao R, Cooper GM, Segal RA, Kaplan DR, Greenberg ME (1997) Regulation of neuronal survival by the serine-threonine protein kinase Akt. *Science* **275**: 661–665.

Duguay SJ, Jin Y, Stein J, Duguay AN, Gardner P, Steiner DF (1998) Post-translational processing of the insulin-like growth factor-2 precursor. Analysis of O-glycosylation and endoproteolysis. *J Biol Chem* **273**: 18443–18451 doi:10.1074/jbc.273.29.18443.

- Dumontet C, Jordan MA, Lee FFY (2009) Ixabepilone: targeting betaIII-tubulin expression in taxane-resistant malignancies. *Mol Cancer Ther* **8**: 17–25 doi:10.1158/1535-7163.MCT-08-0986.
- Eckstein N, Servan K, Hildebrandt B, Politz A, Jonquieres GV, Wolf-Kummeth S, Napierski I, Hamacher A, Kassack MU, Budczies J, Beier M, Dietel M, Royer-Pokora B, Denkert C, Royer HD (2009) Hyperactivation of the Insulin-like Growth Factor Receptor I Signaling Pathway Is an Essential Event for Cisplatin Resistance of Ovarian Cancer Cells. *Cancer Res* **69**: 2996–3003 doi:10.1158/0008-5472.CAN-08-3153.
- Ekstrom TJ, Cui H, Li X, Ohlsson R (1995) Promoter-specific IGF2 imprinting status and its plasticity during human liver development. *Development* **121**: 309–316.
- Erickson BK, Conner MG, Landen CN (2013) The role of the fallopian tube in the origin of ovarian cancer. *Am J Obstet Gynecol* **209**: 409–414 doi:10.1016/j.ajog.2013.04.019.
- Eva A, Robbins KC, Andersen PR, Srinivasan A, Tronick SR, Reddy EP, Ellmore NW, Galen AT, Lautenberger JA, Papas TS, Westin EH, Wong-Staal F, Gallo RC, Aaronson SA (1982) Cellular genes analogous to retroviral onc genes are transcribed in human tumour cells. *Nature* **295**: 116–119.
- Fukuda I, Hizuka N, Ishikawa Y, Yasumoto K, Murakami Y, Sata A, Morita J, Kurimoto M, Okubo Y, Takano K (2006) Clinical features of insulin-like growth factor-II producing non-islet-cell tumor hypoglycemia. *Growth Horm IGF Res* **16**: 211–216 doi:10.1016/j.ghir.2006.05.003.
- Fung-Kee-Fung M, Oliver T, Elit L, Oza A, Hirte HW, Bryson P (2007) Optimal chemotherapy treatment for women with recurrent ovarian cancer. *Curr Oncol* **14**: 195–208.
- Gallagher EJ, LeRoith D (2011) Minireview: IGF, Insulin, and Cancer. *Endocrinology* **152**: 2546–2551 doi:10.1210/en.2011-0231.
- Gao J, Chesebrough JW, Cartlidge SA, Ricketts S-A, Incognito L, Veldman-Jones M, Blakey DC, Tabrizi M, Jallal B, Trail PA, Coats S, Bosslet K, Chang YS (2011) Dual IGF-I/II–Neutralizing Antibody MEDI-573 Potently Inhibits IGF Signaling and Tumor Growth. *Cancer Res* **71**: 1029–1040 doi:10.1158/0008-5472.CAN-10-2274.
- Gao W, Gu Y, Li Z, Cai H, Peng Q, Tu M, Kondo Y, Shinjo K, Zhu Y, Zhang J, Sekido Y, Han B, Qian Z, Miao Y (2014) miR-615-5p is epigenetically inactivated and functions as a tumor suppressor in pancreatic ductal adenocarcinoma. *Oncogene* **0**: doi:10.1038/onc.2014.101.
- García-Echeverría C, Pearson MA, Marti A, Meyer T, Mestan J, Zimmermann J, Gao J, Brueggen J, Capraro H-G, Cozens R, Evans DB, Fabbro D, Furet P, Porta DG, Liebetanz J, Martiny-Baron G, Ruetz S, Hofmann F (2004) In vivo antitumor activity of NVP-AEW541-A

novel, potent, and selective inhibitor of the IGF-IR kinase. *Cancer Cell* **5**: 231–239 doi: 10.1038/nrc1352.

Garofalo C, Manara MC, Nicoletti G, Marino MT, Lollini P-L, Astolfi A, Pandini G, López-Guerrero JA, Schaefer K-L, Belfiore A, Picci P, Scotlandi K (2011) Efficacy of and resistance to anti-IGF-1R therapies in Ewing's sarcoma is dependent on insulin receptor signaling. *Oncogene* **30**: 2730–2740 doi:10.1038/onc.2010.640.

Gebeshuber CA, Martinez J (2013) miR-100 suppresses IGF2 and inhibits breast tumorigenesis by interfering with proliferation and survival signaling. *Oncogene* **32**: 3306–3310 doi:10.1038/onc.2012.372.

Giannakakou P, Nakano M, Nicolaou KC, O'Brate A, Yu J, Blagosklonny MV, Greber UF, Fojo T (2002) Enhanced microtubule-dependent trafficking and p53 nuclear accumulation by suppression of microtubule dynamics. *Proc Natl Acad Sci USA* **99**: 10855–10860 doi:10.1073/pnas.132275599.

Goodman HM, Harlow BL, Sheets EE, Muto MG, Brooks S, Steller M, Knapp RC, Berkowitz RS (1992) The role of cytoreductive surgery in the management of stage IV epithelial ovarian carcinoma. *Gynecol Oncol* **46**: 367–371 doi:10.1016/0090-8258(92)90234-A.

Gotlieb WH, Bruchim I, Gu J, Shi Y, Camirand A, Blouin M-J, Zhao Y, Pollak MN (2006) Insulin-like growth factor receptor I targeting in epithelial ovarian cancer. *Gynecol Oncol* **100**: 389–396 doi:10.1016/j.ygyno.2005.09.048.

Greenall SA, Bentley JD, Pearce LA, Scoble JA, Sparrow LG, Bartone NA, Xiao X, Baxter RC, Cosgrove LJ, Adams TE (2013) Biochemical characterization of individual human glycosylated pro-insulin-like growth factor (IGF)-II and big-IGF-II isoforms associated with cancer. *J Biol Chem* **288**: 59–68 doi:10.1074/jbc.M112.432013.

Gregory AD, Houghton AM (2011) Tumor-associated neutrophils: new targets for cancer therapy. *Cancer Res* **71**: 2411–2416 doi:10.1158/0008-5472.CAN-10-2583.

Haley VL, Barnes DJ, Sandovici I, Constancia M, Graham CF, Pezzella F, Bühnemann C, Carter EJ, Hassan AB (2012) IGF2 pathway dependency of the Trp53 developmental and tumour phenotypes. *EMBO Mol Med* **4**: 705–718 doi:10.1002/emmm.201101105.

Haluska P, Carboni JM, TenEyck C, Attar RM, Hou X, Yu C, Sagar M, Wong TW, Gottardis MM, Erlichman C (2008) HER receptor signaling confers resistance to the insulin-like growth factor-I receptor inhibitor, BMS-536924. *Mol Cancer Ther* **7**: 2589–2598 doi: 10.1158/1535-7163.MCT-08-0493.

Hamilton TC, Young RC, Ozols RF (1984) Experimental model systems of ovarian cancer: applications to the design and evaluation of new treatment approaches. *Semin Oncol* **11**: 285–298.

Harris LK, Westwood M (2012) Biology and significance of signalling pathways activated by IGF-II. *Growth Factors* **30**: 1–12 doi:10.3109/08977194.2011.640325.

He L, Jagtap PG, Kingston DG, Shen HJ, Orr GA, Horwitz SB (2000) A common pharmacophore for Taxol and the epothilones based on the biological activity of a taxane molecule lacking a C-13 side chain. *Biochemistry* **39**: 3972–3978 doi:10.1021/bi992518p.

He L, Yang CP, Horwitz SB (2001) Mutations in beta-tubulin map to domains involved in regulation of microtubule stability in epothilone-resistant cell lines. *Mol Cancer Ther* **1**: 3–10 doi:10.1038/277665a0.

Hellström I, Raycraft J, Hayden-Ledbetter M, Ledbetter JA, Schummer M, McIntosh M, Drescher C, Urban N, Hellström KE (2003) The HE4 (WFDC2) protein is a biomarker for ovarian carcinoma. *Cancer Res* **63**: 3695–3700 doi:10.1002/1097-0142(19951115)76:10+<2092::AID-CNCR2820761331>3.0.CO;2-T.

Hizuka N, Fukuda I, Takano K, Okubo Y, Asakawa-Yasumoto K, Demura H (1998) Serum insulin-like growth factor II in 44 patients with non-islet cell tumor hypoglycemia. *Endocr J* **45 Suppl**: S61–S65.

Holthuizen PE (2003) The Many Levels of Control of IGF-II Expression. In *Insulin-Like Growth Factors*, (Eurekah.com and Kluwer Academic / Plenum Publishers), pp. 91–103.

Hope-Roberts M, Horobin RW, Wainwright M (2011) Identifying apoptotic cells with the 3-hydroxyflavone derivative F2N12S, a ratiometric fluorescent small molecule probe selective for plasma membranes: a possible general mechanism for selective uptake into apoptotic cells. *Biotech Histochem* **86**: 255–261 doi:10.3109/10520291003723426.

Horwitz SB (1994) Taxol (paclitaxel): mechanisms of action. *Ann Oncol* **5 Suppl 6**: S3–S6.

Howlander N, Noone A, Krapcho M, Garshell J, Miller D, Altekruse SF, Kosary CL, Yu M, Ruhl J, Tatalovich Z, Mariotto A, Lewis DR, Chen HS, Feuer EJ, Cronin KA (2014) SEER Cancer Statistics Review, 1975-2011. seer.cancer.gov

Hu L, Hofmann J, Lu Y, Mills GB, Jaffe RB (2002) Inhibition of phosphatidylinositol 3'-kinase increases efficacy of paclitaxel in in vitro and in vivo ovarian cancer models. *Cancer Res* **62**: 1087–1092.

Huang GS, Brouwer-Visser J, Ramirez MJ, Kim CH, Hebert TM, Lin J, Arias-Pulido H, Qualls CR, Prossnitz ER, Goldberg GL, Smith HO, Horwitz SB (2010) Insulin-like Growth

Factor 2 Expression Modulates Taxol Resistance and Is a Candidate Biomarker for Reduced Disease-Free Survival in Ovarian Cancer. *Clin Cancer Res* **16**: 2999–3010 doi:10.1158/1078-0432.CCR-09-3233.

Huang GS, Lopez-Barcons L, Freeze BS, Smith AB, Goldberg GL, Horwitz SB, McDaid HM (2006) Potentiation of taxol efficacy and by discodermolide in ovarian carcinoma xenograft-bearing mice. *Clin Cancer Res* **12**: 298–304 doi:10.1158/1078-0432.CCR-05-0229.

Huang Y-F, Cheng W-F, Wu Y-P, Cheng Y-M, Hsu K-F, Chou C-Y (2014) Circulating IGF system and treatment outcome in epithelial ovarian cancer. *Endocr Relat Cancer* **21**: 217–229 doi:10.1530/ERC-13-0274.

Jainchill JL, Aaronson SA, Todaro GJ (1969) Murine sarcoma and leukemia viruses: assay using clonal lines of contact-inhibited mouse cells. *J Virol* **4**: 549–553.

Jordan MA, Wilson L (2004) Microtubules as a target for anticancer drugs. *Nat Rev Cancer* **4**: 253–265 doi:10.1038/nrc1317.

Kanatsuna N, Taneera J, Vaziri-Sani F, Wierup N, Larsson HE, Delli A, Skärstrand H, Balhuizen A, Bennet H, Steiner DF, Törn C, Fex M, Lernmark Å (2013) Autoimmunity against INS-IGF2 protein expressed in human pancreatic islets. *J Biol Chem* **288**: 29013–29023 doi:10.1074/jbc.M113.478222.

Kavallaris M (2010) Microtubules and resistance to tubulin-binding agents. *Nat Rev Cancer* **10**: 194–204 doi:10.1038/nrc2803.

Kim J, Coffey DM, Creighton CJ, Yu Z, Hawkins SM, Matzuk MM (2012) High-grade serous ovarian cancer arises from fallopian tube in a mouse model. *Proc Natl Acad Sci USA* **109**: 3921–3926 doi:10.1073/pnas.1117135109.

Klein LE, Freeze BS, Smith AB, Horwitz SB (2005) The microtubule stabilizing agent discodermolide is a potent inducer of accelerated cell senescence. *Cell Cycle* **4**: 501–507.

Kulik G, Klippel A, Weber MJ (1997) Antiapoptotic signalling by the insulin-like growth factor I receptor, phosphatidylinositol 3-kinase, and Akt. *Mol Cell Biol* **17**: 1595–1606.

Kurman RJ (2013) Origin and molecular pathogenesis of ovarian high-grade serous carcinoma. *Annals of Oncology* **24 Suppl 10**: x16–x21 doi:10.1093/annonc/mdt463.

Lancaster JM, Dressman HK, Whitaker RS, Havrilesky L, Gray J, Marks JR, Nevins JR, Berchuck A (2004) Gene expression patterns that characterize advanced stage serous ovarian cancers. *J Soc Gynecol Investig* **11**: 51–59.

- Landen CN, Birrer MJ, Sood AK (2008) Early events in the pathogenesis of epithelial ovarian cancer. *J Clin Oncol* **26**: 995–1005 doi:10.1200/JCO.2006.07.9970.
- Lee AV, Darbre P, King RJB (1994) Processing of insulin-like growth factor-II (IGF-II) by human breast cancer cells. *Molecular and Cellular Endocrinology* **99**: 211–220 doi:10.1016/0303-7207(94)90010-8.
- Lee Y, Miron A, Drapkin R, Nucci MR, Medeiros F, Saleemuddin A, Garber J, Birch C, Mou H, Gordon RW, Cramer DW, McKeon FD, Crum CP (2007) A candidate precursor to serous carcinoma that originates in the distal fallopian tube. *J Pathol* **211**: 26–35 doi:10.1002/path.2091.
- Li B, Tsao SW, Chan KW, Ludwig DL, Novosyadlyy R, Li YY, He QY, Cheung ALM (2014a) Id1-induced IGF-II and its autocrine/endocrine promotion of esophageal cancer progression and chemoresistance--implications for IGF-II and IGF-IR-targeted therapy. *Clin Cancer Res* **20**: 2651–2662 doi:10.1158/1078-0432.CCR-13-2735.
- Li J, Neumann I, Volkmer I, Staeger MS (2011) Down-regulation of achaete-scute complex homolog 1 (ASCL1) in neuroblastoma cells induces up-regulation of insulin-like growth factor 2 (IGF2). *Mol Biol Rep* **38**: 1515–1521 doi:10.1007/s11033-010-0259-z.
- Li X, Nadauld L, Ootani A, Corney DC, Pai RK, Gevaert O, Cantrell MA, Rack PG, Neal JT, Chan CW-M, Yeung T, Gong X, Yuan J, Wilhelmy J, Robine S, Attardi LD, Plevritis SK, Hung KE, Chen C-Z, Ji HP, Kuo CJ (2014b) Oncogenic transformation of diverse gastrointestinal tissues in primary organoid culture. *Nat Med* **20**: 769–777 doi:10.1038/nm.3585.
- Liu JP, Baker J, Perkins AS, Robertson EJ, Efstratiadis A (1993) Mice carrying null mutations of the genes encoding insulin-like growth factor I (Igf-1) and type 1 IGF receptor (Igf1r). *Cell* **75**: 59–72.
- Liu M, Roth A, Yu M, Morris R, Bersani F, Rivera MN, Lu J, Shioda T, Vasudevan S, Ramaswamy S, Maheswaran S, Diederichs S, Haber DA (2013) The IGF2 intronic miR-483 selectively enhances transcription from IGF2 fetal promoters and enhances tumorigenesis. *Genes Dev* **27**: 2543–2548 doi:10.1101/gad.224170.113.
- Livingstone C (2013) IGF2 and cancer. *Endocr Relat Cancer* **20**: R321–R339 doi:10.1530/ERC-13-0231.
- Lu L, Katsaros D, Wiley A, Rigault de la Longrais IA, Risch HA, Puopolo M, Yu H (2006) The relationship of insulin-like growth factor-II, insulin-like growth factor binding protein-3, and estrogen receptor-alpha expression to disease progression in epithelial ovarian cancer. *Clin Cancer Res* **12**: 1208–1214 doi:10.1158/1078-0432.CCR-05-1801.

Ludwig T, Eggenschwiler J, Fisher P, D'Ercole AJ, Davenport ML, Efstratiadis A (1996) Mouse mutants lacking the type 2 IGF receptor (IGF2R) are rescued from perinatal lethality in *Igf2* and *Igf1r* null backgrounds. *Dev Biol* **177**: 517–535 doi:10.1006/dbio.1996.0182.

Lui JC, Baron J (2013) Evidence that *Igf2* down-regulation in postnatal tissues and up-regulation in malignancies is driven by transcription factor E2f3. *Proc Natl Acad Sci USA* **110**: 6181–6186 doi:10.1073/pnas.1219079110.

Luo Y, Shoemaker AR, Liu X, Woods KW, Thomas SA, de Jong R, Han EK, Li T, Stoll VS, Powlas JA, Oleksijew A, Mitten MJ, Shi Y, Guan R, McGonigal TP, Klinghofer V, Johnson EF, Levenson JD, Bouska JJ, Mamo M, Smith RA, Gramling-Evans EE, Zinker BA, Mika AK, Nguyen PT, Oltersdorf T, Rosenberg SH, Li Q, Giranda VL (2005) Potent and selective inhibitors of Akt kinases slow the progress of tumors in vivo. *Mol Cancer Ther* **4**: 977–986 doi:10.1158/1535-7163.MCT-05-0005.

Mabuchi S, Ohmichi M, Kimura A, Hisamoto K, Hayakawa J, Nishio Y, Adachi K, Takahashi K, Arimoto-Ishida E, Nakatsuji Y, Tasaka K, Murata Y (2002) Inhibition of phosphorylation of BAD and Raf-1 by Akt sensitizes human ovarian cancer cells to paclitaxel. *J Biol Chem* **277**: 33490–33500 doi:10.1074/jbc.M204042200.

Maenhaut C, Dumont JE, Roger PP, van Staveren WCG (2010) Cancer stem cells: a reality, a myth, a fuzzy concept or a misnomer? An analysis. *Carcinogenesis* **31**: 149–158 doi:10.1093/carcin/bgp259.

Manara MC, Landuzzi L, Nanni P, Nicoletti G, Zambelli D, Lollini PL, Nanni C, Hofmann F, García-Echeverría C, Picci P, Scotlandi K (2007) Preclinical in vivo study of new insulin-like growth factor-I receptor--specific inhibitor in Ewing's sarcoma. *Clin Cancer Res* **13**: 1322–1330 doi:10.1158/1078-0432.CCR-06-1518.

Marangoni E, Vincent-Salomon A, Auger N, Degeorges A, Assayag F, de Cremoux P, de Plater L, Guyader C, De Pinieux G, Judde JG, Rebucci M, Tran-Perennou C, Sastre-Garau X, Sigal-Zafrani B, Delattre O, Dieras V, Poupon MF (2007) A new model of patient tumor-derived breast cancer xenografts for preclinical assays. *Clin Cancer Res* **13**: 3989–3998 doi:10.1158/1078-0432.CCR-07-0078.

Marcelletti JF, Multani PS, Lancet JE, Baer MR, Sikic BI (2009) Leukemic blast and natural killer cell P-glycoprotein function and inhibition in a clinical trial of zosuquidar infusion in acute myeloid leukemia. *Leukemia Research* **33**: 769–774 doi:10.1016/j.leukres.2008.09.020.

McCluggage WG (2011) Morphological subtypes of ovarian carcinoma: a review with emphasis on new developments and pathogenesis. *Pathology* **43**: 420–432 doi:10.1097/PAT.0b013e328348a6e7.

McDaid HM, Horwitz SB (2001) Selective potentiation of paclitaxel (taxol)-induced cell death by mitogen-activated protein kinase inhibition in human cancer cell lines. *Mol Pharmacol* **60**: 290–301.

McDaid HM, Lopez-Barcons L, Grossman A, Lia M, Keller S, Pérez-Soler R, Horwitz SB (2005) Enhancement of the therapeutic efficacy of taxol by the mitogen-activated protein kinase inhibitor CI-1040 in nude mice bearing human heterotransplants. *Cancer Res* **65**: 2854–2860 doi:10.1158/0008-5472.CAN-04-4391.

McMillin DW, Delmore J, Weisberg E, Negri JM, Geer DC, Klippel S, Mitsiades N, Schlossman RL, Munshi NC, Kung AL, Griffin JD, Richardson PG, Anderson KC, Mitsiades CS (2010) Tumor cell-specific bioluminescence platform to identify stroma-induced changes to anticancer drug activity. *Nat Med* **16**: 483–489 doi:10.1038/nm.2112.

Mineo R, Fichera E, Liang S-J, Fujita-Yamaguchi Y (2000) Promoter Usage for Insulin-like Growth Factor-II in Cancerous and Benign Human Breast, Prostate, and Bladder Tissues, and Confirmation of a 10th Exon. *Biochem Biophys Res Commun* **268**: 886–892 doi:10.1006/bbrc.2000.2225.

Mitsiades CS, Mitsiades NS, McMullan CJ, Poulaki V, Shringarpure R, Akiyama M, Hideshima T, Chauhan D, Joseph M, Libermann TA, García-Echeverría C, Pearson MA, Hofmann F, Anderson KC, Kung AL (2004) Inhibition of the insulin-like growth factor receptor-1 tyrosine kinase activity as a therapeutic strategy for multiple myeloma, other hematologic malignancies, and solid tumors. *Cancer Cell* **5**: 221–230 doi:10.1038/nrc1352.

Molina R, Escudero JM, Augé JM, Filella X, Foj L, Torné A, Lejarcegui J, Pahisa J (2011) HE4 a novel tumour marker for ovarian cancer: comparison with CA 125 and ROMA algorithm in patients with gynaecological diseases. *Tumour Biology* **32**: 1087–1095 doi:10.1007/s13277-011-0204-3.

Monk D (2006) Imprinting of IGF2 P0 transcript and novel alternatively spliced INS-IGF2 isoforms show differences between mouse and human. *Hum Mol Genet* **15**: 1259–1269 doi:10.1093/hmg/ddl041.

Moody G, Beltran PJ, Mitchell P, Cajulis E, Chung Y-A, Hwang D, Kendall R, Radinsky R, Cohen P, Calzone FJ (2014) IGF1R blockade with ganitumab results in systemic effects on the GH-IGF axis in mice. *J Endocrinol* **221**: 145–155 doi:10.1530/JOE-13-0306.

Mor G, Visintin I, Lai Y, Zhao H, Schwartz P, Rutherford T, Yue L, Bray-Ward P, Ward DC (2005) Serum protein markers for early detection of ovarian cancer. *Proc Natl Acad Sci USA* **102**: 7677–7682 doi:10.1073/pnas.0502178102.

Nie Z-L, Pan Y-Q, He B-S, Gu L, Chen L-P, Li R, Xu Y-Q, Gao T-Y, Song G-Q, Hoffman AR, Wang S-K, Hu J-F (2012) Gene therapy for colorectal cancer by an oncolytic adenovirus that targets loss of the insulin-like growth factor 2 imprinting system. *Mol Cancer* **11**: 86 doi:10.1186/1476-4598-11-86.

Ogawa T, Ogawa K, Shiga K, Furukawa T, Nagase H, Hashimoto S, Kobayashi T, Horii A (2010) Upregulation of IGF2 is associated with an acquired resistance for cis-diamminedichloroplatinum in human head and neck squamous cell carcinoma. *Eur Arch Otorhinolaryngol* **267**: 1599–1606 doi:10.1007/s00405-010-1257-4.

Orr GA, Verdier-Pinard P, McDaid H, Horwitz SB (2003) Mechanisms of Taxol resistance related to microtubules. *Oncogene* **22**: 7280–7295 doi:10.1038/sj.onc.1206934.

Pandini G, Frasca F, Mineo R, Sciacca L, Vigneri R, Belfiore A (2002) Insulin/insulin-like growth factor I hybrid receptors have different biological characteristics depending on the insulin receptor isoform involved. *J Biol Chem* **277**: 39684–39695 doi:10.1074/jbc.M202766200.

Parekh H, Wiesen K, Simpkins H (1997) Acquisition of taxol resistance via P-glycoprotein- and non-P-glycoprotein-mediated mechanisms in human ovarian carcinoma cells. *Biochem Pharmacol* **53**: 461–470.

Pearce CL, Doherty JA, Van Den Berg DJ, Moysich K, Hsu C, Cushing-Haugen KL, Conti DV, Ramus SJ, Gentry-Maharaj A, Menon U, Gayther SA, Pharoah PDP, Song H, Kjaer SK, Hogdall E, Hogdall C, Whittemore AS, McGuire V, Sieh W, Gronwald J, Medrek K, Jakubowska A, Lubinski J, Chenevix-Trench G, AOCS/ACS Study Group, Beesley J, Webb PM, Berchuck A, Schildkraut JM, Iversen ES, Moorman PG, Edlund CK, Stram DO, Pike MC, Ness RB, Rossing MA, Wu AH (2011) Genetic variation in insulin-like growth factor 2 may play a role in ovarian cancer risk. *Hum Mol Genet* **20**: 2263–2272 doi:10.1093/hmg/ddr087.

Philip PA, Goldman B, Ramanathan RK, Lenz H-J, Lowy AM, Whitehead RP, Wakatsuki T, Iqbal S, Gaur R, Benedetti JK, Blanke CD (2014) Dual blockade of epidermal growth factor receptor and insulin-like growth factor receptor-1 signaling in metastatic pancreatic cancer: Phase Ib and randomized phase II trial of gemcitabine, erlotinib, and cixutumumab versus gemcitabine plus erlotinib (SWOG S0727). *Cancer* doi:10.1002/cncr.28744.

Piek JMJ, Verheijen RHM, Kenemans P, Massuger LF, Bulten H, van Diest PJ (2003) BRCA1/2-related ovarian cancers are of tubal origin: a hypothesis. *Gynecol Oncol* **90**: 491.

Pollak M (2012) The insulin and insulin-like growth factor receptor family in neoplasia: an update. *Nat Rev Cancer* **12**: 159–169 doi:10.1038/nrc3215.

Pollard JW (2004) Opinion: Tumour-educated macrophages promote tumour progression and metastasis. *Nat Rev Cancer* **4**: 71–78 doi:10.1038/nrc1256.

Potti A, Dressman HK, Bild A, Riedel RF, Chan G, Sayer R, Cragun J, Cottrill H, Kelley MJ, Petersen R, Harpole D, Marks J, Berchuck A, Ginsburg GS, Febbo P, Lancaster J, Nevins JR (2006) Genomic signatures to guide the use of chemotherapeutics. *Nat Med* **12**: 1294–1300 doi:10.1038/nm1491.

Rancourt RC, Harris HR, Barault L, Michels KB (2013) The prevalence of loss of imprinting of H19 and IGF2 at birth. *FASEB J* **27**: 3335–3343 doi:10.1096/fj.12-225284.

Rao S, Orr GA, Chaudhary AG, Kingston DG, Horwitz SB (1995) Characterization of the taxol binding site on the microtubule. 2-(m-Azidobenzoyl)taxol photolabels a peptide (amino acids 217–231) of beta-tubulin. *J Biol Chem* **270**: 20235–20238.

Ratajczak MZ (2012) Igf2-H19, an imprinted tandem gene, is an important regulator of embryonic development, a guardian of proliferation of adult pluripotent stem cells, a regulator of longevity, and a ‘passkey’ to cancerogenesis. *Folia Histochemica et Cytobiologica* **50**: 171–179 doi:10.5603/FHC.2012.0026.

Ratajczak MZ, Shin D-M, Schneider G, Ratajczak J, Kucia M (2013) Parental imprinting regulates insulin-like growth factor signaling: a Rosetta Stone for understanding the biology of pluripotent stem cells, aging and cancerogenesis. *Leukemia* **27**: 773–779 doi:10.1038/leu.2012.322.

Rawahi Al T, Lopes AD, Bristow RE, Bryant A, Elattar A, Chattopadhyay S, Galaal K (2013) Surgical cytoreduction for recurrent epithelial ovarian cancer. *Cochrane Database Syst Rev* **2**: CD008765 doi:10.1002/14651858.CD008765.pub3.

Rikhof B, van der Graaf WTA, Suurmeijer AJH, van Doorn J, Meersma GJ, Groenen PJTA, Schuurin EMD, Meijer C, de Jong S (2012) ‘Big’-insulin-like growth factor-II signaling is an autocrine survival pathway in gastrointestinal stromal tumors. *Am J Pathol* **181**: 303–312 doi:10.1016/j.ajpath.2012.03.028.

Rodon J, DeSantos V, Ferry RJ, Kurzrock R (2008) Early drug development of inhibitors of the insulin-like growth factor-I receptor pathway: lessons from the first clinical trials. *Mol Cancer Ther* **7**: 2575–2588 doi:10.1158/1535-7163.MCT-08-0265.

Romero I, Bast RC, Bast RC Jr. (2012) Minireview: human ovarian cancer: biology, current management, and paths to personalizing therapy. *Endocrinology* **153**: 1593–1602 doi:10.1210/en.2011-2123.

Sawiris GP, Sherman-Baust CA, Becker KG, Cheadle C, Teichberg D, Morin PJ (2002) Development of a highly specialized cDNA array for the study and diagnosis of epithelial ovarian cancer. *Cancer Res* **62**: 2923–2928.

Sayer RA, Lancaster JM, Pittman J, Gray J, Whitaker R, Marks JR, Berchuck A (2005) High insulin-like growth factor-2 (IGF-2) gene expression is an independent predictor of poor survival for patients with advanced stage serous epithelial ovarian cancer. *Gynecol Oncol* **96**: 355–361 doi:10.1016/j.ygyno.2004.10.012.

Schiff PB, Fant J, Horwitz SB (1979) Promotion of microtubule assembly in vitro by taxol. *Nature* **277**: 665–667.

Sciacca L, Mineo R, Pandini G, Murabito A, Vigneri R, Belfiore A (2002) In IGF-I receptor-deficient leiomyosarcoma cells autocrine IGF-II induces cell invasion and protection from apoptosis via the insulin receptor isoform A. *Oncogene* **21**: 8240–8250 doi:10.1038/sj.onc.1206058.

Shahabi S, Yang C-PH, Goldberg GL, Horwitz SB (2010) Etoposide B enhances surface EpCAM expression in ovarian cancer Hey cells. *Gynecol Oncol* **119**: 345–350 doi:10.1016/j.ygyno.2010.07.005.

Sherman-Baust CA, Becker KG, Wood Iii WH, Zhang Y, Morin PJ (2011) Gene expression and pathway analysis of ovarian cancer cells selected for resistance to cisplatin, paclitaxel, or doxorubicin. *J Ovarian Res* **4**: 21 doi:10.1186/1757-2215-4-21.

Shield K, Ackland ML, Ahmed N, Rice GE (2009) Multicellular spheroids in ovarian cancer metastases: Biology and pathology. *Gynecol Oncol* **113**: 143–148 doi:10.1016/j.ygyno.2008.11.032.

Shin DH, Lee H-J, Min H-Y, Choi SP, Lee M-S, Lee JW, Johnson FM, Mehta K, Lippman SM, Glisson BS, Lee H-Y (2013) Combating resistance to anti-IGFR antibody by targeting the integrin β 3-Src pathway. *J Natl Cancer Inst* **105**: 1558–1570 doi:10.1093/jnci/djt263.

Siegel R, Ma J, Zou Z, Jemal A (2014) Cancer statistics, 2014. *CA: A Cancer Journal for Clinicians* **64**: 9–29 doi:10.3322/caac.21208.

Singer CF, Mogg M, Koestler W, Pacher M, Marton E, Kubista E, Schreiber M (2004) Insulin-like growth factor (IGF)-I and IGF-II serum concentrations in patients with benign and malignant breast lesions: free IGF-II is correlated with breast cancer size. *Clin Cancer Res* **10**: 4003–4009 doi:10.1158/1078-0432.CCR-03-0093.

Skehan P, Storeng R, Scudiero D, Monks A, McMahon J, Vistica D, Warren JT, Bokesch H, Kenney S, Boyd MR (1990) New colorimetric cytotoxicity assay for anticancer-drug screening. *JNCI Journal of the National Cancer Institute* **82**: 1107–1112.

StatBite: Ovarian cancer: risk of recurrence by stage of diagnosis. (2009) StatBite: Ovarian cancer: risk of recurrence by stage of diagnosis. *J Natl Cancer Inst* **101**: 1234 doi:10.1093/jnci/djp308.

Stewart JM, Shaw PA, Gedye C, Bernardini MQ, Neel BG, Ailles LE (2011) Phenotypic heterogeneity and instability of human ovarian tumor-initiating cells. *Proc Natl Acad Sci USA* **108**: 6468–6473 doi:10.1073/pnas.1005529108.

Stordal B, Hamon M, McEneaney V, Roche S, Gillet J-P, O'Leary JJ, Gottesman M, Clynes M (2012) Resistance to paclitaxel in a cisplatin-resistant ovarian cancer cell line is mediated by P-glycoprotein. *PLoS ONE* **7**: e40717 doi:10.1371/journal.pone.0040717.

Swierczak A, Cook AD, Lenzo JC, Restall CM, Doherty JP, Anderson RL, Hamilton JA (2014) The Promotion of Breast Cancer Metastasis Caused by Inhibition of CSF-1R/CSF-1 Signaling Is Blocked by Targeting the G-CSF Receptor. *Cancer Immunol Res* **2**: 765–776 doi:10.1158/2326-6066.CIR-13-0190.

Szakács G, Paterson JK, Ludwig JA, Booth-Genthe C, Gottesman MM (2006) Targeting multidrug resistance in cancer. *Nat Rev Drug Discov* **5**: 219–234 doi:10.1038/nrd1984.

Tada Y, Yamaguchi Y, Kinjo T, Song X, Akagi T, Takamura H, Ohta T, Yokota T, Koide H (2014) The stem cell transcription factor ZFP57 induces IGF2 expression to promote anchorage-independent growth in cancer cells. *Oncogene* doi:10.1038/onc.2013.599.

Tan DSP, Ang JE, Kaye SB (2008) Ovarian cancer: can we reverse drug resistance? *Adv Exp Med Biol* **622**: 153–167 doi:10.1007/978-0-387-68969-2_13.

Tazearslan C, Huang J, Barzilai N, Suh Y (2011) Impaired IGF1R signaling in cells expressing longevity-associated human IGF1R alleles. *Aging Cell* **10**: 551–554 doi:10.1111/j.1474-9726.2011.00697.x.

Torres K, Horwitz SB (1998) Mechanisms of Taxol-induced cell death are concentration dependent. *Cancer Res* **58**: 3620–3626.

Trimble EL, Alvarez RD (2006) Intraperitoneal chemotherapy and the NCI clinical announcement. *Gynecol Oncol* **103**: S18–S19 doi:10.1016/j.ygyno.2006.08.020.

Ulanet DB, Ludwig DL, Kahn CR, Hanahan D (2010) Insulin receptor functionally enhances multistage tumor progression and conveys intrinsic resistance to IGF-1R targeted therapy. *Proc Natl Acad Sci USA* **107**: 10791–10798 doi:10.1073/pnas.0914076107.

Vanneman M, Dranoff G (2012) Combining immunotherapy and targeted therapies in cancer treatment. *Nat Rev Cancer* **12**: 237–251 doi:10.1038/nrc3237.

Vaughan S, Coward JI, Bast RC, Berchuck A, Berek JS, Brenton JD, Coukos G, Crum CC, Drapkin R, Etemadmoghadam D, Friedlander M, Gabra H, Kaye SB, Lord CJ, Lengyel E, Levine DA, McNeish IA, Menon U, Mills GB, Nephew KP, Oza AM, Sood AK, Stronach EA, Walczak H, Bowtell DD, Balkwill FR (2011) Rethinking ovarian cancer: recommendations for improving outcomes. *Nat Rev Cancer* **11**: 719–725 doi:10.1038/nrc3144.

Visintin I, Feng Z, Longton G, Ward DC, Alvero AB, Lai Y, Tenthorey J, Leiser A, Flores-Saaib R, Yu H, Azori M, Rutherford T, Schwartz PE, Mor G (2008) Diagnostic markers for early detection of ovarian cancer. *Clin Cancer Res* **14**: 1065–1072 doi:10.1158/1078-0432.CCR-07-1569.

Wang N, Feng Y, Wang Q, Liu S, Xiang L, Sun M, Zhang X, Liu G, Qu X, Wei F (2014) Neutrophils infiltration in the tongue squamous cell carcinoma and its correlation with CEACAM1 expression on tumor cells. *PLoS ONE* **9**: e89991 doi:10.1371/journal.pone.0089991.

Wu B, Chao JA, Singer RH (2012) Fluorescence fluctuation spectroscopy enables quantitative imaging of single mRNAs in living cells. *Biophys J* **102**: 2936–2944 doi:10.1016/j.bpj.2012.05.017.

Wu JD, Odman A, Higgins LM, Haugk K, Vessella R, Ludwig DL, Plymate SR (2005) In vivo effects of the human type I insulin-like growth factor receptor antibody A12 on androgen-dependent and androgen-independent xenograft human prostate tumors. *Clin Cancer Res* **11**: 3065–3074 doi:10.1158/1078-0432.CCR-04-1586.

Yang B, Wagner J, Damaschke N, Yao T, Wuerzberger-Davis SM, Lee M-H, Svaren J, Miyamoto S, Jarrard DF (2014) A novel pathway links oxidative stress to loss of insulin growth factor-2 (IGF2) imprinting through NF- κ B activation. *PLoS ONE* **9**: e88052 doi:10.1371/journal.pone.0088052.

Yasui K, Mihara S, Zhao C, Okamoto H, Saito-Ohara F, Tomida A, Funato T, Yokomizo A, Naito S, Imoto I, Tsuruo T, Inazawa J (2004) Alteration in copy numbers of genes as a mechanism for acquired drug resistance. *Cancer Res* **64**: 1403–1410.

Yee D (2012) Insulin-like Growth Factor Receptor Inhibitors: Baby or the Bathwater? *JNCI Journal of the National Cancer Institute* **104**: 975–981 doi:10.1093/jnci/djs258.

Zinzi L, Capparelli E, Cantore M, Contino M, Leopoldo M, Colabufo NA (2014) Small and Innovative Molecules as New Strategy to Revert MDR. *Front Oncol* **4**: 2 doi:10.3389/fonc.2014.00002.